Summer 8-15-2018

Exploring Fatty Acid Metabolism for the Biosynthesis of Non-Natural Chemicals

Wen Jiang
Washington University in St. Louis

WASHINGTON UNIVERSITY IN ST. LOUIS

Energy, Environmental and Chemical Engineering

Dissertation Examination Committee:
Fuzhong Zhang, Chair
Michael Jewett
Tae Seok Moon
Himadri Pakrasi
Yinjie Tang

Exploring Fatty Acid Metabolism for the Biosynthesis of Non-Natural Chemicals

by
Wen Jiang

A dissertation presented to
The Graduate School
of Washington University in
partial fulfillment of the
requirements for the degree
of Doctor of Philosophy

August 2018
St. Louis, Missouri

Table of Contents

List of Figures

List of Tables

Acknowledgments

First of all, I would like to express my sincere gratitude to my advisor Dr. Fuzhong Zhang for his guidance and care during the past five years. Since joining the lab in December 2013, Dr. Zhang has always given me freedom to choose my research projects based on my interest and expertise, while providing guidance and assistance whenever needed. For each project, he has been inspiring me with passions and great ideas and impressing me with his solid background knowledge and experience. Additionally, his courage to take on novel challenging projects has always encouraged me to pursue new tasks.

Moreover, I would like to give my appreciation to my coworkers, especially Dr. Gayle Bentley, Dr. Yanfang Jiang, Dr. Yi Xiao, Dr. Di Liu, Dr. Nathan Crook (WU Medical School), and Ashty Karim (Northwestern University) for their careful tutor and patient assistance. Their contributions are essential to help me fulfill this dissertation work and develop communication and collaboration skills. I would also acknowledge my committee members, Dr. Michael Jewett (Northwestern University), Dr. Tae Seok Moon, Dr. Himadri Pakrasi, and Dr. Yinjie Tang, for their invaluable comments and inputs to polish my dissertation, as well as their insights to guide my path towards further improvement in my future research and professional development. Last but not least, I would like to express my honor to have a summer internship in Monsanto Company. This opportunity expanded my insight for gene editing, and my managers, Dr. Larry Gilbertson and Dr. Edward Cargill, offered me great guidance for career development.

Thanks to all Zhang Lab members for making my life much easier and happier here. Dr. Di Liu and Dr. Yi Xiao have provided countless help and support for me to adapt to the lab as quick as possible; The safety instruction and assistance provided by Cameron Sargent and Eugene Kim

has always facilitated my work; The encouragement and help between Chris Bowen and I have escorted us to pass through all the challenges in our PhD study; The formation of “shitty group” among Chris Hartline, Alex Schmitz and I has been offering us the platform to learn about single-cell works together. Not to mention the time I spent with Dr. Gayle Bentley, Dr. Yanfang Jiang and Dr. Linda Guaman to finish our research project and enjoy our lives.

Thanks to all my friends to make my life more enjoyable and less homesick. I have had a relaxed and enjoyable daily life after work with my roommates, Dr. Wei Xiong, Dr. Lijie Zhang and Yuanzi Sun, for five years. I will always remember our graduation trip to the Great Smoky Mountain before we separated. In addition, many other friends, who left before me (like Dr. Jie Sun and Dr. Lian He), or who came after me (like Jiayu Li and Yunzhu Zhang), have had great impact on my life, and have passed on our tradition and spirit forever.

Finally, I am deeply grateful to my parents for understanding and supporting me to study abroad, and for their forever love to me.

This work has been supported by Defense Advanced Research Projects Agency (DARPA).

Wen Jiang

Washington University in St. Louis

August 2018

Dedicated to my parents.

ABSTRACT OF THE DISSERTATION

Exploring Fatty Acid Metabolism for the Biosynthesis of Non-Natural Chemicals

by

Wen Jiang

Doctor of Philosophy in Energy, Environmental and Chemical Engineering

Washington University in St. Louis, 2018

Professor Fuzhong Zhang, Chair

The global energy crisis and increasing environmental concerns have spurred the sustainable production of biofuels and other fossil-fuel-derived chemicals. One approach is to engineer microbial metabolic pathways to convert renewable feedstocks (e.g. lignocellulosic biomass) to compounds that have structures similar to those of petroleum-derived fuels and chemicals. The microbial fatty acid (FA) biosynthetic pathway is attractive because FAs are common precursors that can be converted to several types of chemicals, including alkanes, alkenes, alcohols, and esters. These chemicals have numerous applications as fuels, fragrances, emollients, plasticizers, thickeners, and detergents. Most work has used *Escherichia coli* as the microbial host due to its exceptionally high rate of fatty acid biosynthesis.

To broaden the use of FA-derived compounds, it is important to diversify the structure of biosynthesized FAs. Unfortunately, wild-type *E. coli* synthesize only straight long-chain FAs (mostly palmitic acid), which limits their range of application. On the other hand, chemicals derived from non-natural fatty acids (NNFAs) have wider applications. For example, branched-chain FA-derived hydrocarbons have better combustion properties than their straight-chain counterparts when used as fuels, and ω-hydroxy acids and di-acids are monomers for polymers.

My dissertation work explored engineering *E. coli* metabolic pathways to produce NNFAs and their derivatives. I started with the production branched-chain fatty acids (BCFAs), and showed that high percentage BCFA (or derivatives) production can be achieved via my engineered strains. The composition of BCFAs was controlled to produce even-chain-iso-, odd-chain-iso-, or odd-chain-anteiso-BCFAs separately. Next, I partitioned the complete pathway into three modules: a precursor formation module, an acyl-CoA activation and malonyl-ACP consumption module, and a final product synthesis module. I engineered and tuned each module separately and combined the optimal modules to produce a high percentage of branched-chain fatty alcohols, alkanes, and esters. Finally, I established a new cell-free framework as a proof-of-concept for *in vitro* production of fatty acid derivatives, providing a platform for rapid screening and prototyping of fatty acid synthetic pathways to produce bifunctional fatty acid derivatives.

The findings of my work have provided a deeper understanding of the potential of the fatty acid synthetic pathway for NNFA production, and the strain-engineering strategies used in this dissertation will open new opportunities for efficient production of chemicals derived from NNFAs.

Chapter 1: Microbial production of non-natural chemicals

1.1 Current progress in microbial bioproduction

The past decade has witnessed rapid advance in microbial bioproduction from renewable resources. Various biosynthetic pathways have been constructed to produce chemicals with diverse structures, and multiple metabolic engineering strategies have been developed to increase titers, yields, productivities and system robustness. The feedstock choices have been expanded from food crops (e.g., corns and oilseeds) to abundant and low-cost non-food biomass (e.g., corn stover and switchgrass) [1], solid wastes (e.g., industrial wastes and sewage sludge) [2], natural resources (syngas, methanol and methane) [3], and carbon dioxide [4]. Meanwhile, the fermentation host choices have expanded beyond the traditional model microorganisms such as *Escherichia coli* and *Saccharomyces cerevisiae* to a wide variety of non-model organisms. These new hosts variously feature unique capabilities in assimilating target feedstock, adapting to specialized fermentation conditions, and producing target chemicals in high efficiencies.

1.2 Strategies for pathway optimization

Once the metabolic pathway is established, several new strategies can be applied to optimize the pathway and to increase product titers, yields, and productivities. Conventional concept of metabolic engineering is to drive the metabolic flux into the production pathway. Various methods have been developed to facilitate this step, including upregulating pathway enzymes [5], deleting or downregulating competing pathways [6], and adjusting the global metabolism by engineering

transcriptional factors [7]. Meanwhile, an increasing number of strategies have been developed to balance metabolic pathways and to engineer host cells by increasing their robustness, enhancing cell viability, and regulating cell populations [8].

Metabolite overproduction often competes with natural metabolism for limited cellular resources and disrupts the host's homeostasis for some metabolites or cofactors [9], leading to impaired cell growth [10]. Therefore, to increase the system robustness and thus to obtain high efficient production, engineered metabolic pathway must be balanced by eliminating pathway bottlenecks while preventing the accumulation of excess proteins or intermediates. A metabolic pathway can be balanced statically via engineering promoters [11] or RBSs [12], or dynamically via a metabolite biosensor to adjust flux in response to a rate-limiting or a toxic metabolite by regulating its production and/or consumption [13, 14]. An alternative strategy to avoid adverse effects on cell growth is to separate the production process from cell growth phase. Several strategies were developed to induce the transition from growth phase to production, including stationary phase signals [15], quorum sensing [16], and depletion of a nutrient [17] that is not needed for metabolite production. For example, based on the Crabtree effect, a GAL regulatory circuit was engineered in *S. cerevisiae* to autosense glucose depletion and simultaneously induce the producing pathway [18, 19].

Furthermore, the accumulation of some products may trigger a variety of detrimental effects on the host cells, mainly physiological changes of cell membranes. By altering the composition of cell membranes FA (e.g. chain length, degree of saturation, and abundance of cyclic rings) [20] and the distribution of phospholipid head groups [21], the engineered hosts could demonstrate enhanced tolerance to various toxic compounds (such as alcohols, carboxylic acids and aromatic compounds) and adverse industrial conditions (such as low pH and high temperature) [20].

In addition, the heterogeneity of producing cells strongly affects ensemble production [22, 23]. A recently developed strategy named PopQC positively links metabolite production with cell growth, enabling the enrichment of high-producing variants from a heterologous culture and leading to several folds enhancement in overall product titers [24]. Selecting non-genetic variants is a promising new path to increase the production yield, with a strong potential for novel development based on the system.

1.3 Metabolic pathways for the synthesis of non-natural chemicals

Typically, based on the inherence of the biosynthetic pathway, the produced chemicals can be broadly classified into three categories: 1) Natural chemicals, such as bioethanol and lactic acid, which are produced inherently through a native pathway; 2) Non-natural chemicals, such as 1-butanol and isobutanol, which are produced in a heterologous host strain by the establishment of heterologous pathways and enzymes; 3) Non-natural created chemicals, which can only be produced by creating synthetic enzymes and pathways with new functions. In this section, I intend to give a brief but comprehensive overview of three heterologous pathways leading to non-natural chemical production in *E. coli*.

1.3.1 α-keto acid pathway

Isobutanol pathway is a great example for non-natural chemical biosynthesis. By combining the short-chain branched-chain amino acid biosynthetic pathway with the alcohol generation pathway, short-chain alcohols (including isobutanol, 3-methyl-1-butanol, and 2-methyl-1-butanol) were produced from cellular short-chain α-keto acid intermediates catalyzed by an α-keto acid decarboxylase and an alcohol dehydrogenase [25](Figure 1-1, light blue). Furthermore, by altering

the substrate specificity of LeuABCD enzymes, the acyl chain length of α-keto acids was further increased by recursively condensing with acetyl-CoA and releasing CO_2. Using this strategy, alcohols with medium chain-lengths (up to C8) or with branched/aromatic terminals were produced [26] (Figure 1-1, green). Meanwhile, α-keto acids or their derived alcohols can also be converted to short-chain acids [27] and alkanes [28], and to acetate-based esters [29].

Table 1- 1 The carbon efficiencies, cofactor balances, and highest titers produced from α-keto acid pathway

Products	Carbon recovery from glucose	Cofactor imbalance	Highest titer
1-butanol	44.4%	+ 6 NADH	1 g/L [30]
isobutanol	66.7%	+ 1 NADH, - 1 NADPH	22 g/L [25]
3-methyl-1-butanol	55.6%	+ 4 NADH, - 1 NADPH	4.4 g/L [31]
2-methyl-1-butanol	83.3%	+ 1 NADH, - 3 NADPH	1.25 g/L [32]
1-pentanol	41.7%	+ 8 NADH	4.3 g/L [33]
1-hexanol	40.0%	+ 10 NADH	302 mg/L [26]
1-heptanol	38.9%	+ 12 NADH	80 mg/L [26]
1-octanol	38.1%	+ 14 NADH	2.0 mg/L [26]

One advantage of the α-keto acid pathway is its ability to add one carbon atom at a time to the acyl-chain, allowing precise control over chain-length. However, this chain elongation process sacrifices carbon efficiency and accumulates NADH (Table 1-1), which might be the reason for the lower titer of medium-chain alcohols (C6-C8) compared to that of isobutanol.

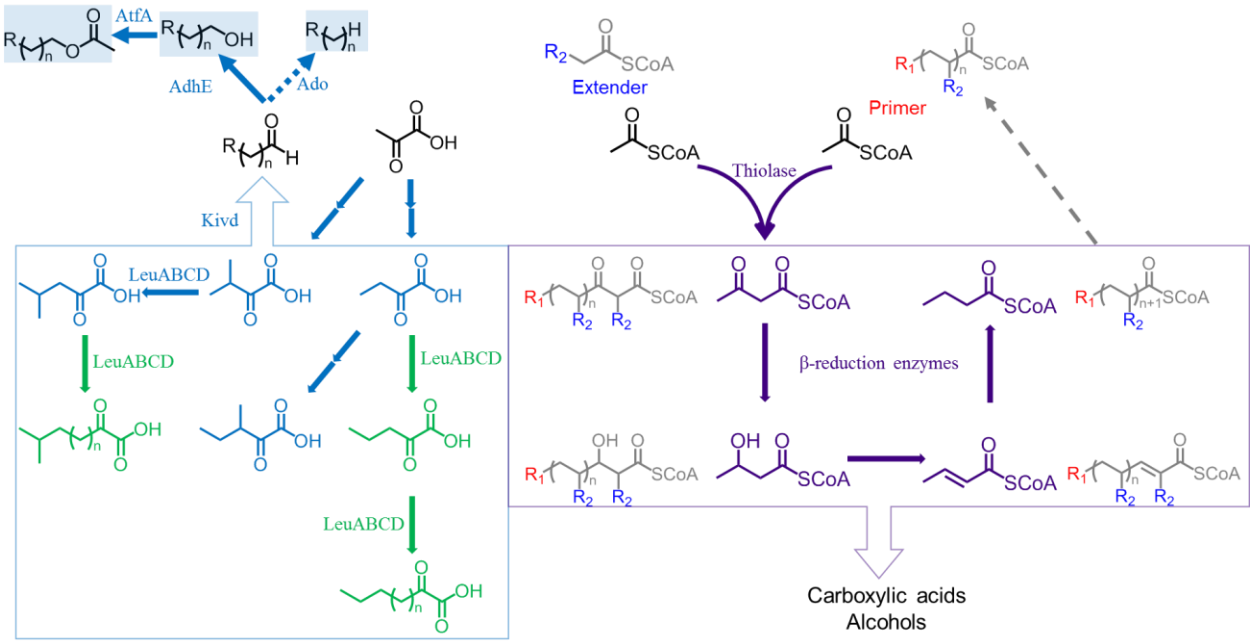

Figure 1- 1 Biofuels produced from the α-keto acid pathway (left) and non-decarboxylative Claisen condensation pathway (right)
α-keto acids can be converted to aldehydes by an α-keto acid decarboxylase (Kivd). Aldehydes can then be converted to alcohols by an aldehyde dehydrogenase (AdhE) or to alkanes by an aldehyde decarbonylase (colored blue). α-keto acids can be elongated by a LeuABCD mutant to yield longer chain α-keto acids (colored green). The natural-occurring non-decarboxylative Claisen condensation pathway is colored purple. The engineered primers and extenders used in the non-decarboxylative Claisen condensation pathway are colored grey.

1.3.2 Non-decarboxylative Claisen condensation pathway

Non-decarboxylative Claisen condensation pathway was first discovered in nature from *Clostridium kluyveri* [34] (Figure 1-1, purple). In this pathway, two molecules of acetyl-CoA are condensed to acetoacetyl-CoA, which is then reduced to butyrate by β-reduction reactions. In contrast to the FA biosynthetic pathway that grows the carbon chain on ACP, the non-decarboxylative Claisen condensation pathway grows the carbon chain on CoA and uses acetyl-CoA or other short-chain acyl-CoAs as primers. Dellomonaco *et al.* engineered a synthetic non-decarboxylative Claisen condensation pathway to elongate carbon chains by reversing β-oxidation pathway [35]. The elongation cycle can be terminated by an acyl-CoA reductase and an alcohol

dehydrogenase to produce straight-chain alcohols, or by an acyl-CoA thioesterase to produce carboxylic acids. By switching thiolases and β-reduction enzymes, researchers further expanded the primer from acetyl-CoA to six other ω-functionalized primers, and incorporated three different extender units [36] (Figure 1, grey structures). This platform has greatly enlarged the structural diversity of biosynthesized molecules, yielding a series of novel bioproducts, such as 2-methylpentanoic acid and 2,3-dihydroxybutyric acid [36].

The non-decarboxylative Claisen condensation pathway has two distinctive advantages: the ability to incorporate internal functional groups (including branch structures) into the product, and the ability to orthogonally control the structures of both primers and extenders. This pathway will become more versatile as new enzymes are discovered to incorporate more extenders and new strategies are developed to precisely control the number and order of elongation cycles.

1.3.3 Isoprenoid pathway

The isoprenoid pathway utilizes C5 isopentenyl pyrophosphate (IPP) and dimethylallyl pyrophosphate (DMAPP) as building blocks, which are produced from either the mevalonate (MVA) or methylerythritol-4-phosphate (MEP) pathway (Figure 1-2). The carbon chain is elongated by iterative assembly of IPP or DMAPP, generating polyisoprenoid diphosphates which are then converted to terpenes or terpenoids by terpene synthases or polyisoprenoid diphosphate modifying enzymes such as hydrolases or esterases.

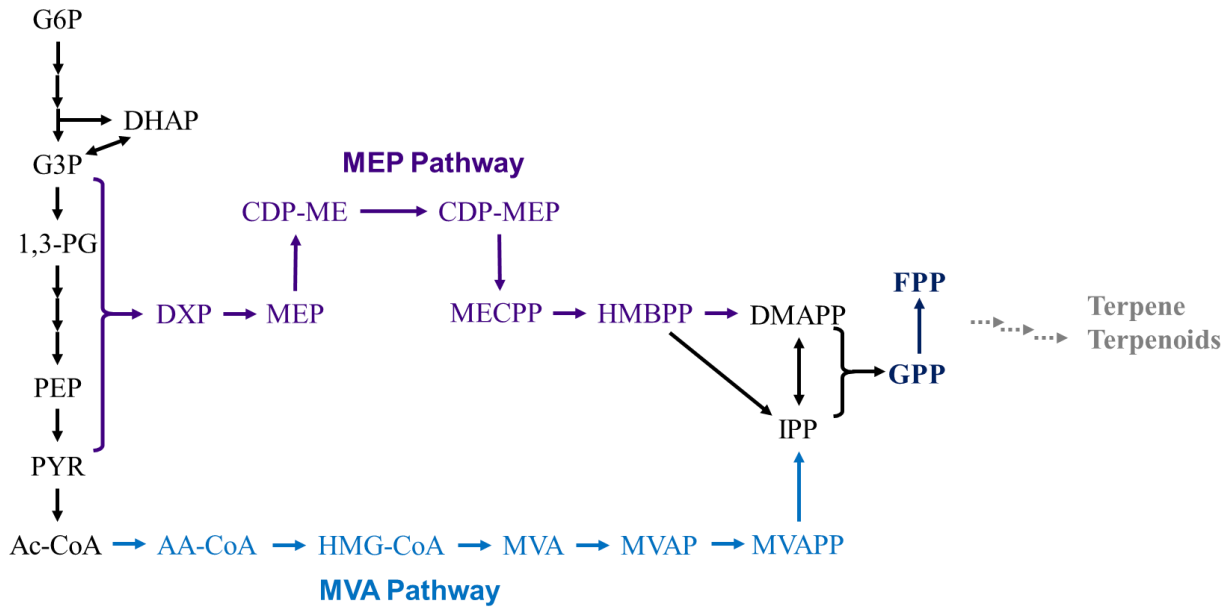

Figure 1- 2 The isoprenoid pathway
Mevalonate pathway is colored light blue. MEP pathway is colored purple. AA-CoA: acetoacetyl-CoA; MVA: mevalonate; MVAP: mevalonate-5-phosphate; MVAPP: mevalonate-diphosphate; MEP: 2-C-methylerythritol-4-phosphate; CDP-ME: 4-diphosphocytidyl-2-C-methylerythritol; CDP-MEP: 4-diphosphocytidyl-2-C-methyl-D-erythritol-2-phosphate; HMB-PP: (E)-4-hydroxy-3-methyl-but-2-enyl pyrophosphate.

Due to the diverse functionality of terpene synthases, the most outstanding feature of the isoprenoid pathway is its capability to generate structurally diverse products. So far, thousands of different terpene structures have been identified [37], and over hundreds of terpene synthases have been sequenced [38]. However, most terpene synthases have not been characterized, and the links between most terpene synthases to their corresponding terpene products have not been established. New methods for high throughput characterization of new terpene synthases could facilitate the discovery of new biosynthetic routes to various specialty chemicals.

1.4 Fatty acid pathway

The commercialization of biodiesel as the first-generation biofuels has attracted much attention on fatty acid pathway. As oilseed-derived biodiesel suffers from inferior low-temperature performance and competes with food supply, engineering efforts have been made to overproduce microbial-based fatty acid-derived fuels and chemicals. Fatty acids (FAs) are biosynthesized *in vivo* by either the discrete fatty acid synthase complex FASII (in most bacteria) or a multifunctional FASI synthase (in eukaryotic cells). In *E. coli*, the initiation step is catalyzed by β-keto-acyl-ACP synthetase III (FabH, encoded by *fabH*), which condenses acetyl-CoA with malonyl-ACP to form acetoacetyl-ACP (Figure 1-3). The four-carbon acyl chain is then elongated on acyl carrier proteins (ACPs) through repeated cycles of reactions catalyzed by FabG, FabA/FabZ, FabI, and FabB/FabF to yield straight long-chain acyl-ACPs for lipid biosynthesis. Straight long-chain acyl-ACP can be hydrolyzed by the overexpression of a cytosolic thioesterase to produce SCFAs [39]. Medium-chain FAs (C8-C12), which are preferred for biodiesel, can be produced in *E. coli* by overexpressing a medium-chain-specific thioesterase [40] (Figure 1-3, Chain-Length Control Module). Similarly, the *S. cerevisiae* FASI has been engineered to produce medium-chain FAs at a titer of 464 mg/L using a rational protein engineering strategy [41]. These medium-chain FAs can then be derived using engineered conversion pathways to alkanes [42], alcohols [43], and esters [44] for various applications (Figure 1-3, α-Terminal Structure Control Module).

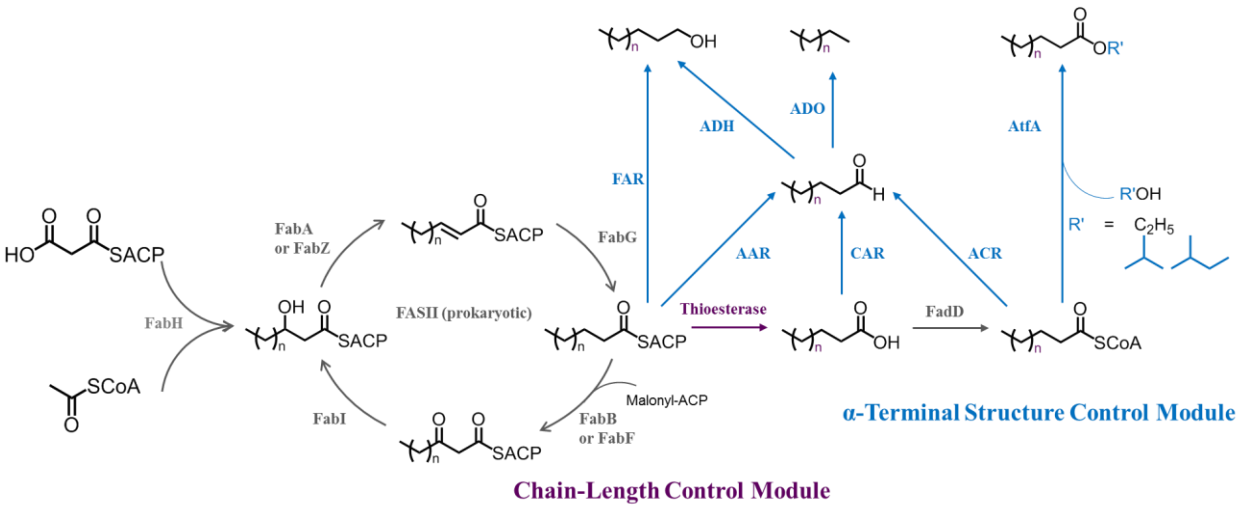

Figure 1- 3 Pathways for the production of fatty acid-derived chemicals

Native *E. coli* fatty acid pathway is colored grey. The chain length control module is colored purple. The α-terminal structure control is colored blue. FabH: β-keto-acyl-ACP synthase III; FabB: β-keto-acyl-ACP synthase I; FabG: β-keto-acyl-ACP reductase; FabZ: β-hydroxyacyl-ACP dehydratase; FabI: enoyl-acyl-ACP reductase; FadD: acyl-CoA synthase; ACR: acyl-CoA reductase; AtfA: wax-ester synthase; AAR: acyl-ACP reductase; ADO: aldehyde decarbonylase; ADH: alcohol dehydrogenase; FAR: fatty acyl reductase.

Several engineering efforts have been developed to overproduce SCFAs in engineered *E. coli* including overexpression of various thioesterases [45, 46], deletion of genes involved in β-oxidation (*fadD* or *fadE*) [45, 47], engineering global regulators of fatty acid pathways [48], and implementing synthetic control systems to dynamically control the expression of pathway genes [13, 14]. Through these efforts, SCFAs have been produced in both high titers and yields [14].

Overall, the highly efficient natural FAS pathways make fatty acid an attractive intermediate for various chemical productions. On the other hand, the essentiality of fatty acid presents challenges to engineering: 1) incorporating non-native fatty acids into the cell membrane may change the membrane fluidity, inhibiting cell growth, 2) expressing native fatty acid biosynthetic genes is often growth-associated, limiting the production to the growth phase, and 3) interaction

between natural FAS enzymes may prevent short- and medium-chain acyl-ACPs from interacting with desired heterologous enzymes in biosynthetic pathways.

1.5 Scope of this research

Current engineering efforts on *E. coli* fatty acid biosynthetic pathway only produce straight chain products, which limits its range of application. On the other hand, chemicals derived from non-natural fatty acids (NNFAs) have broad applications. For example, branched-chain-fatty-acid-derived hydrocarbons have better fuel combustion properties, and ω-hydroxy acids and di-acids are monomer starting points for producing polymers. Ideally, diversifying the structure of biosynthesized fatty acids from *E. coli* could produce non-natural molecules that have exactly the same chemical structures as petroleum-derived chemicals, and the high rate machinery of *E. coli* fatty acid synthesis will facilitate the broad application of these FA-derived compounds.

This dissertation aims to engineer *E. coli* metabolic pathways to produce NNFAs and their derivatives. Specifically, I aim to start engineering an *E. coli* strain to produce branched-chain fatty acids (BCFAs) in Chapter 2. Then I apply the engineered platform to produce branched-chain hydrocarbons and to develop strategies to optimize pathway robustness, efficiencies, and yields in Chapter 3. Finally, I aim to extend the diversity of biologically synthesized fatty acids by testing the capacity of the fatty acid biosynthetic pathway to incorporate functional terminal groups based on my engineered pathways in Chapter 4 and Chapter 5. Successful completion of this study will generate a series of pathways for the biosynthesis of NNFA-derived products, which cannot be currently produced from renewable resources. Furthermore, the modular-controlled production system will allow the fine tuning of chemical structures and compositions, making it suitable for a variety of applications.

Chapter 2: Engineer an *E. coli* strain to produce branched-chain fatty acids in high percentage

2.1 Introduction

Engineering microbial metabolic pathways allows the production of advanced biofuel and biochemical with desired structures and properties. Among them, the fatty acid biosynthetic pathway is particularly attractive because fatty acids are common precursors that can be readily converted to several types of chemicals including alkanes [42, 49], alkenes [50], alcohols [39, 51], and esters [52-54] through either biological [55] or chemical conversion [45]. However, the majority of previous engineering efforts have focused on microbial production of straight-chain fatty acids (SCFAs) and their derivatives, which have limited cold-flow properties and thus can be only used during warm weather [56, 57]. The low-temperature operability of fatty acid-derived fuels can be improved by introducing branches to the fuel molecule, which requires the synthesis of branched-chain fatty acids (BCFAs) [58].

Naturally, *E. coli* synthesizes only SCFAs through the multi-enzyme fatty acid type II biosynthesis system (FASII). The initiation step is catalyzed by the only β-keto-acyl-ACP synthetase III (FabH, encoded by *fabH*), which condenses acetyl-CoA with malonyl-ACP to form acetoacetyl-ACP. Then the four-carbon acyl chain product is elongated on acyl carrier proteins (ACPs) through repeated cycles of reactions to yield straight long-chain acyl-ACPs (C14-C18) for lipid synthesis (Figure 2-1A, blue arrow).

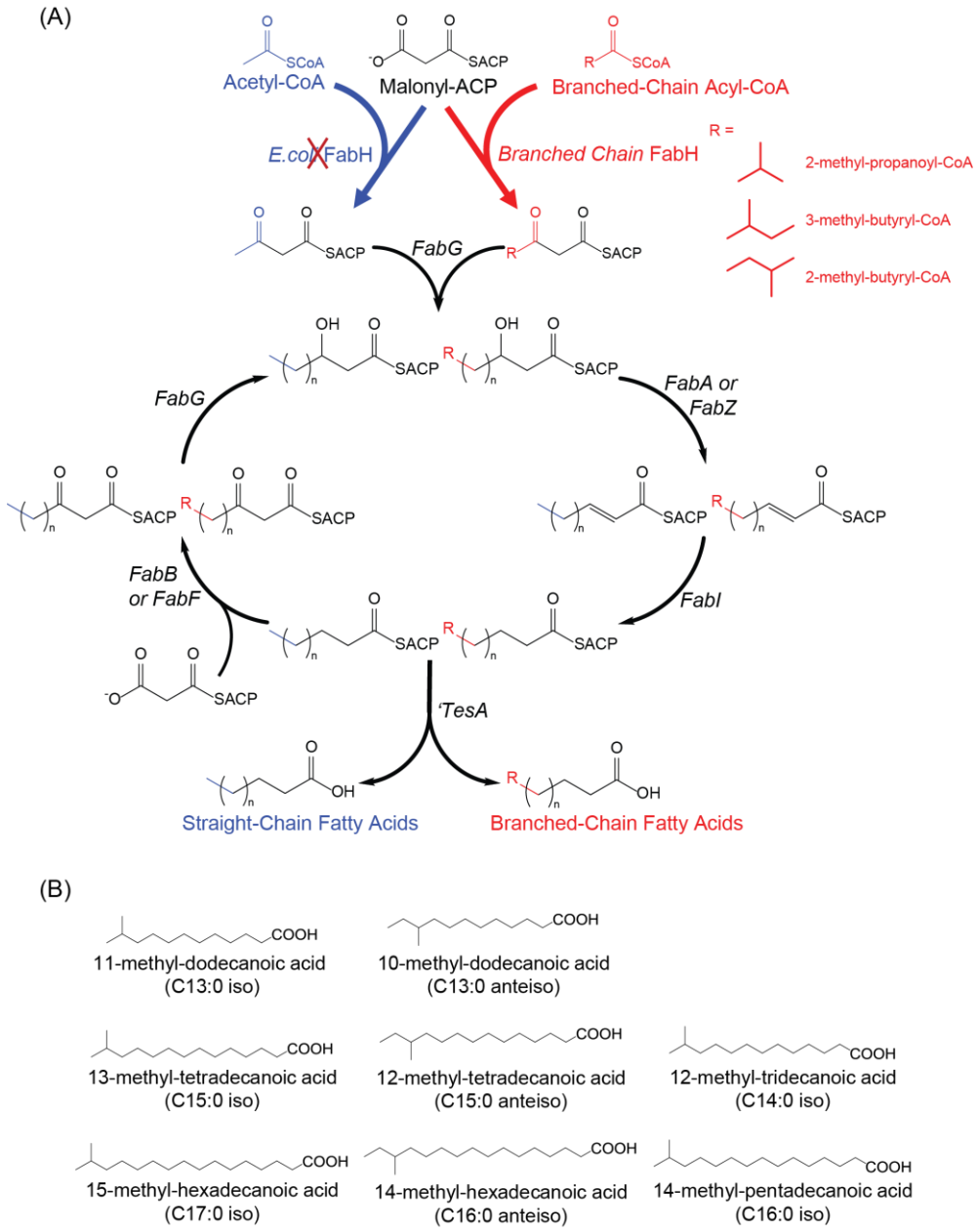

Figure 2- 1 SCFAs and BCFAs biosynthetic pathways

(A) Incorporation of branch groups (R) to fatty acids is determined by the substrate specificity of FabH. $_{Ec}$FabH (blue) uses acetyl-CoA as a substrate. Branched-chain-acyl-CoA-specific FabHs (red) preferentially use branched-chain acyl-CoAs as substrates. (B) BCFAs produced from this study.

Previous studies have shown that FabH plays a key role for the production BCFAs in some Gram-positive bacteria. While *E. coli* FabH ($_{Ec}$FabH) can only take acetyl-CoA, and to a lesser

extent, propionyl-CoA as substrates, some FabHs from Gram-positive bacteria such as *Bacillus subtilis, Listeria monocytogenes,* and *Staphylococcus aureus* use branched-chain acyl-CoAs (such as 2-methylpropanoyl-CoA) as starters [59]. Additionally, branched-chain acyl-CoAs can be synthesized from α-keto acids by the overexpression of a branched-chain α-keto acid dehydrogenases (BKD, encoded by the *bkd* operon) [54, 60-62]. Using such biochemistry, a BCFA biosynthetic pathway was recently constructed by overexpressing the *B. subtilis* BKD and FabH2 ($_{Bs}$FabH2) [63] (Figure 2-1A, red arrow). However, the engineered strain only produced a low fraction of equivalent BCFAs [63]. Instead, a significant proportion of equivalent SCFAs were co-produced, making it extremely difficult to separate the desired BCFAs from the predominant SCFA products. Thus, it is imperative to increase the proportion of BCFAs in total free fatty acids (FFAs).

I reasoned that the low BCFA titer and proportion are due to the competition of two FabHs for the same pool of substrate malonyl-ACP and the higher concentration of acetyl-CoA (substrate of $_{Ec}$FabH) compared to branched-chain acyl-CoAs (substrate of $_{Bs}$FabH2). In this chapter, the acetyl-CoA-specific *E. coli* FabH was replaced with a branched-chain-acyl-CoA-specific FabH to direct the carbon flux to the synthesis of BCFAs, enhancing BCFA titer by 81-fold compared to a strain containing both acetyl-CoA- and branched-chain-acyl-CoA-specific FabHs. Furthermore, the overexpression of BKD to synthesize branched-chain-acyl-CoA precursors was discovered toxic to *E. coli* due to depletion of protein lipoylation capacity. Engineering a complementary protein lipoylation pathway alleviated the toxicity and improved BCFA production to 276 mg/L and 85% of total free fatty acids, the highest BCFA titer and percentage to date. Finally, I achieved fine-tuning of BCFA branch positions by engineering the upstream pathway to control the supply

of branched-chain acyl-CoAs, eventually producing 181 mg/L BCFAs at 72% of total FFA from glucose.

2.2 Materials and Methods

2.2.1 Materials and Media

Phusion DNA polymerase was purchased from New England Biolabs (Beverly, MA, USA). Restriction enzymes, T4 ligase, gel purification kits, and plasmid miniprep kits were purchased from Thermo Scientific (Waltham, Massachusetts, USA). All primers were synthesized by Integrated DNA Technologies (Coralville, IA, USA). BCFA standards (Bacterial Acid Methyl Ester Mix), SCFA standards (GLC-20 and GLC-30) and all the other reagents were purchased from Sigma Aldrich (St. Louis, MO, USA).

Minimal medium (M9 medium supplemented with 75 mM MOPS at pH 7.4, 2 mM $MgSO_4$, 1 mg/L thiamine, 50 μg/mL lipoic acid, 10 μM $FeSO_4$, 0.1 mM $CaCl_2$ and micronutrients including 3 μM $(NH_4)_6Mo_7O_{24}$, 0.4 mM boric acid, 30 μM $CoCl_2$, 15 μM $CuSO_4$, 80 μM $MnCl_2$, and 10 μM $ZnSO_4$) containing 2% glucose as carbon source was used for cell growth and fatty acid production.

2.2.2 Plasmids and strains

Plasmids used in this study were listed in Table 2-1. Gene encoding *S. aureus* ($_{Sa}$FabH) was codon-optimized for *E. coli* expression and synthesized by Integrated DNA Technologies (Coralville, IA, USA), respectively, whereas other genes were amplified by PCR from templates. To create all plasmids (Table 3-1), the corresponding genes were assembled into the backbones of BioBrick plasmids [64], using either restriction sites, Golden-Gate DNA assembly method [65], or Gibson isothermal assembling method [66].

Table 2- 1 Plasmids used in Chapter 2

Plasmids	Replication ori	Overexpressed operon	Resistance	Refs
pA5a-tesA	pA15a	P_{lacUV5}-*tesA*(*E.coli*)	Amp^R	This chapter
pB5c-rfp	pBBR1	P_{lacUV5}-*rfp*	Cm^R	This chapter
pE1k-$_{Bs}$fabH2	ColE1	P_{Trc}-*fabH2*(*B.subtilis*)	Kan^R	This chapter
pB5c-bkd	pBBR1	P_{lacUV5}-*bkd*(*B.subtilis*)	Cm^R	This chapter
pB8k-$_{Bs}$fabH2	pBBR1	P_{BAD}-*fabH2*(*B.subtilis*)	Kan^R	This chapter
pE8c-bkd	ColE1	P_{BAD}-*bkd*(*B.subtilis*)	Cm^R	This chapter
pSa-P_{ecfabH}-$_{Bs}$fabH1	SC101	P_{ecfabH}-*fabH1*(*B.subtilis*)	Amp^R	This chapter
pSa-P_{ecfabH}-$_{Bs}$fabH2	SC101	P_{ecfabH}-*fabH2*(*B.subtilis*)	Amp^R	This chapter
pSa-P_{ecfabH}-$_{Sa}$fabH	SC101	P_{ecfabH}-*fabH* (*S.aureus*)	Amp^R	This chapter
pB5c-tesA-bkd	pBBR1	P_{lacUV5}-*tesA*(*E.coli*)-*bkd*(*B.subtilis*)	Cm^R	This chapter
pE8c-tesA-bkd	ColE1	P_{BAD}-*tesA*(*E.coli*)-*bkd*(*B.subtilis*)	Cm^R	This chapter
pE8k-lplA	ColE1	P_{BAD}-*lplA*(*E. coli*)	Kan^R	This chapter
pA5k-fadR-lplA	pA15a	P_{lacUV5}-*fadR-lplA* (*E. coli*)	Kan^R	This chapter
pE8c-tesA-mleuABCD	ColE1	P_{BAD}-*tesA-mleuABCD* (*E. coli*)	Cm^R	This chapter
pA6k-alsS-ilvCD	pA15a	$P_{LlacO-1}$- *alsS-ilvCD* (*E. coli*)	Kan^R	

E. coli DH10B was used for cloning purposes. *E. coli* strains DH1(*ΔfadE*) and CL111 [67] (a gift from Dr. John Cronan's Lab, University of Illinois at Urbana-Champaign) were used for fatty acid production. Strains BC11-13 were created by transforming the corresponding *fabH* plasmids into CL111 followed by deletion of the *Salmonella enterica* Serovar Typhimurium *fabH* ($_{Se}$*fabH*) using P1 transduction [67]. To created strain BC13(*ΔKan*), *Kan* antibiotic marker in the genome of CL111 strain was deleted using plasmid pCP20 [68]. Plasmid pSa-P_{ecfabH}-$_{Sa}$fabH was transformed into the *kan* deleted CL111 strain and the $_{Se}$*fabH* was knocked out by P1 transduction. Strain BC33 was created by integrating the *bkd* operon (*lpdV, bkdAA, bkdAB,* and *bkdB*) at the *fadE* locus in the genome under the control of a P_{LacUV5} promoter using a previously described technique [69], followed by transforming plasmid pSa-P_{ecfabH}-$_{Sa}$fabH and knocking out the $_{Se}$*fabH* by P1 transduction [67]. The corresponding plasmids were then transformed into different parental strains to yield all the production strains.

Table 2- 2 Strains used in Chapter 2

Strains	Relevant genotype	*fabH* gene	Reference
CL111	UB1005, attHK022::(*plsX'fabH*; *aadA*) *fabH*::kan	*Se**fabH*	[67]
BC01	DH1(*ΔfadE*) pB8k-$_{Bs}$fabH2, pE8c-bkd, pA5a-tesA	*Ec**fabH Bs**fabH2*	This chapter
BC02	DH1(*ΔfadE*) pE1k-$_{Bs}$fabH2, pB5c-bkd, pA5a-tesA	*Ec**fabH Bs**fabH2*	This chapter
SC01	DH1(*ΔfadE*) pA5a-tesA	*Ec**fabH*	This chapter
SC02	DH1(*ΔfadE*) pB5c-rfp, pA5a-tesA	*Ec**fabH*	This chapter
SC03	DH1(*ΔfadE*) pE8c-tesA-bkd	*Ec**fabH*	This chapter
BC11	CL111 (*plsX'fabH*; *aadA*)::Tet^A pSa-P$_{ecfabH}$-$_{Bs}$fabH2	*Bs**fabH2*	This chapter
BC12	CL111 (*plsX'fabH*; *aadA*)::Tet^A pSa-P$_{ecfabH}$-$_{Bs}$fabH1	*Bs**fabH1*	This chapter
BC13	CL111 (*plsX'fabH*; *aadA*)::Tet^A pSa-P$_{ecfabH}$-$_{Sa}$fabH	*Sa**fabH*	This chapter
BC10A	CL111 pSa-P$_{ecfabH}$-$_{Bs}$fabH2 pE8c-tesA-bkd	*Se**fabH Bs**fabH2*	This chapter
BC11A	CL111 (*plsX'fabH*; *aadA*)::Tet^A pSa-P$_{ecfabH}$-$_{Bs}$fabH2, pE8c-tesA-bkd	*Bs**fabH2*	This chapter
BC12A	CL111 (*plsX'fabH*; *aadA*)::Tet^A pSa-P$_{ecfabH}$-$_{Bs}$fabH1, pE8c-tesA-bkd	*Bs**fabH1*	This chapter
BC13A	CL111 (*plsX'fabH*; *aadA*)::Tet^A pSa-P$_{ecfabH}$-$_{Sa}$fabH, pB5c-tesA-bkd	*Sa**fabH*	This chapter
BC11L	CL111 ((*plsX'fabH*; *aadA*)::Tet^A, *△Kan,* pSa-P$_{ecfabH}$-$_{Bs}$fabH2, pB5c-tesA-bkd, pE8k-lplA	*Bs**fabH2*	This chapter
BC13L	CL111 (*plsX'fabH*; *aadA*)::Tet^A, *△Kan,* pSa-P$_{ecfabH}$-$_{Sa}$fabH, pB5c-tesA-bkd, pE8k-lplA	*Sa**fabH*	This chapter
BC13FL	CL111 (*plsX'fabH*; *aadA*)::Tet^A, *△Kan,* pSa-P$_{ecfabH}$-$_{Sa}$fabH, pE8c-tesA-bkd, pA5k-fadR-lplA	*Sa**fabH*	This chapter
BC30	CL111(*⊿kan*) *fadE*:: *$_{bs}$lpdV-$_{bs}$bkdAA-$_{bs}$bkdAB-$_{bs}$bkdB*	*Se**fabH*	This chapter
BC33	CL111(*⊿kan*) (*plsX'fabH*; *aadA*)::Tet^A *fadE*:: *$_{bs}$lpdV-$_{bs}$bkdAA-$_{bs}$bkdAB-$_{bs}$bkdB* pSa-P$_{ecfabH}$-$_{Sa}$*fabH*	*Sa**fabH*	This chapter
BC33C	CL111 (*plsX'fabH*; *aadA*)::Tet^A, *△Kan, fadE::bkd, ldhA::fadR-lplA,* pSa-P$_{ecfabH}$-$_{Sa}$fabH, pE8c-tesA-mleuABCD, pA6k-alsS-ilvCD	*Sa**fabH*	This chapter

2.2.3 Cell culturing and α-keto acids supplementation

Cells were pre-cultivated in LB medium with proper antibiotics. Overnight cultures were inoculated 2% v/v into M9 minimal medium (described in section 2.2.1) with corresponding

antibiotics for adaptation. Overnight cultures in minimal medium were then used to inoculate 5 mL of the same fresh minimal medium, with an initial OD_{600} of 0.08. When OD_{600} reached 0.8, cells were induced with proper inducers (1mM isopropyl β-D-1-thiogalactopyranoside (IPTG), 0.4% arabinose, and/or 200 nM anhydrotetracycline (aTc), or as otherwise specified). For α-keto acid supplementation experiments, one of the α-keto acids (3-methyl-2-oxobutyric acid, 3-methyl-2-oxopentanoic acid, or 4-methyl-2-oxopentanoic acid) was added at OD_{600} = 0.8 to a final concentration of 1 g/L. Cells were harvested three days after induction.

Cell growth curves were recorded on an Infinite F200PRO (TECAN) plate reader. Overnight LB cultures were used to inoculate modified M9 medium with 2% glucose. Overnight cultures were then used to inoculate 5 mL of the same fresh minimal medium with an initial OD_{600} of 0.08. Upon inoculation, 150 μl of the culture was aliquoted into a 96-well plate. The 5 mL culture was used for fatty acid quantification, while the 96-well plate was incubated inside the plate reader with shaking (218.3 rpm, 37 °C) to record cell growth. Relative cell density (in arbitrary units) was measured by monitoring absorption at 600 nm. Data were taken every 1500 s until cell cultures reached late stationary phase.

2.2.4 qRT-PCR

qRT-PCR was performed using a previously published method [70]. Strains DH1(*ΔfadE*), BC13 and BC13A were cultivated as described in section 2.2.3 and induced with 1 mM of IPTG and the supplementation of 1g/L 4-methyl-2-oxopentanoic acid. Total RNAs were extracted from exponentially growing cells in duplicate using TRIzol Max Bacterial RNA Isolation Kit (life technologies). Contaminating DNA was removed with RNase-free DNase I (Thermo Scientific), and cDNAs were synthesized using a Revert Aid First Strand cDNA Synthesis Kit (Thermo Scientific) with random hexamer primers following the manufacturer's protocol. The synthesized

cDNAs were normalized to 0.2 μg/μL, and 1 μL was amplified using the Power SYBR Green PCR Master Mix (Applied Biosystems) and primers specific to the genes of interest in a 20 μL reaction system. The reaction for each gene in each sample was performed in triplicates. qRT-PCR assays were carried out on an ABI7500 fast machine with the thermal cycling conditions recommended by the manufacturer. For data analysis, expression levels of the house keeping gene *dnaK* were used as a control for normalization between samples. Fold changes of genes of interest were calculated as $2^{-\Delta\Delta CT}$.

2.2.5 Quantification of the free fatty acids

Titers of free fatty acids were quantified using a previously published method [48]. Specifically, 1 mL of cell culture was acidified with 100 μL of concentrated HCl (12N). Free fatty acids were extracted twice with 0.5 mL ethyl acetate, which was spiked with 20 μg/mL of C19:0 fatty acid as an internal standard. The extracted fatty acids were methylated to fatty acid methyl esters (FAMEs) by adding 10 μL concentrated HCl, 90 μL methanol, and 120 μL of TMS-diazomethane, and incubated at room temperature for 15 min. FAMEs were quantified using a GC-MS (Hewlett-Packard model 7890A, Agilent Technologies) equipped with a 30 m DB5-MS column (J&W Scientific) and a mass spectrometer (5975C, Agilent Technologies) or a FID (Agilent Technologies) detector. For each sample, the column was equilibrated at 80 °C for 1 min, followed by a ramp to 280 °C at 30°C/min, and was then held at 280 °C for 3 min. Individual BCFA peaks were identified by comparing their retention time to those of standard BCFA methyl esters (Bacterial Acid Methyl Ester Mix, Sigma Aldrich) and by comparing their mass spectra to the Probability Based Matching (PBM) Mass Spectrometry Library. Concentrations of each fatty acid were determined by comparing the area of each FAME peak to a standard curve generated by standard FAME mixtures (GLC-20, GLC-30, and Bacterial Acid Methyl Ester Mix, Sigma Aldrich)

eluted using the same method. BCFA titer for each strain was measured in biological triplicate (starting from three different colonies) and average values are reported.

2.2.6 Western blotting and protein analysis

Whole culture, volume normalized by optical density at 600 nm, was incubated with loading buffer (2x Laemmli Sample Buffer (Bio-Rad) and β-mercaptoethanol) at 99ºC for 10 minutes with vigorous shaking. Then, 15 µl of whole culture lysates was loaded onto two 12% polyacrylamide denaturing gels and separated by electrophoresis. Gels were duplicated and run in parallel. One gel was then stained with Coomassie blue and the other was immunoblotted. For immunoblotting, protein was blotted to a polyvinylidine fluoride (PVDF) membrane using a standard protocol (Gallagher et al., 2008). Lipoate modified enzymes were detected using a rabbit-anti-lipoyl primary antibody (EMD-Millipore) followed by a goat-anti-rabbit secondary antibody conjugated to horseradish peroxidase (Santa Cruz Biotechnology). Stained membranes were imaged using a GE ImageQuant (LAS 4000 mini).

2.3 Results

2.3.1 Construction of BCFA biosynthetic pathway

I first constructed a BCFA biosynthetic pathway similar to previous work [63]. In detail, the *B. subtilis* BKD complex (encoded by *ipdV*, *bkdAA*, *bkdAB* and *bkdB*), $_{Bs}$FabH2, and a cytosolic *E. coli* thioesterase TesA (encoded by *'tesA*) were overexpressed in a *fadE* deleted *E. coli* DH1 background. The resulting strain (BC01) only produced 0.9% BCFAs at a titer of 2.7 mg/L (Figure 2-2). No significant increase in BCFA titer or proportion was observed even with the enhanced expression level of $_{Bs}$FabH2 by changing its promoter from a relative weak (about one third of expression level compared to standard) P_{BAD} (induced with 0.4% arabinose in the presence of 2%

glucose in the medium) to a very strong (about 4 times of expression level compared to standard) P_{trc} (induced with 1 mM of IPTG) [64] (from 2.7 mg/L, 0.9% in BC01 to 3.5 mg/L, 1.9% in BC02, Figure 2-2). In both cases, SCFAs were the dominant products (Supplementary Figure 2-1A). The low BCFA proportion is consistent with previous studies [63, 71].

2.3.2 Replacement of $_{Ec}$FabH with branched-chain-specific FabHs

The key enzyme for the production of SCFA *v.s.* BCFAs is FabH, which catalyzes the condensation of malonyl-ACP and acetyl-CoA in the case of SCFAs or the condensation of malonyl-ACP and a branched-chain acyl-CoA in the case of BCFAs. Overexpression of $_{Bs}$FabH2 in previously engineered *E. coli* strains resulted in two FabHs competing for malonyl-ACP [63, 71]. In these strains, the $_{Ec}$FabH may outcompete $_{Bs}$FabH2 because the specific activity of $_{Ec}$FabH to acetyl-CoA is 3-6 folds higher than the activity of $_{Bs}$FabH2 to branched-chain acyl-CoAs based on *in vitro* characterization [59]. Furthermore, acetyl-CoA is abundant in *E. coli* (0.61 mM) [72], but it is difficult to accumulate branched-chain acyl-CoAs to concentrations close to or higher than acetyl-CoA. As a result, SCFAs were produced predominantly (>98%) even when $_{Bs}$FabH2 was overexpressed from a strong promoter.

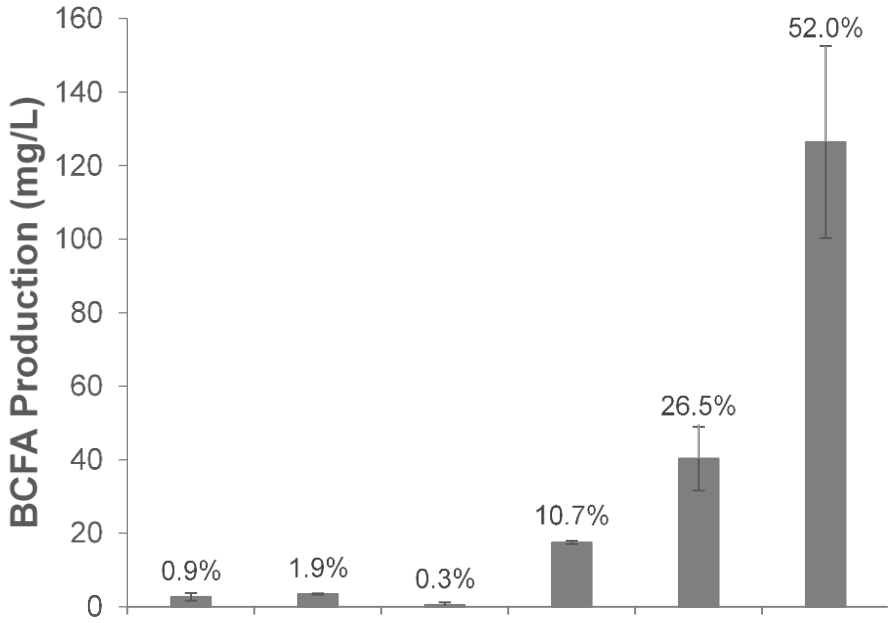

Strain name	BC01	BC02	BC10A	BC11A	BC13A	BC13A
fabH promoter	P_{BAD}	P_{trc}	P_{ecfabH}	P_{ecfabH}	P_{ecfabH}	P_{ecfabH}
$_{Ec}$FabH or $_{Se}$FabH	+	+	+	-	-	-
$_{Bs}$FabH2	+	+	+	+	-	-
$_{Sa}$FabH	-	-	-	-	+	+
α-keto acid supply	-	-	-	-	-	+

Figure 2- 2 BCFA titers produced by engineered E. coli strains in this study
$_{Ec}$FabH, $_{Se}$FabH, $_{Bs}$FabH2, and $_{Sa}$FabH are FabHs from *E. coli*, *S. enterica*, *B. subtilis*, and *S. aureus*, respectively. Cells were cultivated as described in Method. BCFA titers from biological triplicate were averaged. Numbers above the column indicate the proportions of BCFA over total FFA production.

I hypothesized that deletion of $_{Ec}$FabH (complete replacement of $_{Ec}$FabH by $_{Bs}$FabH2) will attenuate the synthesis of SCFAs. Although $_{Bc}$FabH2 also recognizes acetyl-CoA as a substrate, its specific activity to acetyl-CoA is 24% and 30% lower than that to 2-methylpropanoyl-CoA and 3-methylbutyryl-CoA, respectively [59]. However, direct replacement of $_{Ec}$FabH with a branched-chain-acyl-CoA-specific FabH is technically challenging because 1) *fabH* is essential for fatty acid biosynthesis [67], and 2) it is the second gene in a *fab* operon that contains several essential genes

in *E. coli* fatty acid biosynthesis [73]. To solve this problem, I used a previously engineered *E. coli* strain (CL111) [67], whose *fabH* was already replaced by an acetyl-CoA-specific *S. enterica fabH* (with similar activity with $_{Ec}$FabH) at the *att*$_{HK022}$ phage attachment site [67]. I cloned the *B. subtilis fabH2* (*$_{Bs}$fabH2*) 3' of the *E. coli fabH* promoter (P_{ecfabH}) to a low copy number plasmid (SC101 ori) and transformed the resulting plasmid pSa-P_{ecfabH}-$_{Bs}$fabH2 to CL111, leading to strain BC10 that have both *$_{Se}$fabH* and *$_{Bs}$fabH2* genes (Table 2-2). The *$_{Se}$fabH* in BC10 was then removed by a genetic manipulation that involved P1 transduction of a Tn10 transposon near the *att*$_{HK022}$ attachment site to yield strain BC11 that contained *$_{Bs}$fabH2* as the only *fabH* gene. Both BC10 and BC11 were transformed with a plasmid encoding BKD and TesA (pE8c-tesA-bkd), resulting in strains BC10A and BC11A, respectively. When cultivated under the same condition, strain BC11A produced 17.5 mg/L of BCFAs, which is 35-fold higher than the strain with both *$_{Se}$fabH* and *$_{Bs}$fabH2* (BC10A, 0.5 mg/L, Figure 2-2). The BCFA proportion was also increased to 11%, 43-fold higher than that of BC10A.

I then used the *fabH* replacement method to test two more FabHs ($_{Bs}$FabH1, $_{Sa}$FabH), whose specificity to branched-chain acyl-CoAs are even higher than $_{Bs}$FabH2 [59, 74]. Strain BC12A expressing $_{Bs}$FabH1 (encoded by *$_{Bs}$fabH1* gene), BKD, and TesA produced 19.4 mg/L of BCFAs, representing 39-fold increase as compared to BC10A. More interestingly, strain BC13A expressing $_{Sa}$FabH (encoded by *$_{Sa}$fabH* gene), BKD, and TesA produced 40.3 mg/L of BCFAs, corresponding to 81-fold enhancement from BC10A (Figure 2-2). Even compared to strain BC01 which cannot undergo β-oxidation, the BCFA titer of strain BC13A is 15-fold higher. The proportion of BCFAs was also increased to 29% and 27% in strains BC12A and BC13A, respectively. In general, the engineered strains produced a variety of BCFAs with chain length

spanning from C13 to C17 and carrying different terminal structures (iso and anteiso) (Figure 2-1B).

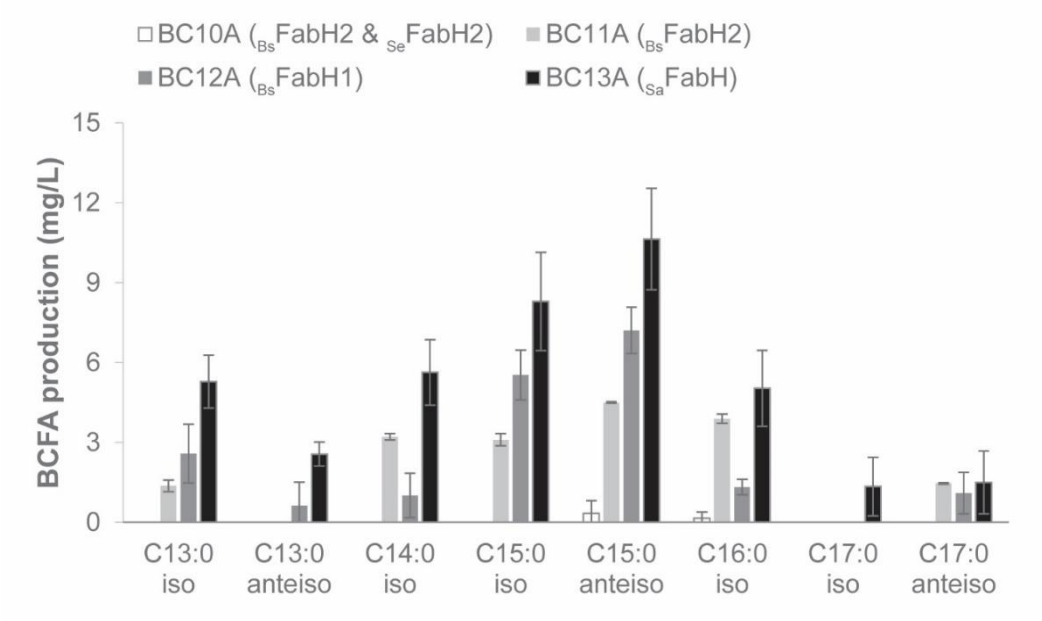

Figure 2- 3 Effects of FabH replacement on BCFA production
Cells were cultivated as described in Methods. BC10A-BC12A were induced with 0.4% arabinose while BC13A was induced with 1 mM IPTG.

Next, BCFA profiles of these strains were analyzed. Although strains BC11A-BC13A expressing different FabHs, their BCFA profiles are similar: C15:0-anteiso-FA is the most abundant BCFA following by either C15:0-iso- or C16:0-iso-FA (Figure 2-3). However, *in vitro* characterization of these FabHs showed different preference towards acyl-CoA substrates [74]. For example, the activity of $_{Bs}$FabH1 to 2-methylbutyryl-CoA was 10-fold higher than 3-methylbutyryl-CoA, whereas the activity of $_{Bs}$FabH2 was 2-fold higher than that to 3-methylbutyryl-CoA [59]. The inconsistency between the *in vitro* FabH specificities and *in vivo* BCFA profiles strongly indicated that BCFA production in the engineered strains was limited by the branched-chain acyl-CoAs supply.

2.3.3 Supplementation of α-keto acids

In the engineered strains, branched-chain acyl-CoAs are biosynthesized by BKD from branched-chain α-keto acids (3-methyl-2-oxobutyric acid, 4-methyl-2-oxopentanoic acid, and 3-methyl-2-oxopentanoic acid), which are naturally produced as precursors for the biosynthesis of valine, leucine and isoleucine, respectively. The intracellular α-keto acids pool might be limited because biosynthesis of branched amino acids is heavily feedback regulated in *E. coli* [75-77]. Thus, it is possible that the production of BCFAs was limited by the supply of branched-chain α-keto acids. To test these hypotheses, I supplemented each of the following α-keto acids: 3-methyl-2-oxobutyric acid (converted 2-methylpropanoyl-CoA), 4-methyl-2-oxopentanoic acid (converted 3-methylbutyryl-CoA), and 3-methyl-2-oxopentanoic acid (converted 2-methylbutyryl-CoA), to strains BC11A-BC13A and tested their BCFA productions.

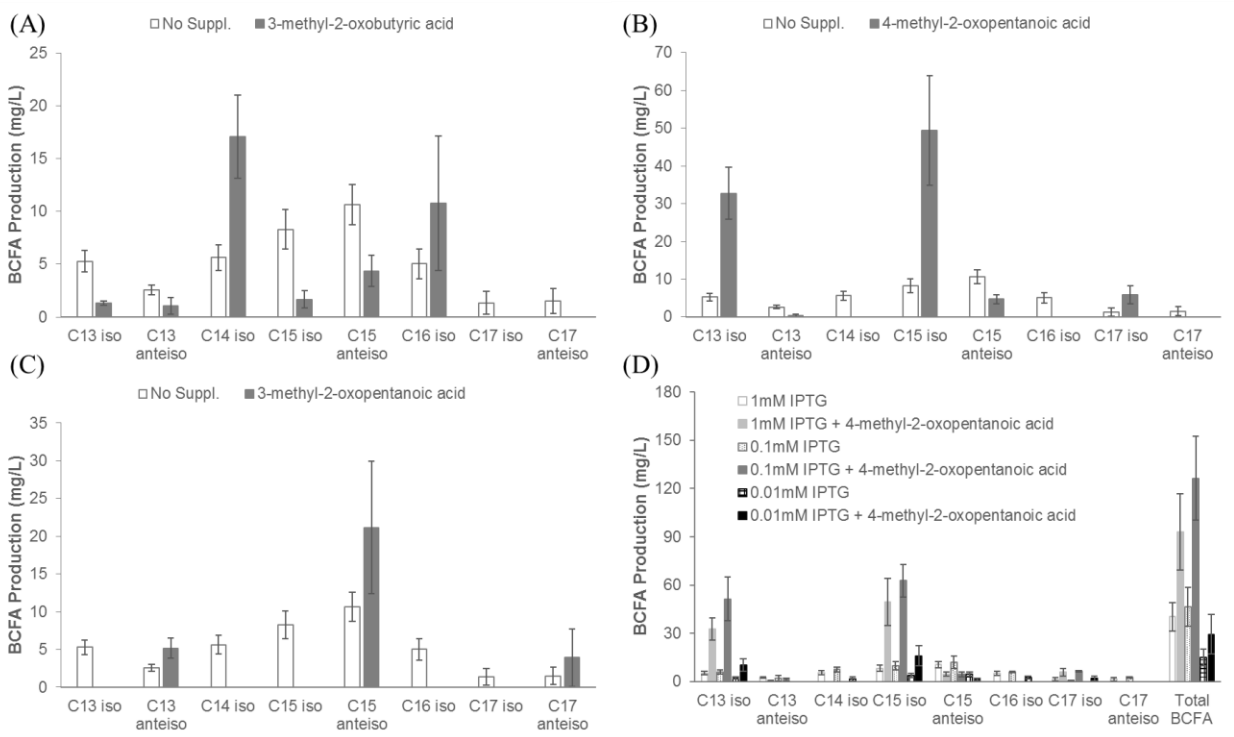

Figure 2- 4 Effect of α-keto acid supplementation to BCFA productions
Strain BC13A (containing $_{Sa}$FabH) was cultivated as described in Methods and induced with 1 mM of IPTG. At the moment of induction, cell cultures were supplemented with 1 g/L of either 3-methyl-2-oxobutyric acid (A, solid columns), 4-methyl-2-oxopentanoic acid (B, solid columns), 3-methyl-2-oxopentanoic acid (C, solid columns), or nothing (A-C, empty columns). (D) BC13A cell cultures were titrated with varied IPTG concentrations.

Supplementation of 1 g/L of 3-methyl-2-oxobutyric acid, 4-methyl-2-oxopentanoic acid, and 3-methyl-2-oxopentanoic acid to strains BC11-13A significantly enhanced the production of even-chain-iso-FAs, odd-chain-iso-FAs, and odd-chain-anteiso-FAs, respectively (Figure 2-4&5, Supplementary Figure 2-2&3), confirming that supply of branched-chain acyl-CoAs (more specifically, α-keto acids) limited the synthesis of BCFAs. The specific enhancement also confirmed that BCFAs were produced through the designed pathways. Interestingly, I observed that supplementation of each α-keto acid also inhibited the production of BCFAs derived from the other two α-keto acids (Figure 2-4, Supplementary Figure 2-2&3), presumably due to the

competition of α-keto acids for available BKD activity. These results indicated that the conversion of α-keto acids to branched-chain acyl-CoAs is a rate-limiting step for the engineered strains when supplied with 1 g/L of α-keto acids. The cross-inhibition also demonstrated that the composition of BCFAs can be controlled by the supply of α-keto acids. For example, when 4-methyl-2-oxopentanoic acid was supplemented to the culture of BC13A (carrying $_{Sa}$FabH), odd-chain-iso-FAs were produced as the predominant BCFAs (95%, Figure 2-4B). On the other hand, when 3-methyl-2-oxopentanoic acid was supplemented to the culture of BC13A, odd-chain-anteiso-FAs were produced as the predominant BCFAs (>99%, Figure 2-4C). Among the tested conditions, supplementing 4-methyl-2-oxopenoate to BC13A produced the highest BCFA titer, 93 mg/L, and the highest BCFA proportion, 43% (Figure 2-5).

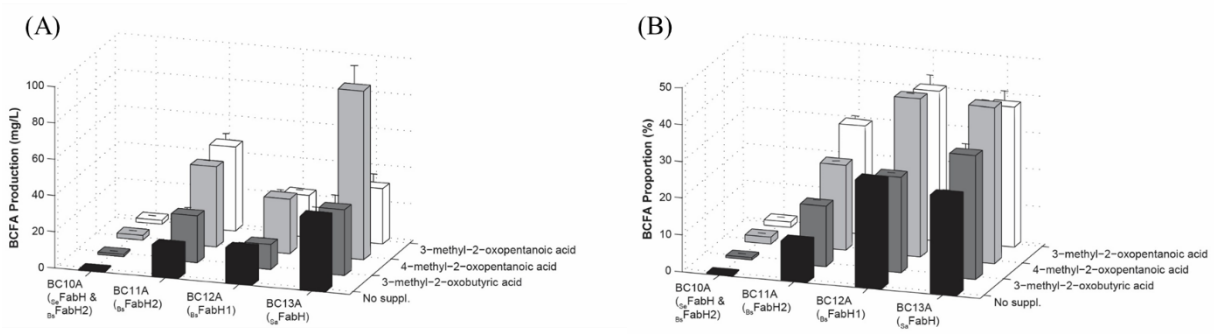

Figure 2- 5 Total BCFA titers (A) and proportions (B) for strains BC11-13A with and without α-keto acid supplementation.

Next, the transcriptional responses to the replacement of *E. coli* native *fabH* with other *fabHs* was investigated. The transcription levels of *fabD* and *fabG*, two downstream genes in the *fab* operon, were analyzed by qRT-PCR (Figure 2-6). Compared to the wide type strain DH1 (*ΔfadE*), the transcription levels of both *fabD* and *fabG* were lower in strain BC13 and BC13A, suggesting that the *fabH* replacement affected the transcription of downstream genes. This might give some explanation for the relatively low total fatty acid production in the engineered strain. However, the

expression level of *fabD* increased in strain BC13A compared to that in strain BC13 (Figure 2-6), likely results from the overexpression of *tesA*. Because the increased acyl-CoA concentration due to the accumulation free fatty acids will help activate FadR expression, which can further activate the P_{fabH} promoter.

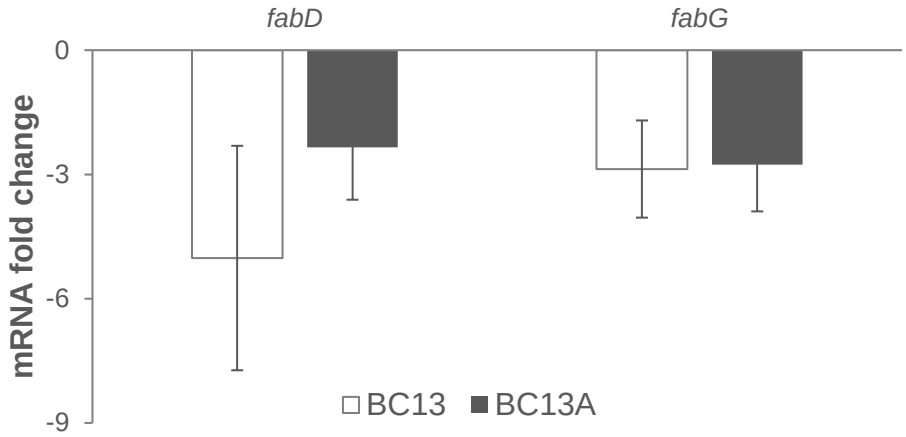

Figure 2- 6 Fold changes of transcription levels of *fabD* and *fabG* in strain BC13 and BC13A compared to wide type strain DH1(*ΔfadE*)

2.3.4 Heterologous BKD expression restricts lipoylation of *E. coli* native 2-oxoacid dehydrogenases

I further titrated the culture of BC13A with varying concentrations of inducer IPTG to find the optimal expression level for TesA and BKD. The highest BCFA titer was obtained when 0.1 mM of IPTG was used, yielding 126 mg/L BCFAs, corresponding to 52% of the total FFAs (Figure 2-4D, Supplementary Figure 2-1B). In contrast, induction with 1 mM IPTG caused stress to the cell and led to modification to the plasmid encoding the BKD and TesA (data not shown).

Next, the impact of BKD and/or TesA overexpression on cell growth and free fatty acid (FFA) production was elucidated individually. To start with, I constructed a FFA-overproducing strain, SC01 by overexpressing TesA in DH1 (*ΔfadE*). The overexpression of *bkd* operon was introduced

to strain SC01, resulting in strain SC03. BKD overexpression significantly reduced cell growth when compared to strain SC03, $p<0.01$ (Figure 2-7A). Expression of a red fluorescent protein (RFP, strain SC02) did not affect cell growth, indicating that the impaired cell growth was likely not caused by metabolic burden from protein expression. When strains SC01 and SC03 were cultivated for FFA production, a significant reduction in total FFA occurred with BKD overexpression, indicating that BKD expression also inhibits total FFA production (Figure 2-7B).

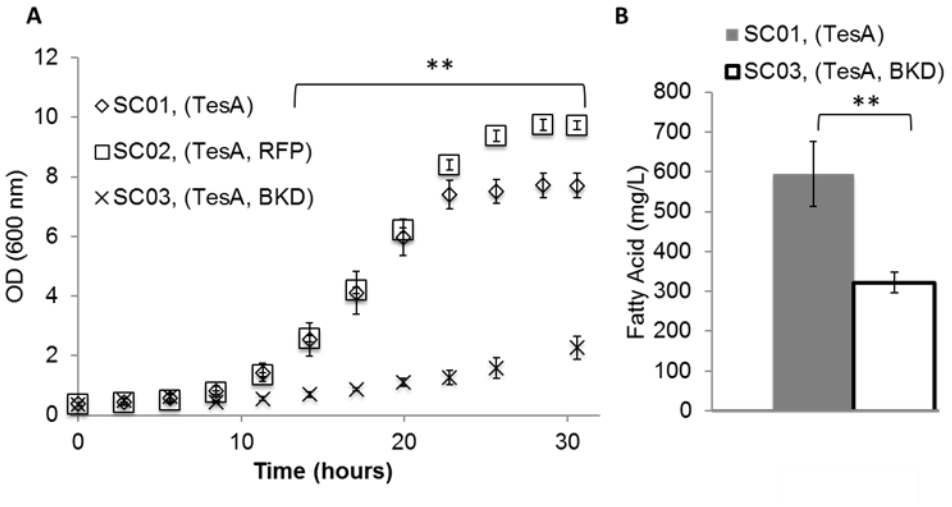

Figure 2- 7 Expression of BKD reduces cell growth and free fatty acid production
(A) Growth of fatty acid-overproducing strains with (SC03) or without (SC01) BKD overexpression ($p<0.01$, Student's T-test). (B) Overexpression of BKD reduced free fatty acid (FFA) production ($p<0.01$). Data generated by and figure courtesy of Dr. Gayle Bentley.

In the quest to understand the observed BKD toxicity, I examined the highly conserved OADH enzyme class. Previous work determined that overexpression of the PDH E2 subunit in *E. coli* repressed PDH activity, suggesting that *E. coli* has limited protein lipoylation capacity [78]. Expression of heterologous BKD requires lipoylation of its E2 subunit, which might similarly deplete the cellular lipoylation capability, leading to unlipoylated PDH and OGD in addition to under-lipoylated BKD (Figure 2-8A, Panel ii). Because both PDH and OGD contribute to central metabolism, I hypothesized that BKD overexpression without expanded lipoylation capacity

restricts lipoylation of PDH and OGD (Figure 2-8A, ii), resulting in the observed growth defect and reduced fatty acid production (Figure 2-7).

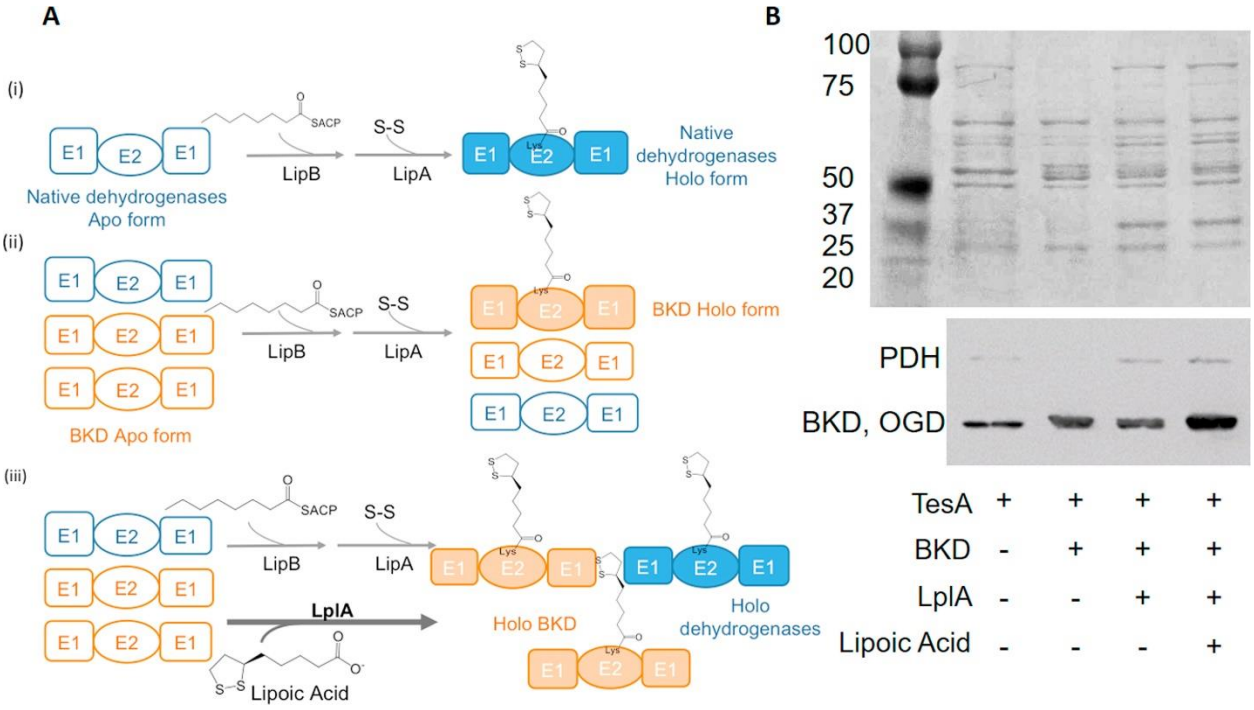

Figure 2- 8 Expression of BKD reduces lipoylation of native 2-oxoacid dehydrogenases (OADHs)
(A) Model illustrating the proposed mechanism of BKD toxicity. (i) Native 2-oxoacid dehydrogenases (OADHs, blue) are lipoylated for proper function. (ii) When BKD (yellow) is overexpressed, protein lipoylation capability is depleted, leading to unlipoylated OADHs. (iii) OADHs can be fully lipoylated through the overexpression of LplA, which ligates lipoic acid to the E2 subunit of each OADH. (B) Top, 12% SDS-PAGE gel stained with Coomassie blue; bottom, Western Blot of the same samples blotted using an anti-lipoyl monoclonal antibody. Conditions for each Western sample are listed beneath each lane. Data generated by and figure courtesy of Dr. Gayle Bentley.

To test my hypothesis, whole cell lysates of strains with (SC03) or without BKD (SC01) overexpression were analyzed by SDS-PAGE and Western Blot using an anti-lipoyl-protein monoclonal antibody (Figure 2-8B). Without BKD, I observed lipoylated proteins corresponding to the molecular weights of the PDH E2 subunit (62 kDa) and the OGD E2 subunit (44 kDa, lane 1 in Figure 2-8B). Strain SC03 with BKD overexpression showed a strong lipoyl-protein band

corresponding to the size of the BKD E2 subunit (45 kDa, cannot be resolved with the 44 kDa OGD E2), but the previously visible band of lipoylated-PDH E2 disappeared (Lane 2 in Figure 2-8B). Overall, this data revealed that BKD overexpression depletes lipoylation of *E. coli* native OADHs, leading to impaired cell growth (Figure 2-7A) and reduced FA production (Figure 2-7B).

2.3.5 Engineering a protein lipoylation pathway restores OADH lipoylation, allowing BCFA production in high percentages

I hypothesized that the protein lipoylation deficiency caused by BKD overexpression could be overcome by engineering a protein lipoylation pathway. *E. coli* utilizes two pathways for protein lipoylation (Figure 2-9). The first pathway synthesizes lipoate *de novo*, for which an octanoyl moiety from octanoyl-ACP is transferred to an E2 subunit, followed by insertion of two sulfur atoms into the octanoyl side chain of an octanolyated E2 subunit, forming a five membered ring (Figure 2-9, red arrows) [79-82]. Alternatively, exogenous lipoic acid can be ligated directly to an E2 subunit by lipoyl ligase A (LplA, encoded by *lplA*) (Figure 2-9, blue arrow) [83-85]. To test the hypothesis, a strain was engineered to utilize exogenous lipoic acid, in order to maximize the availability of octanoyl-ACP for fatty acid elongation. The *lplA* gene was cloned under the control of a P_{BAD} promoter and transformed to strain BC11A, resulting in strain BC11L. Overexpression of LplA on a plasmid partially improved PDH lipoylation (Lane 3 in Figure 2-8B). Completing the lipoylation pathway via lipoic acid supplementation further improved PDH E2 and BKD E2 lipoylation (Lane 4 in Figure 2-8B), demonstrating that the engineered pathway improved lipoylation of not only PDH, but also BKD and ODH.

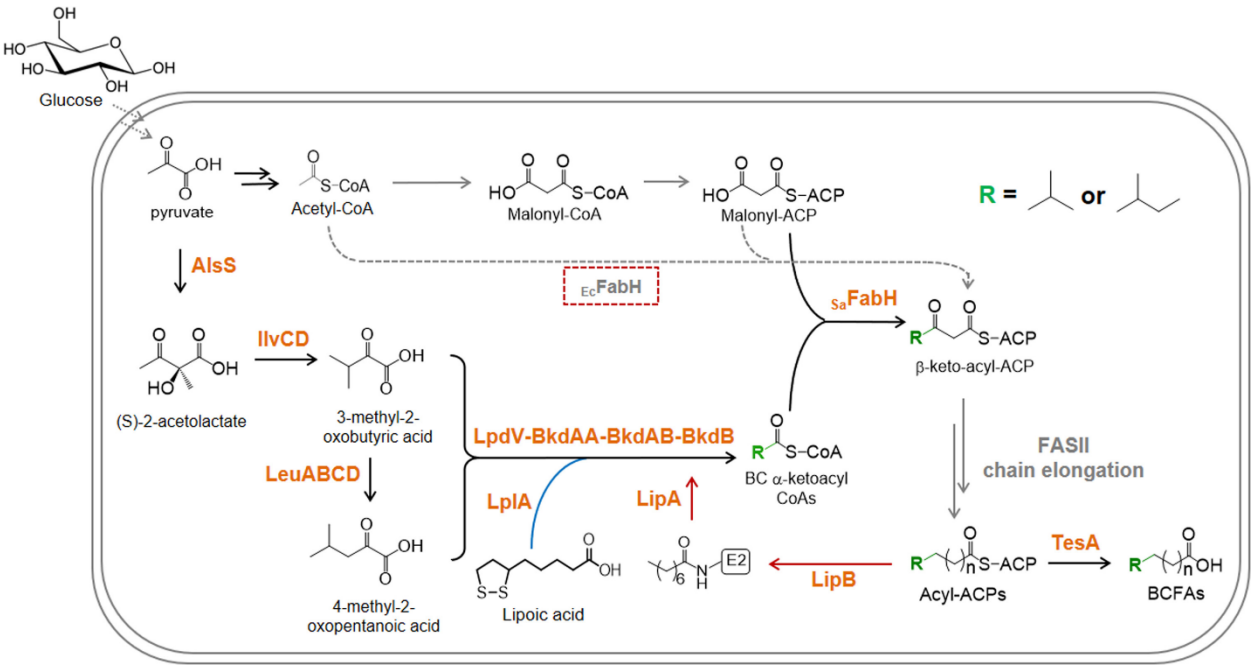

Figure 2- 9 Engineered pathway for the production of high percentage branched-chain fatty acids (BCFAs) in *E. coli*
The percentage of BCFA products can be dramatically enhanced by engineering protein lipoylation, either through an endogenous pathway (overexpression of LipB and LipA) or an exogenous pathway (LplA overexpression in combination with lipoic acid supplement). Cellular branched-chain α-ketoacid precursors can be enriched by engineering a branched-chain amino acid biosynthesis pathway (eg. AlsS, IlvCD, and LeuABCD). Data generated by and figure courtesy of Dr. Gayle Bentley.

Then I tested whether lipoylation restoration could increase BCFA titer and percentage. Without lipoic acid supplementation, strain BC11L produced 49 mg/L BCFA, statistically indistinguishable from its parental strain lacking plasmid LplA (BC11A, Figure 2-10A). Supplementing lipoic acid in the BC11L culture dramatically improved BCFA production by 4-fold, reaching 200 mg/L and 81% compared to 29% BCFA without plasmid LplA (BC11A, Figure 2-10A). BCFA production alone in BC11L surpassed total FFA in the parental strain BC11A, suggesting that lipoylation additionally improved cellular capacity for fatty acid production, presumably by improving cell fitness through native OADH lipoylation. Among the produced BCFAs, odd-chain-iso FAs, 11-methyldodecanoic acid (C13 iso) and 13-methyltetradecanoic acid

(C15 iso), are the major products, individually representing 34% and 53% of total FFAs, respectively (Figure 2-10B). Lipoic acid added to a strain lacking LplA (BC11A) did not affect fatty acid production (data not shown). Furthermore, leaky expression of LplA (without arabinose, P_{BAD}-*lplA*) restored BCFA production to the same level as with fully induced LplA, consistent with its role as a protein-modifying enzyme rather than a metabolic enzyme (data not shown). Similarly, when $_{Sa}$FabH was used instead of $_{Bs}$FabH2, BCFA production was improved with LplA overexpression (Strain BC13L; 220 mg/L, 79% BCFA) compared to the parental strain lacking LplA (Strain BC13A; 126 mg/L, 56% BCFA) (Figure 2-10C&D). Expression of FadR, a global regulator of fatty acid biosynthesis [48, 86], further increased BCFA production to 276 mg/L and 85% of total FFA (Strain BC13FL, Figure 2-10C&D). Overall, the results demonstrated that engineering the protein lipoylation pathway promotes native OADH and BKD lipoylation, leading to enhanced BCFA production and a significant increase in BCFA percentage.

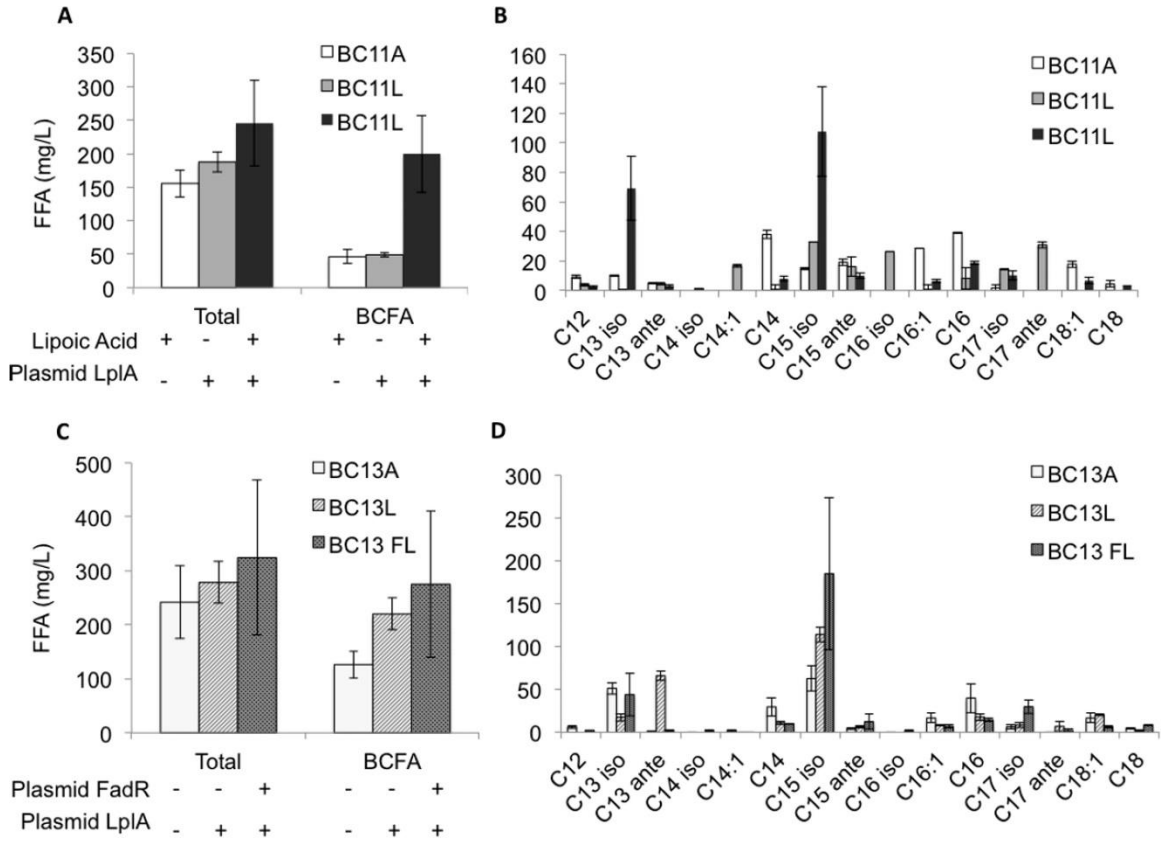

Figure 2- 10 LplA expression with lipoic acid supplementation increases BCFA production
(A) FFA production from strains expressing $_{Bs}$FabH2 as the sole FabH. Strain BC11A was modified to overexpress LplA (BC11L) (B) fatty acid species produced by each strain, under the same condition as the bar in (A). (C), (D) Strains expressing the $_{Sa}$FabH as the sole FabH. Strain BC13A was engineered to express a plasmid LplA, generating strain BC13L. Expression of FadR in strain BC13L generates strain BC13FL. All cultures (C), (D) were supplemented with 50 mg/L lipoic acid. All cultures (A)–(D) were supplemented with 1 g/L 4-methyl-2-oxopentanoate. Data generated by and figure courtesy of Dr. Gayle Bentley.

I next supplemented different kinds of α-keto acids to tailor the chain structures of produced BCFAs. The highest performing strain, BC13FL, was cultured and supplemented with 1 g/L 3-methyl-2-oxobutyric acid, 4-methyl-2-oxopentanoic acid, or 3-methyl-2-oxopentanoic acid. BCFA production strictly mirrored the branch structure of the supplemented α-ketoacid, generating even-chain-iso, odd-chain-iso, and odd-chain-anteiso fatty acids as the major products, respectively (Figure 2-11). Under all conditions, BCFA production exceeded 83% of total FFA.

Specifically, when supplemented with 4-methyl-2-oxopentanoic acid, 93% of BCFA were odd-chain-iso fatty acids. Likewise, when supplemented with 3-methyl-2-oxopentanoic acid or 3-methyl-2-oxobutyric acid, 93% and 74% of BCFA produced were odd-chain-anteiso or even-chain-iso fatty acids, respectively.

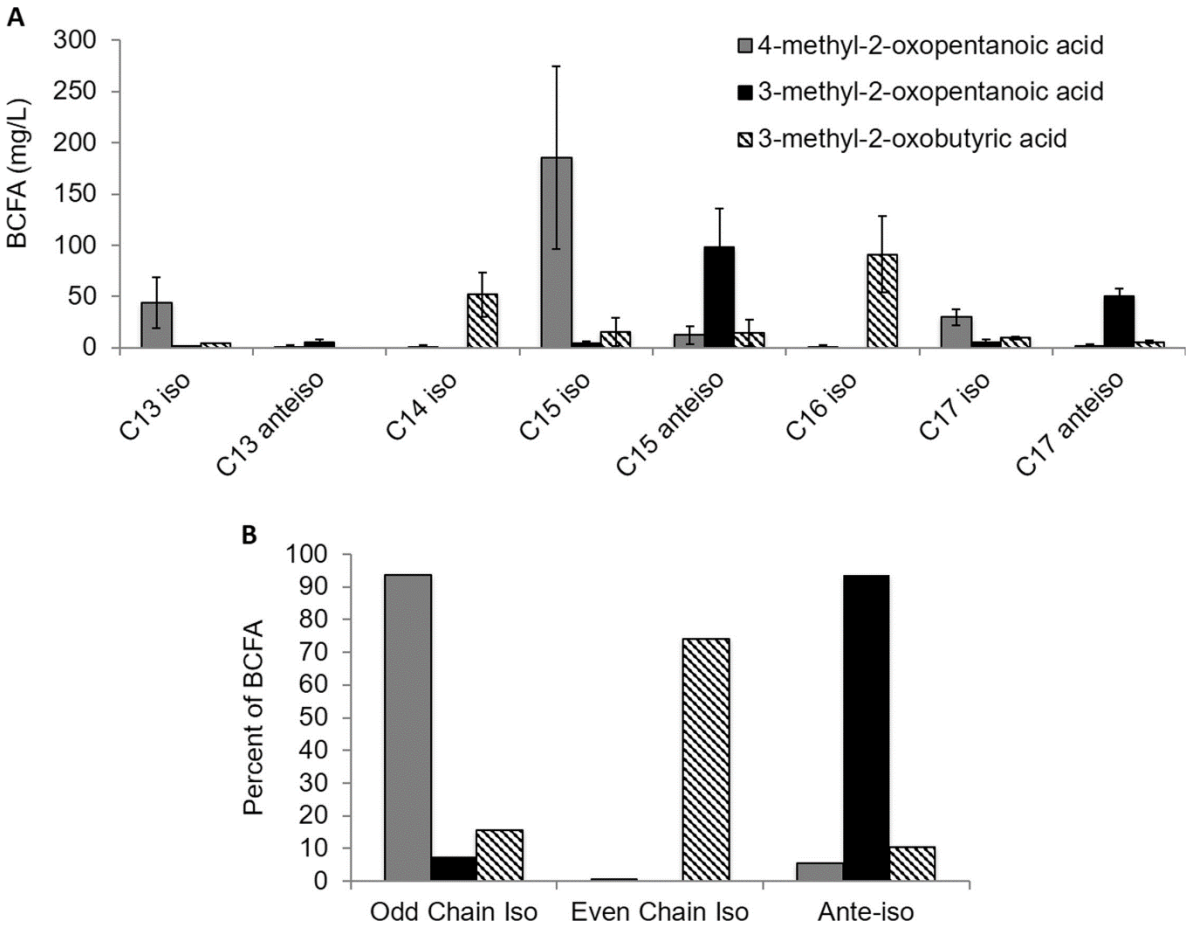

Figure 2- 11 Production of high percentage even chain iso, odd chain iso, and ante-iso BCFA species

Strain BC13FL was supplemented with 1 g/L of 4-methyl-2-oxopentanoic acid, 3-methyl-2-oxopentanoic acid, or 3-methyl-2-oxobutyric acid, separately. (A) FFA profiles of the strain under each cultivation condition are shown. (B) Percent of BCFAs corresponding to each branch position with the corresponding α-ketoacid shown in (A). Data generated by and figure courtesy of Dr. Gayle Bentley.

2.3.6 Production of BCFA from glucose

After releasing the lipoylation bottleneck, I attempted to generate BCFA from glucose by engineering the branched-chain amino acid pathway to enrich for branched-chain α-ketoacid precursors (Figure 2-9). In order to accommodate additional genes required for the branched-chain amino acid pathway, several operons were integrated into the genome at strategically selected integration loci to simultaneously eliminate competing pathways. I first integrated the *bkd* operon at the *fadE* locus to reduce potential metabolic burden caused by BKD overexpression and to prevent potential BCFA consumption in β-oxidation. Next, a synthetic operon containing *fadR-lplA* was integrated at the *ldhA* locus to direct flux away from D-lactate production. Meanwhile, the *B. subtilis alsS* and the *E. coli ilvCD* gene clusters were expressed to convert pyruvate to 3-methyl-2-oxobutyric acid (Figure 2-9). An engineered *E. coli leuABCD* operon carrying a feedback-resistant *leuA* was expressed together with *tesA* to convert 3-methyl-2-oxobutyric acid to 4-methyl-2-oxopentanoic acid [87]. Overall, the resulting strain BC33L overexpressed 15 enzymes and produced 181 mg/L BCFAs from glucose, comprising 71% of total FFA (Figure 2-12A&B). As expected, 13-methyl-tetradecanoic acid (C15 iso) was the major FA species (72% of the BCFA) due to the accumulation of 4-methyl-2-oxopentanoic acid.

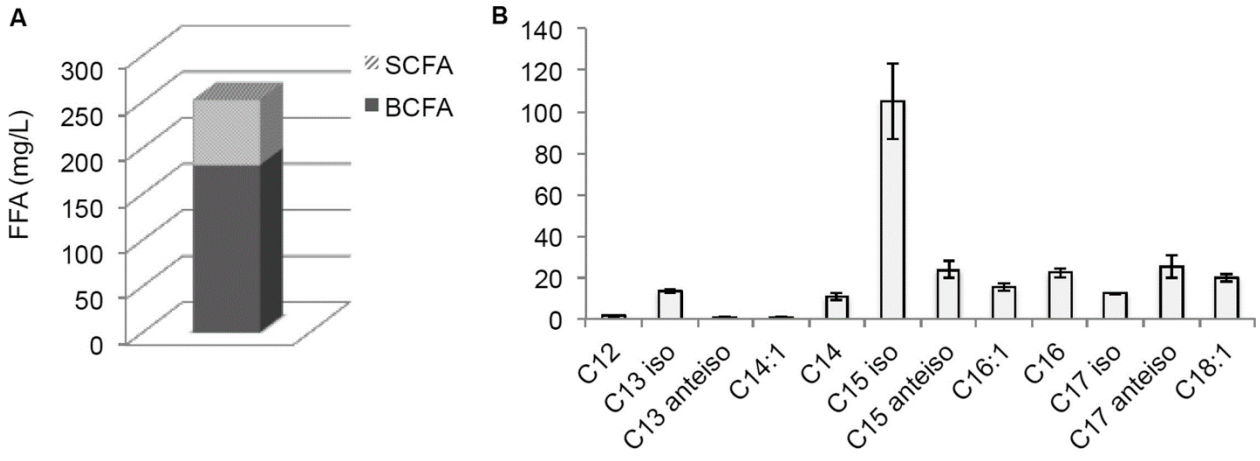

Figure 2- 12 Production of BCFA from glucose
Strain BC33C contains an engineered 4-methyl-2-oxopentanoic acid-producing pathway to generate BCFA from glucose (A) Percent composition of straight chain fatty acid (SCFA) and BCFA of strain BC33C (B) Free fatty acid species produced by strain BC33 from glucose. Data generated by and figure courtesy of Dr. Gayle Bentley.

2.4 Discussion

Previously, several groups attempted to engineer *E. coli* to produce BCFAs, but the highest BCFA percentage was 20% [71], implying a limit to the percentage of BCFA that can be produced in *E. coli*, a strictly SCFA-producing organism. In this chapter, I have demonstrated the capability to engineer *E. coli* to generate a high percentage of BCFA. By the deletion of *E. coli* native *fabH*, I have increased the BCFA proportions (strain BC13A, 52% in the presence of 4-methyl-2-oxopentanoic acid) without sacrificing BCFA titers. Furthermore, I demonstrated that incomplete protein lipoylation restricted previous BCFA production and a high percentage of BCFA (85% of total FFA) can be produced in *E. coli* by engineering its protein lipoylation pathway. Production of a high proportion of BCFA is key to improve the property of FA-derived fuels because separation of BCFAs from SCFAs represents significant technical challenges. These approaches provide a complementary strategy to other engineering efforts.

Furthermore, while branched-chain-acyl-CoA-specific FabH is essential for incorporating branches to FAs, I found its overexpression in the presence of $_{Ec}$FabH did not increase BCFA production (strain BC02 compared to BC01). In fact, when $_{Bs}$FabH2 expression level was increased by changing from a medium strength promoter (P_{BAD} in the presence of 0.4% arabinose and 2% glucose) to a strong promoter (P_{trc} induced with 1 mM IPTG), total FFA titer decreased (from 284 mg/L to 183 mg/L). This observation is consistent with previous findings where FabH at concentrations higher than other FASII enzymes inhibited fatty acid production from an *in vitro* reconstructed FASII [88]. Similar inhibition of total FA production by $_{Bs}$FabH2 was also observed during the development of strain JBEI-7802. Although FASII enzymes are expressed as separate polypeptide chains, effects of relative protein concentrations to FA production suggests interaction between FASII proteins, probably in a fashion similar to the integrated type I FAS. Optimizing the expression level of branched-chain-acyl-CoA-specific FabHs might alleviate such inhibition, further enhancing BCFA production.

2.5 Conclusion

In general, I have demonstrated that replacing the acetyl-CoA-specific FabH with one of the three tested branched-chain-acyl-CoA-specific FabHs increased the titer of BCFAs up to 81-fold relative to the strain containing both FabHs and engineering a protein lipoylation pathway restored protein lipoylation and further increased the biosynthesis of BCFA. Moreover, even-chain-iso, odd-chain-iso, and odd-chain-anteiso fatty acids can be separately produced by supplying 3-methyl-2-oxobutyric acid, 4-methyl-2-oxopentanoic acid, and 3-methyl-2-oxopentanoic acid to growth media, respectively, indicating the capability to control the terminal group of FAs. Engineering the 4-methyl-2-oxobutyric acid biosynthetic pathway allowed producing odd-chain-iso fatty acids at up to 181 mg/L, and BCFA percentage up to 79% from glucose. As BCFAs

are important precursors for the production of biofuels with improved cold flow properties, the method to increase BCFA production by replacing $_{Ec}$FabH and engineering a protein lipoylation pathway should open new venues for efficient production of advanced biofuels derived from BCFAs.

Supplementary Materials

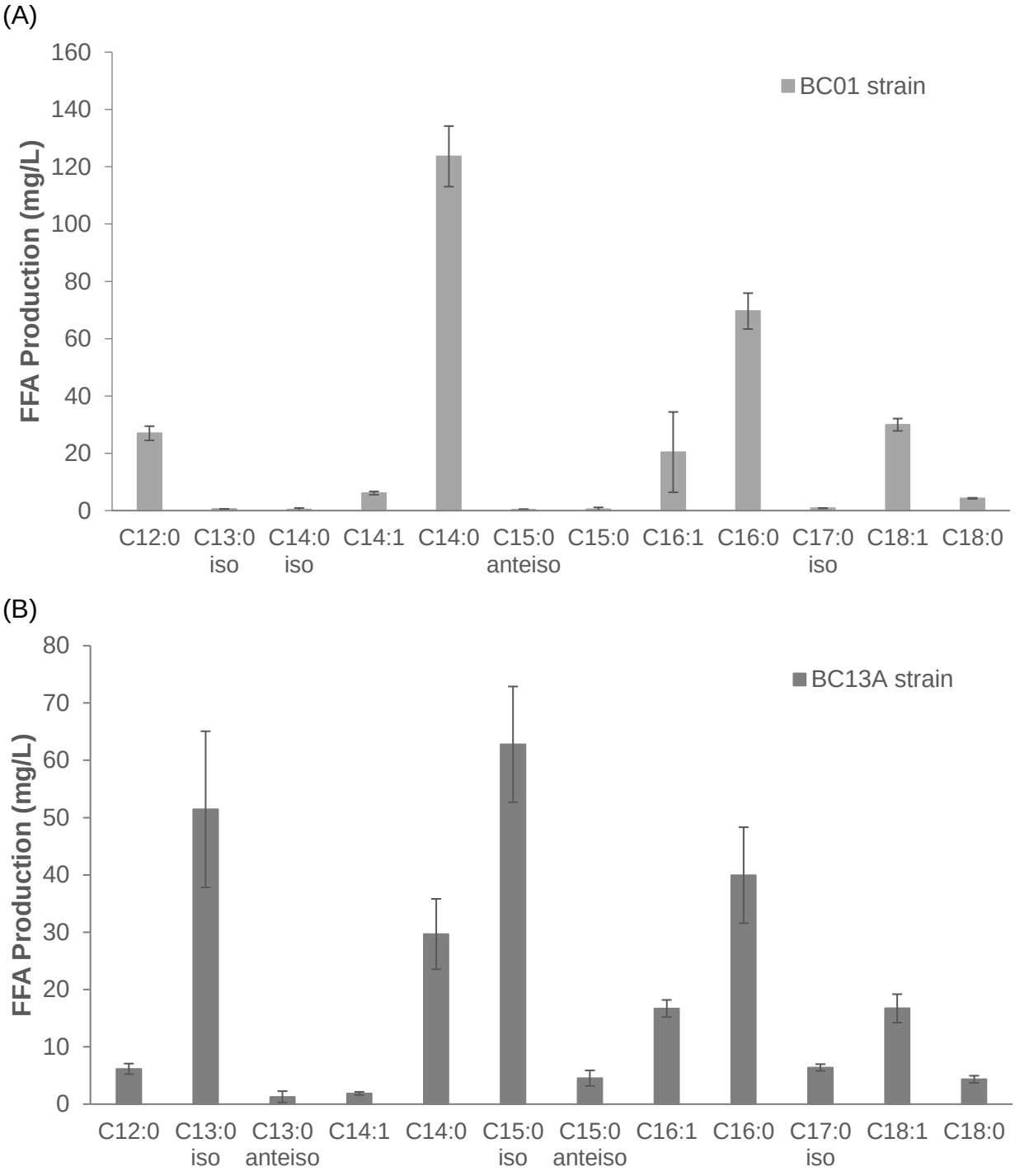

Supplementary Figure 2-1. Fatty acid production profiles of (A) strain BC01 (containing $_{Ec}$FabH& $_{Bs}$FabH2) and (B) the top-performing strain, BC13A (containing $_{Sa}$FabH), with the supplement of 1 g/L 4-methyl-2-oxopentanoic acid.

(A)

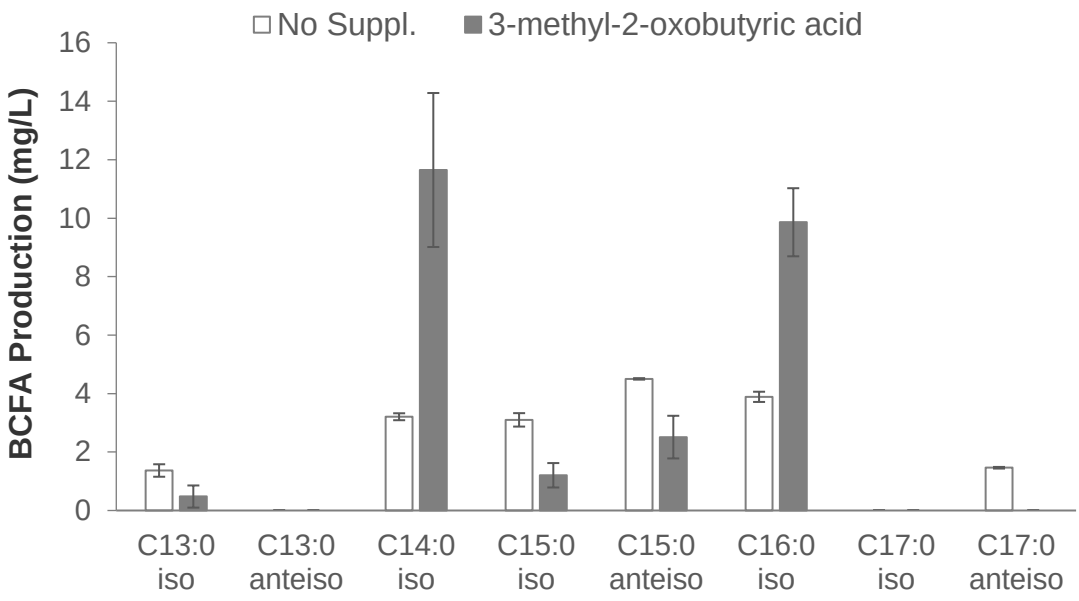
No Suppl.
3-methyl-2-oxobutyric acid
BCFA Production (mg/L)
16
14
12
10
8
6
4
2
0
C13:0 iso
C13:0 anteiso
C14:0 iso
C15:0 iso
C15:0 anteiso
C16:0 iso
C17:0 iso
C17:0 anteiso

(B)

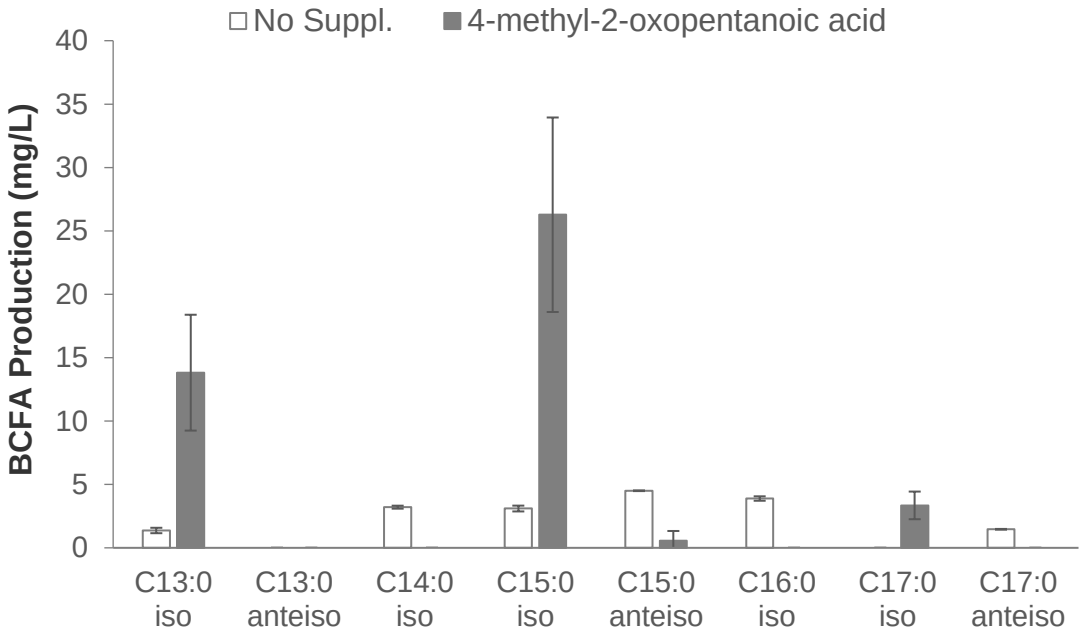
No Suppl.
4-methyl-2-oxopentanoic acid
BCFA Production (mg/L)
40
35
30
25
20
15
10
5
0
C13:0 iso
C13:0 anteiso
C14:0 iso
C15:0 iso
C15:0 anteiso
C16:0 iso
C17:0 iso
C17:0 anteiso

(C)

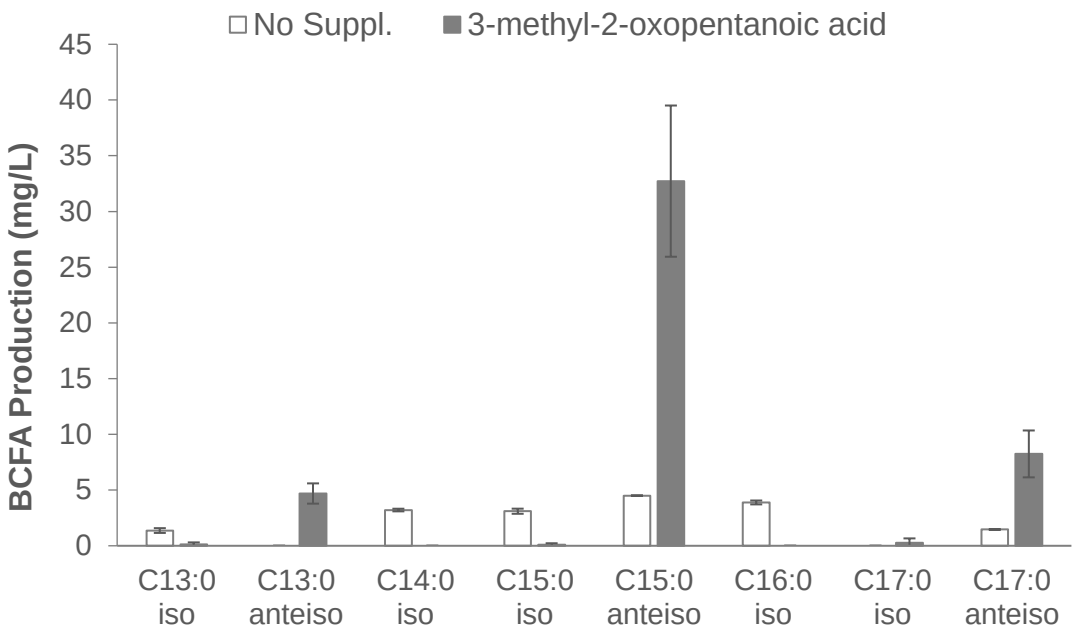

Supplementary Figure 2-2. Effect of α-keto acid supplementation to BCFA productions. Strain BC11A (containing $_{Bs}$FabH2) was cultivated as described in Methods and induced with 0.4% arabinose. At the moment of induction, cell cultures were supplemented with 1 g/L of either 3-methyl-2-oxobutyric acid (A, solid columns), 4-methyl-2-oxopentanoic acid (B, solid columns), 3-methyl-2-oxopentanoic acid (C, solid columns), or nothing (A-C, empty columns).

(A)

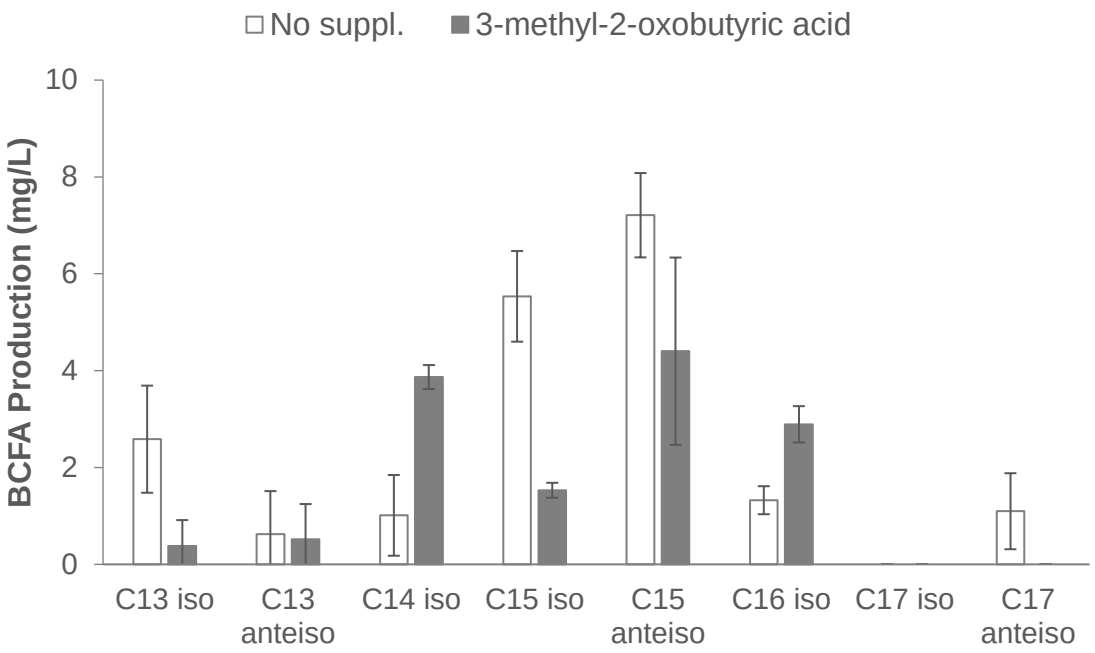
No suppl.
3-methyl-2-oxobutyric acid
BCFA Production (mg/L)
10
8
6
4
2
0
C13 iso
C13 anteiso
C14 iso
C15 iso
C15 anteiso
C16 iso
C17 iso
C17 anteiso

(B)

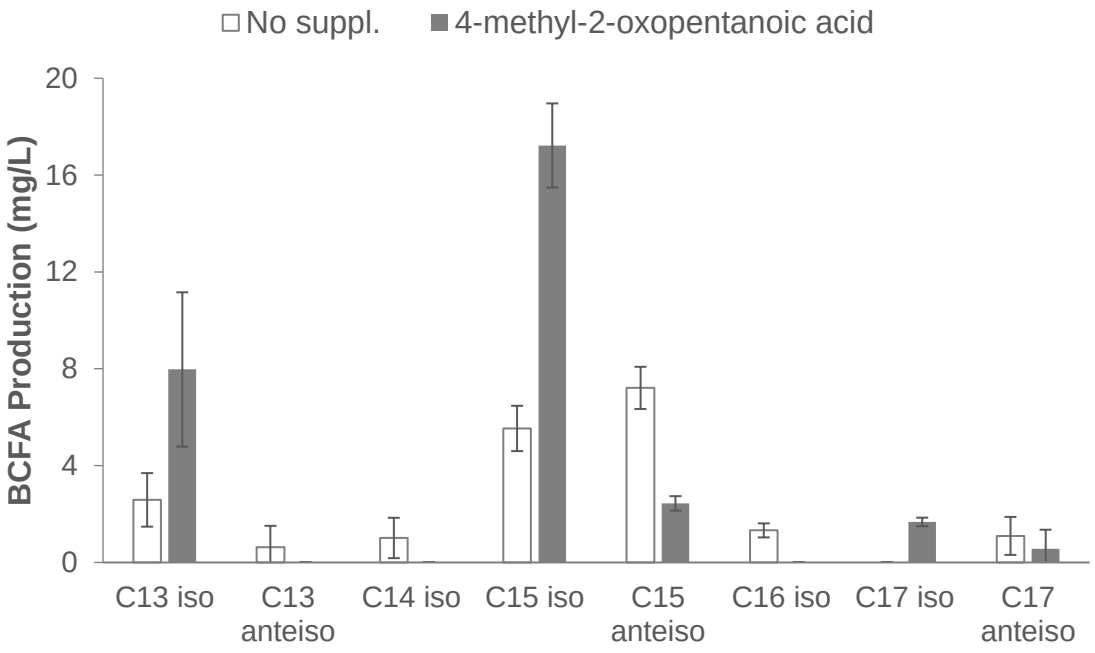
No suppl.
4-methyl-2-oxopentanoic acid
BCFA Production (mg/L)
20
16
12
8
4
0
C13 iso
C13 anteiso
C14 iso
C15 iso
C15 anteiso
C16 iso
C17 iso
C17 anteiso

(C)

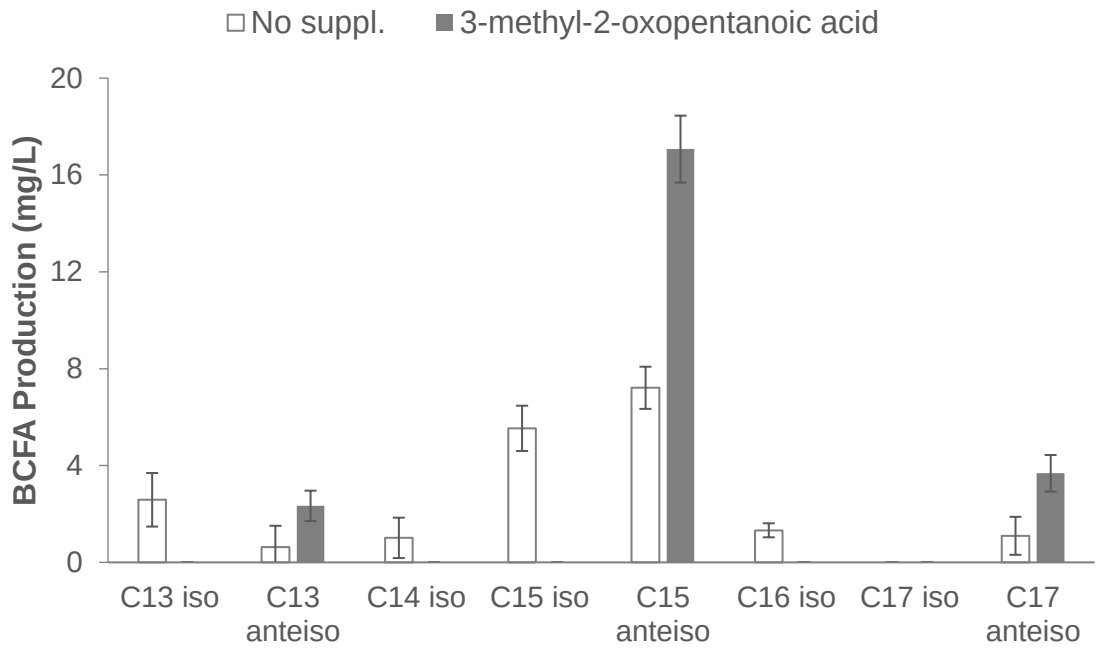

Supplementary Figure 2-3. Effect of α-keto acid supplementation to BCFA productions. Strain BC12A (containing $_{Bs}$FabH1) was cultivated as described in Methods and induced with 0.4% arabinose. At the moment of induction, cell cultures were supplemented with 1 g/L of either 3-methyl-2-oxobutyric acid (A, solid columns), 4-methyl-2-oxopentanoic acid (B, solid columns), 3-methyl-2-oxopentanoic acid (C, solid columns), or nothing (A-C, empty columns).

Chapter 3: Modular pathway engineering for the production of branched-chain fatty alcohols

3.1 Introduction

Finite energy resources and increased environmental concerns demand the development of sustainable and renewable approaches to the production of fuels, chemicals, and materials. Engineering microbial metabolic pathways to synthesize desired products is an attractive approach. With recent advances in genetic techniques and metabolic engineering methodologies, various engineered microbes have been developed to produce an array of chemicals derived from inexpensive and renewable substrates [55, 89] . Target molecules are typically designed to replace or mimic those obtained from petroleum or other non-renewable sources [90, 91]. Among these chemicals, long-chain fatty alcohols (LCFLs) in the range of C12 to C18 have numerous applications as fuels, emollients, plasticizers, thickeners, and detergents [92-94]. At the industrial scale, LCFLs are currently produced either through hydrogenation of pretreated natural fats and oils (oleochemicals) or hydroformylation of petrochemicals (e.g. crude oil, natural gas) [43, 95, 96]. Because both processes require harsh reaction conditions and release harmful byproducts to the environment [97], microbial production of fatty alcohols from renewable sugars is a promising alternative.

LCFLs have been recently biosynthesized from engineered microbes through fatty acid biosynthetic pathway [43, 92, 97-101]. The majority of previously biosynthesized LCFLs contain straight aliphatic chains. Straight LCFLs have relatively high freezing points and viscosities

compared to their branched-chain isomers, thus limiting their low-temperature operability—an essential feature for industrial emollients, lubricants, detergents, and most especially, diesel fuels [102, 103]. For example, the most abundant biosynthetically produced LCFL, straight-chain palmityl alcohol (C16, often called cetyl alcohol), melts at 49.3°C and exists as a solid at room temperature, making it difficult to use as a lubricant or an aircraft hydraulic fluid [104]. In comparison, the branched isomer, isocetyl alcohol, is a clear liquid at room temperature (melting point -30°C) with significantly enhanced fluidity and low-temperature operability, and thus is used in a number of detergent formulations that require low-temperature operability [105]. Introducing degrees of unsaturation has been used as an alternative method to improve the fluidity of straight-chain molecules [106]. However, these molecules are vulnerable to oxidation and color instability, both of which do not occur in BLFLs, even at high temperatures and pressures [103]. BLFLs additionally are ranked low in eye and skin irritation, allowing their use in cosmetics and fragrances [102]. Given the clear breadth BLFL applications, chemical engineers have developed methods to synthesize naturally scarce BLFLs [107-109]. BLFLs are currently produced from straight LCFLs using a multi-step, catalytic process that requires high temperature (180-300°C), strong acids/bases, and multiple operation unites, and the conversion process is unpredictable [102]. Recently, branched-short-chain alcohols in the range of (C3 to C7) were produced by engineered microbes [26, 110] as gasoline replacements. However, due to their short chain-length and high volatility, branched-short-chain alcohols are not suitable for the above-mentioned applications. Given BLFLs' lack of natural abundance, their complex synthesis process, and the demand for their distinctive properties, it is imperative to develop biosynthetic approaches to produce BLFLs from renewable feedstock.

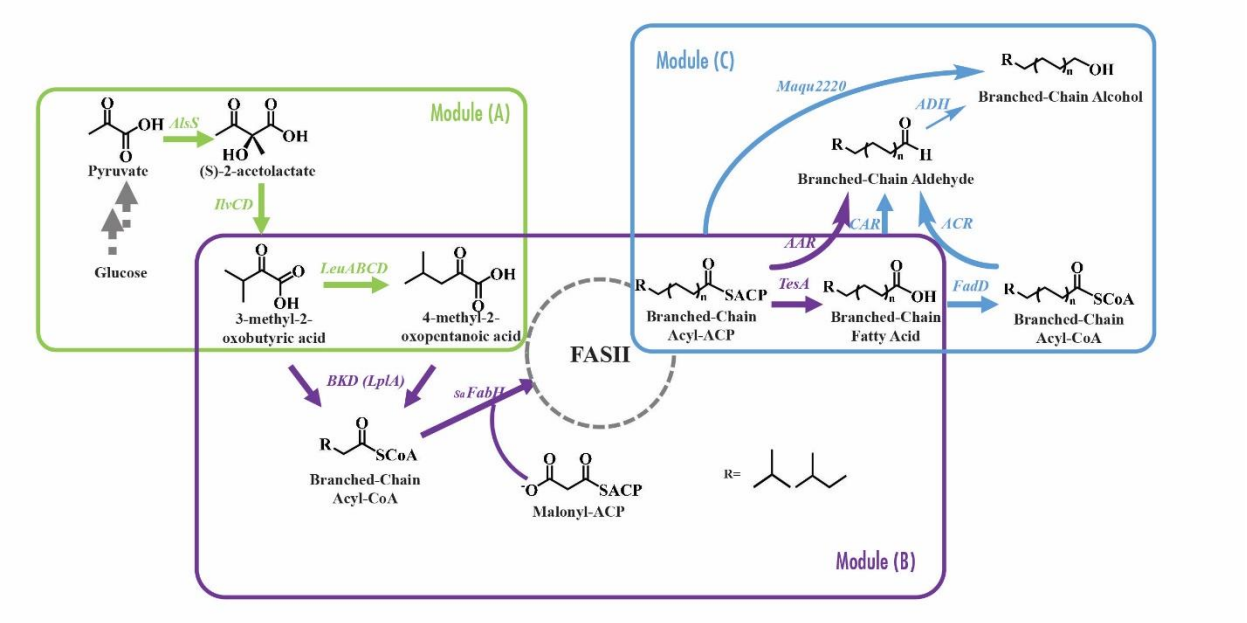

Figure 3- 1 Biosynthetic pathways for BLFL production
α-Keto Acid Generation Module (Module A) converts pyruvate to α-keto acid: 3-methyl-2-oxobutyric acid or 4-methyl-2-oxopentanoic acid. Acyl-ACP Generation Module (Module B) incorporates α-keto acid to the fatty acid biosynthetic pathway. Alcohol Formation Module (Module C) converts branched-chain acyl-ACPs to BLFLs.

Since straight LCFLs have been biologically or chemically derived from free fatty acid precursors [111], BLFLs theoretically can be derived from branched-chain fatty acids (BCFAs). BCFAs have been recently biosynthesized in engineered *E. coli* by overexpressing a heterologous branched-chain α-keto acid dehydrogenase complex (BKD), a branched-chain-acyl-CoA-specific β-ketoacyl-acyl-carrier protein (FabH) and a thioesterase (TesA) [112, 113]. This system ultimately produced BCFA in high percentages from glucose (181 mg/L and 80% BCFA) by engineering a protein lipoylation pathway and an α-keto acid biosynthetic pathway. However, highly efficient conversion of BCFAs to BLFLs has not been explored. It was not known whether the branched-chain intermediates, such as branched long-chain acyl-ACPs, BCFAs, and branched long-chain acyl-CoAs, are compatible with alcohol-conversion enzymes, even though some

enzymes have activities towards branched short-chain-ACP or CoA intermediates [114, 115]. Furthermore, because the BLFL pathway involves in multiple untested reaction, balancing activities of each sub-pathway to prevent accumulation of branched-chain intermediate is necessary to obtain high titer and yield [116-119].

To achieve these goals, I constructed and tested four metabolic pathways that convert branched-chain acyl-ACPs to BLFLs. To optimize productivity, the entire BLFL pathway was divided into three modules (Figure 3-1): an α-Keto Acid Synthesis Module that converts glucose to α-keto acids, an Acyl-ACP Generation Module that converts α-keto acids to branched-chain acyl-ACPs, and an Alcohol Formation Module that converts branched-chain acyl-ACPs to final branched-chain products. To begin, I experimentally determined the most efficient enzyme combinations to convert branched-chain acyl-ACPs to BLFLs using an engineered branched-chain-acyl-ACP-producing basal strain (BC33). This initial pathway identification allowed us to ascertain whether BLFL production was even feasible, given the available enzymes. Next, I optimized each module separately and later the entire pathway collectively to produce even-chain-iso and odd-chain-iso fatty alcohols from glucose. This modular approach enabled the isolation of each module for testing and optimization, without confounding the system by simultaneously engineering the other modules.

3.2 Materials and Methods

3.2.1 Materials and Media

Phusion DNA polymerase was purchased from New England Biolabs (Beverly, MA, USA). Restriction enzymes, T4 ligase, gel purification kits, and plasmid miniprep kits were purchased from Thermo Fisher Scientific (Waltham, Massachusetts, USA). All primers were synthesized by

Integrated DNA Technologies (Coralville, IA, USA). BCFA standards (Bacterial Acid Methyl Ester Mix), SCFA standards (GLC-20 and GLC-30), and all the other reagents were purchased from Sigma Aldrich (St. Louis, MO, USA).

Minimal medium (M9 medium supplemented with 75 mM MOPS at pH 7.4, 2 mM $MgSO_4$, 1 mg/L thiamine, 50 μg/mL lipoic acid, 10 μM $FeSO_4$, 0.1 mM $CaCl_2$, and micronutrients, including 3 μM $(NH_4)_6Mo_7O_{24}$, 0.4 mM boric acid, 30 μM $CoCl_2$, 15 μM $CuSO_4$, 80 μM $MnCl_2$, and 10 μM $ZnSO_4$) containing 2% glucose and 0.5% yeast extract as carbon sources was used for cell growth and fatty alcohol production.

3.2.2 Plasmids and strains

Plasmids used in this study were listed in Table 3-1. Genes encoding *S. elongatus* AAR (*aar*), *M. marinum* CAR (*car*), and *B. subtilis* Sfp (*sfp*) were codon-optimized for *E. coli* expression and synthesized by Integrated DNA Technologies (Coralville, IA, USA). Genes encoding ACR (*maqu2507*) and Maqu2220 (*maqu2220*) were amplified by PCR from templates provided by Dr. Brett M. Barney (University of Minnesota, MN) and Dr. Jay D. Keasling (Joint BioEnergy Institute, CA). To create all plasmids (Table 3-1), the corresponding genes were assembled into the backbones of BioBrick plasmids [64], using either restriction sites or Golden-Gate DNA assembly method [65].

E. coli DH10B was used for cloning purposes. *E. coli* strain CL111 [67] was used for production purposes. Strains BO33A-J were created by transforming the corresponding plasmids (Table 3-2) into BC33 competent cells, respectively. Strain BC43 was created by switching native *leuABCD* promoter P_{leuLp} and P_{leuLp2} to P_{lacUV5} promoter, using a previously described CRISPR-Cas9 gene replacement method [120]. Similarly, to create strain BC63, the *fadR-lplA* operon under

the control of a P_{LacUV5} promoter was integrated to the *ldhA* locus of BC43 strain by the same CRISPR-Cas9 gene replacement method. Strains BO63V and BO63L were created by transforming the corresponding plasmids into strain BC63.

3.2.3 Cell culturing and α-keto acids supplementation

Cells were pre-cultivated in LB medium with proper antibiotics. Overnight cultures were inoculated 2% v/v into M9 minimal medium (described in section 3.2.1) with corresponding antibiotics for adaptation. Overnight cultures in minimal medium were then used to inoculate 5 mL of the same fresh minimal medium, with an initial OD_{600} of 0.08. When OD_{600} reached 0.8, cells were induced with proper inducers (1mM IPTG, 0.4% arabinose, and/or 200 nM aTc, or as otherwise specified). For α-keto acid supplementation experiments, one of the α-keto acids (3-methyl-2-oxobutyric acid or 4-methyl-2-oxopentanoic acid) was added at OD_{600} = 0.8 to a final concentration of 1 g/L. Cells were harvested three days after induction.

3.2.4 Fermentation

Fed-batch fermentation was carried out using a New Brunswick Bioflo 110 fermenter with a pH meter, a dissolved oxygen electrode, and a temperature electrode. M9 medium (described in section 2.1, 500 mL) was inoculated with an overnight culture of strain BO63L to an initial OD_{600} to 0.08, along with appropriate antibiotics and 0.001% Antifoam 204. The fermentation was initiated with the following settings: Temperature was set to 30 °C, pH was controlled at 7.4 by automatic feeding of 6N ammonium hydroxide, the airflow rate was kept at 1.5 L/min, and the average stirring rate was maintained at 500 rpm. Gene expression was induced at OD_{600} = 10 by addition of 1 mM IPTG, 0.4% arabinose, and 0.22 μM aTc (final concentration). A glucose stock solution (400 g/L glucose and 12 g/L $MgSO_4$) was intermittently pulsed into the bioreactor to re-

supply glucose, and a yeast extract solution (20%) was intermittently added into the bioreactor. Broth samples (~3 ml) were collected at a series of time points to measure cell density and alcohol titer.

3.2.5 Quantification of the fatty alcohols

For the quantification of alcohols, 1 mL of cell culture was acidified with 100 μL of concentrated HCl (12N). Alcohols were extracted twice with 0.5 mL ethyl acetate, and the organic layers were isolated. Next, 200 μL of the organic layer from each sample was transferred to one 2 mL clear glass GC vial (Agilent Technologies, Santa Clara, CA), mixed with 200 μL of N,O-bis(trimethylsilyl)trifluoroacetamide (BSTFA) with 1% v/v chlorotrimethylsilane, and incubated at 60 °C for 2 h. Alcohol derivatives were quantified using a GC-MS (Hewlett-Packard model 7890A, Agilent Technologies) equipped with a 30 m DB5-MS column (J&W Scientific) and a mass spectrometer (5975C, Agilent Technologies) or a FID (Agilent Technologies) detector. For each sample, the column was equilibrated at 80 °C, followed by a ramp to 300 °C at 20°C/min, and was then held at 300 °C for 3 min. Individual alcohol peaks were identified by comparing their retention time to that of a standard (a mixture of 1-tetradecanol, 1-hexadecanol, and 1-octadecanol, prepared and derivatized identically to samples) and by comparing their mass spectra to the National Institute of Standards and Technology (NIST) Mass Spectral Library. Concentrations of each alcohol were determined by comparing the area of each sample peak to a standard curve generated by standards eluted using the same method. Product titer for each strain was measured in biological triplicate (starting from three different colonies) and average values are reported.

Table 3- 1 Plasmids used in Chapter 3

Plasmids	Replication ori	Overexpressed operon	Resistance	Reference
pSa-P_{ecfabH}-*$_{Sa}$fabH*	SC101	P_{ecfabH}-*$_{Sa}$fabH* (*S. aureus*)	Amp^R	Chapter 2
pB5k-*aar-lplA*	pBBR1	P_{lacUV5}-*aar*(*S. elongatus*)-*lplA*(*E. coli*)	Kan^R	This chapter
pB5k-*sfp-car*	pBBR1	P_{lacUV5}-*sfp*(*B. subtilis*)-*car*(*M. marinum*)	Kan^R	This chapter
pE8c-*tesA-lplA*	ColE1	P_{BAD}-*tesA*(*E. coli*)-*lplA*(*E. coli*)	Cm^R	This chapter
pB5k-*maqu2507-lplA*	pBBR1	P_{lacUV5}-*maqu2507*(*M. aquaeolei* VT8)-*lplA*(*E. coli*)	Kan^R	This chapter
pE5c-*tesA-fadD*	ColE1	P_{lacUV5}-*tesA*(*E. coli*)-*fadD*(*E. coli*)	Cm^R	[121]
pB5k-*maqu2220*	pBBR1	P_{lacUV5}-*maqu2220*(*M. aquaeolei* VT8)	Kan^R	[121]
pB5k-*maqu2220-lplA*	pBBR1	P_{lacUV5}-*maqu2220*(*M. aquaeolei* VT8)-*lplA*(*E. coli*)	Kan^R	This chapter
pB5k-*adhA*	pBBR1	P_{lacUV5}-*adhA*(*L. lactis*)	Kan^R	This chapter
pB5k-*yqhD*	pBBR1	P_{lacUV5}-*yqhD*(*E. coli*)	Kan^R	This chapter
pB5k-*yjgB*	pBBR1	P_{lacUV5}-*yjgB*(*E. coli*)	Kan^R	This chapter
pA8c-*aar-lplA*	pA15a	P_{BAD}-*aar*(*S. elongatus*)-*lplA*(*E. coli*)	Cm^R	This chapter
pB2k-*alsS-ilvCD-yjgB*	pBBR1	P_{tet}-*alsS*(*B. subtilis*)-*ilvCD*(*E. coli*)-*yjgB*(*E. coli*)	Kan^R	This chapter
pE2c-*aar-lplA-yjgB*	ColE1	P_{tet}-*aar*(*S. elongatus*)-*lplA*(*E. coli*)-*yjgB*(*E. coli*)	Cm^R	This chapter
pA6k-*alsS-ilvCD*	pA15a	P_{LlacO}-*alsS*(*B. subtilis*)-*ilvCD*(*E. coli*)	Kan^R	[122]
pB2k-*alsS-ilvCD*	pBBR1	P_{tet}-*alsS*(*B. subtilis*)-*ilvCD*(*E. coli*)	Kan^R	This chapter
pB5c-*aar-lplA-yjgB*	pBBR1	P_{lacUV5}-*aar*(*S. elongatus*)-*lplA*(*E. coli*)-*yjgB*(*E. coli*)	Cm^R	This chapter
pB5c-*maqu2220-lplA*	pBBR1	P_{lacUV5}-*maqu2220*(*M. aquaeolei* VT8)-*lplA*(*E. coli*)	Cm^R	This chapter
pA8c-*leuA^{mut}BCD*	pA15a	P_{BAD}-*leuA^{mut}BCD*(*E. coli*)	Cm^R	This chapter
pE8c-*leuA^{mut}BCD*	ColE1	P_{BAD}-*leuA^{mut}BCD*(*E. coli*)	Cm^R	This chapter
pB5k-*maqu2220-leuA^{mut}BCD*	pBBR1	P_{lacUV5}-*maqu2220*(*M. aquaeolei* VT8)-*leuA^{mut}BCD*(*E. coli*)	Kan^R	This chapter
pA8c-*lplA*	pA15a	P_{BAD}-*lplA*(*E. coli*)	Cm^R	This chapter
pE8c-*adhA*	ColE1	P_{BAD}-*adhA*(*L. lactis*)	Cm^R	This chapter
pE8c-*yqhD*	ColE1	P_{BAD}-*yqhD*(*E. coli*)	Cm^R	This chapter
pE8c-*yjgB*	ColE1	P_{BAD}-*yjgB*(*E. coli*)	Cm^R	This chapter
pE2s-*alsS-ilvCD*	ColE1	P_{tet}-*alsS*(*B. subtilis*)-*ilvCD*(*E. coli*)	$Spec^R$	This chapter

Table 3- 2 Strains used in Chapter 3

Strains	Relevant genotype	Reference
Parental strains		
CL111	UB1005, attHK022::(*plsX'fabH*; *aadA*) *fabH*::kan	[67]
CL111(*⊿kan*)	UB1005, attHK022::(*plsX'fabH*; *aadA*), ⊿kan	Chapter 2
BC30	CL111(*⊿kan*) *fadE*:: *$_{bs}$lpdV-$_{bs}$bkdAA-$_{bs}$bkdAB-$_{bs}$bkdB*	Chapter 2
BC33	CL111(*⊿kan*) (*plsX'fabH*; *aadA*)::Tet^{A} *fadE*:: *$_{bs}$lpdV-$_{bs}$bkdAA-$_{bs}$bkdAB-$_{bs}$bkdB* pSa-P$_{ecfabH\text{-}Sa}$*fabH*	Chapter 2
BC43	BC33 *leuO-leuL-leuA::P$_{lacUV5}$-leuA^{mut}*	This study
BC63	BC43 *ldhA*::*fadR-lplA*	This study
Alcohol-producing strains		
BO33A	BC33 pB5k-*aar-lplA*	This study
BO33B	BC33 pB5k-*sfp-car*, pE8c-*tesA-lplA*	This study
BO33C	BC33 pB5k-*maqu2507-lplA*, pE5c-*tesA-fadD*	This study
BO33D	BC33 pB5k-*maqu2220-lplA*	This study
BO33E1	BC33 pA8c-*aar-lplA*, pB5k-*adhA*	This study
BO33E2	BC33 pA8c-*aar-lplA*, pB5k-*yqhD*	This study
BO33E3	BC33 pA8c-*aar-lplA*, pB5k-*yjgB*	This study
BO33E4	BC33 pE2c-*aar-lplA-yjgB*	This study
BO33F	BC33 pA8c-*aar-lplA*, pB2k-*alsS-ilvCD-yjgB*	This study
BO33F1	BC33, pE2c-*aar-lplA-yjgB*, pA6k-*alsS-ilvCD*	This study
BO33F2	BC33, pE2c-*aar-lplA-yjgB*, pB2k-*alsS-ilvCD*	This study
BO33F3	BC33, pB5c-*aar-lplA-yjgB*, pA6k-*alsS-ilvCD*	This study
BO33G1	BC33, pA8c-*leuA^{mut}BCD*, pB5k-*aar-lplA*	This study
BO33G2	BC33, pE8c-*leuA^{mut}BCD*, pB5k-*aar-lplA*	This study
BO33H1	BC33 pB5k-*maqu2220-lplA*, pE8c-*adhA*	This study
BO33H2	BC33 pB5k-*maqu2220-lplA*, pE8c-*yqhD*	This study
BO33H3	BC33 pB5k-*maqu2220-lplA*, pE8c-*yjgB*	This study
BO33I1	BC33, pA6k-*alsS-ilvCD*, pB5c-*maqu2220-lplA*	This study
BO33I2	BC33, pE2k-*alsS-ilvCD*, pB5c-*maqu2220-lplA*	This study
BO33J1	BC33, pA8c-*leuA^{mut}BCD*, pB5k-*maqu2220-lplA*	This study
BO33J2	BC33, pA8c-*lplA*, pB5k-*maqu2220-leuA^{mut}BCD*	This study
BO43I	BC43 pB5c-*maqu2220-lplA*, pE2s-*alsS-ilvCD*	This study
BO63V	BC63 pB5k-*maqu2220*, pE2s-*alsS-ilvCD*	This study
BO63L	BC63 pB5k-*maqu2220*, pE2s-*alsS-ilvCD*, pA8c-*leuABCD*	This study

3.3 Results

3.3.1 Engineering Alcohol Formation Modules in BCFA-producing strains

To create the branched-chain-acyl-ACP-producing basal strain BC33, the *E. coli fabH* was first replaced by *Staphylococcus aureus fabH* ($_{Sa}$*fabH*), a modification which was previously demonstrated to enhance branched-chain fatty acid production [113]. The acyl-CoA dehydrogenase gene (*fadE*) was next replaced by *Bacillus subtilus bkd*, functionally inhibiting β-oxidation (Δ*fadE*) and allowing the activation of branched-chain α-keto acids to branched-chain acyl-CoAs that can enter the FASII system (Δ*fadE::bkd*) (Table 3-1 & 2). Next, three Alcohol Formation Modules were separately constructed in strain BC33 (Table 3-2), resulting in alcohol-producing strains BO33A-C. Strain BO33A utilizes the *Synechococcus elongatus* acyl-ACP reductase (AAR, encoded by *aar*, Figure 3-1) to convert acyl-ACPs to fatty aldehydes [99]. Strain BO33B first generates FFAs via expression of the *E. coli* cytosolic thioesterase (TesA), which are then converted to fatty aldehydes by the *Mycobacterium marinum* carboxylic acid reductase (CAR, encoded by *car*) with *Bacillus subtilis* Sfp (encoded by *sfp*) coexpression [92] (Figure 3-1). Strain BO33C also expresses cytosolic TesA to generate FFAs and overexpresses an *E. coli* acyl-CoA synthetase (FadD) to activate FFAs to fatty acyl-CoAs, which are then converted to aldehydes by overexpressing an acyl-CoA reductase from *Marinobacter aquaeolei* VT8 (ACR, encoded by *maqu2507*) [123] (Figure 3-1). All strains rely on native *E. coli* alcohol dehydrogenases (ADHs) to reduce aldehydes to alcohols. The native *E. coli* lipoyl ligase (encoded by *lplA*) is also expressed in all strains to improve the lipoylation of 2-oxoacid dehydrogenases including BKD, which requires lipoylation to function [112].

a

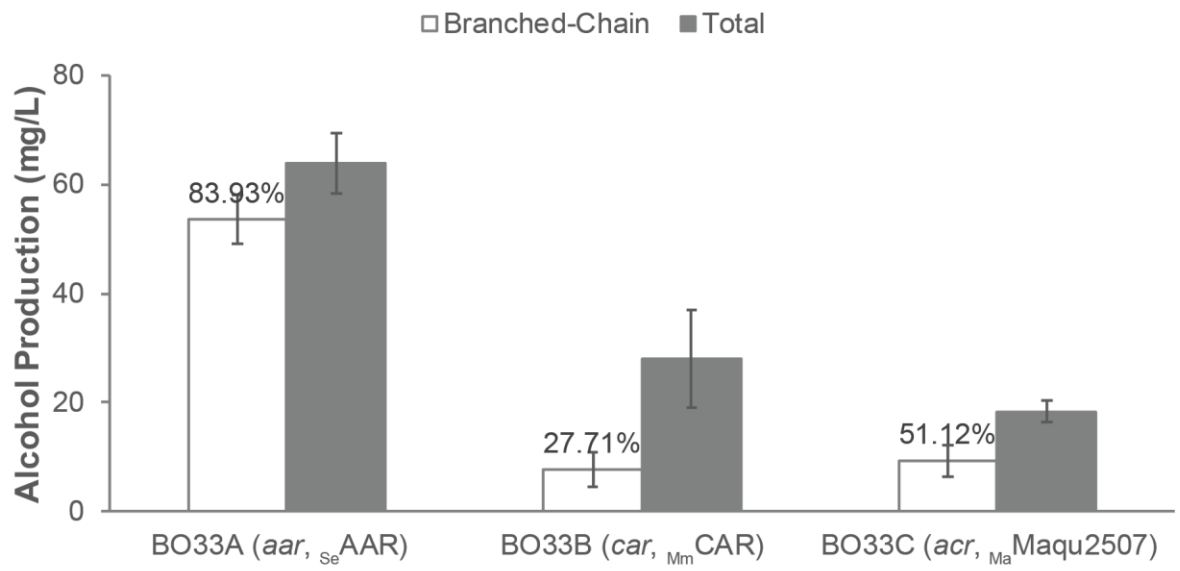
Branched-Chain
Total
Alcohol Production (mg/L)
80
60
40
20
0
83.93%
27.71%
51.12%
BO33A (aar, SeAAR)
BO33B (car, MmCAR)
BO33C (acr, MaMaqu2507)

b

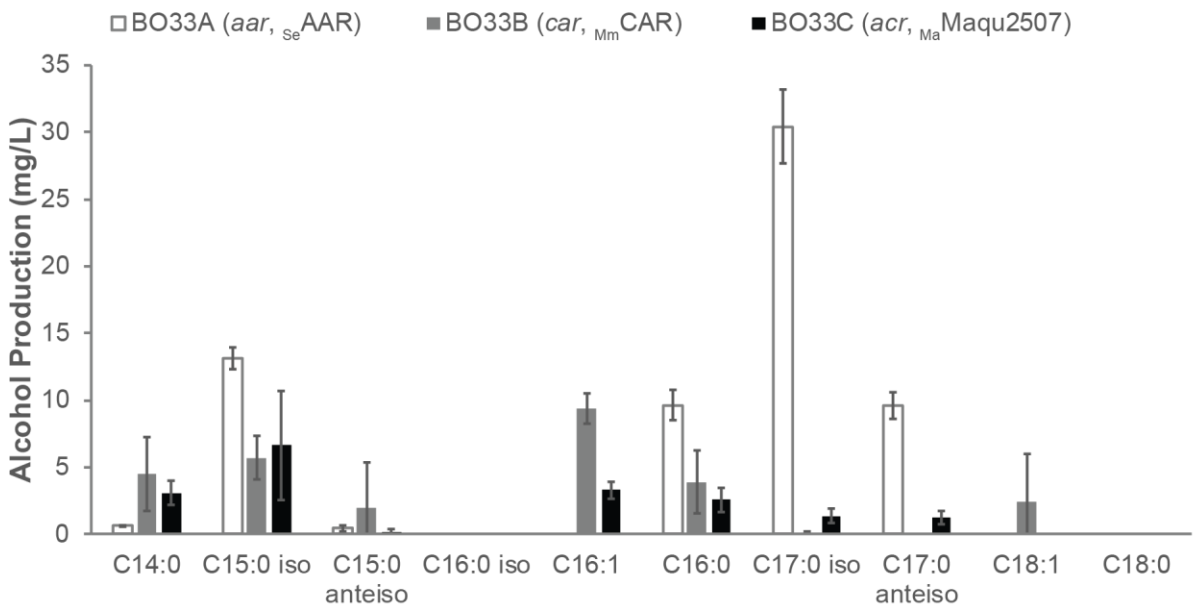
BO33A (aar, SeAAR)
BO33B (car, MmCAR)
BO33C (acr, MaMaqu2507)
Alcohol Production (mg/L)
35
30
25
20
15
10
5
0
C14:0
C15:0 iso
C15:0 anteiso
C16:0 iso
C16:1
C16:0
C17:0 iso
C17:0 anteiso
C18:1
C18:0

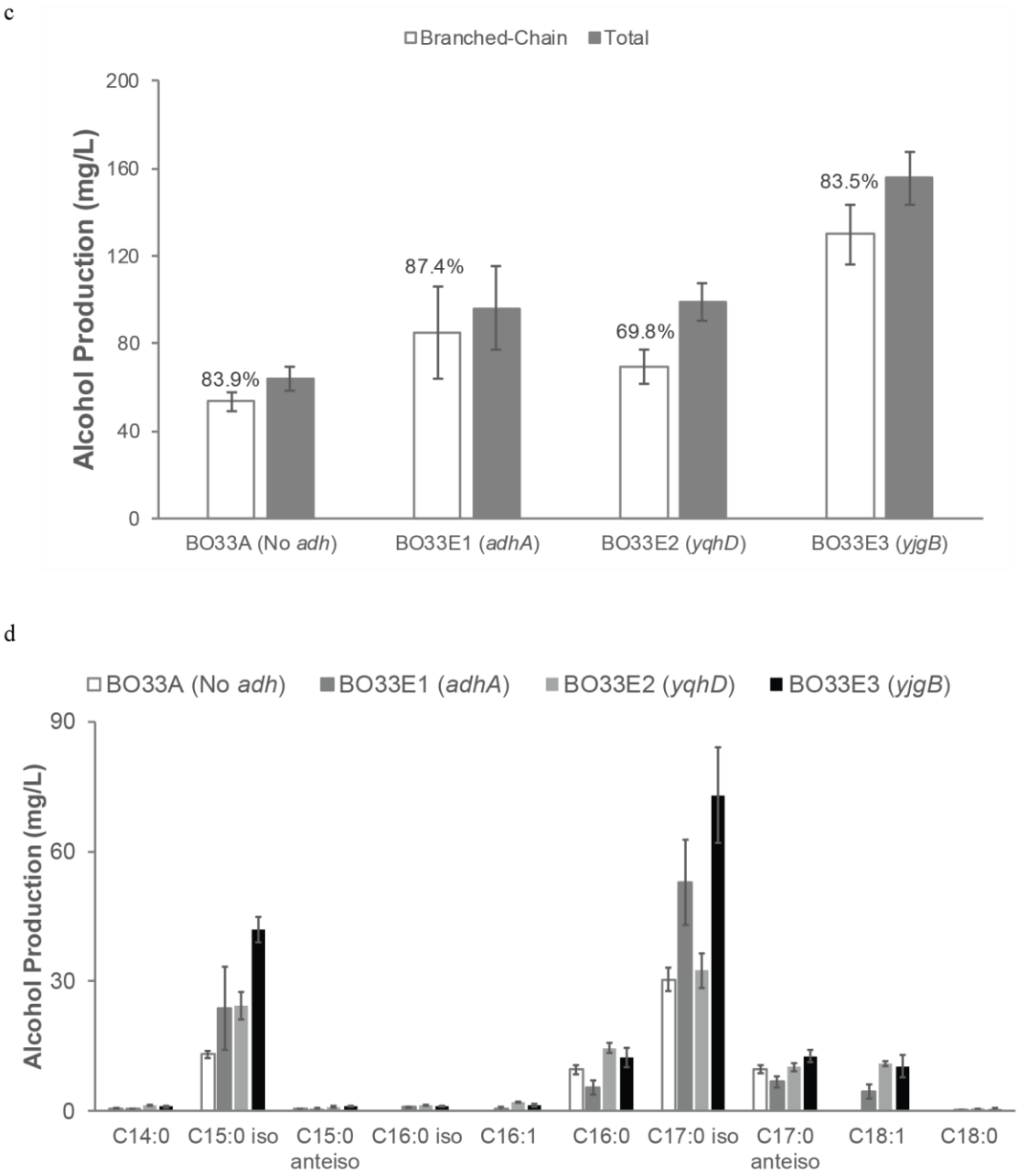

Figure 3- 2 Testing three Alcohol Formation Modules

(a) Overall titer distribution and (b) chain-length of three BLFL-producing strains with different Alcohol Formation Modules, BO33A-C (Table 3-2). $_{Se}$AAR, $_{Mm}$CAR, and $_{Ma}$Maqu2507 are reductases from *S. elongatus*, *M. marinum*, and *M. aquaeolei* VT8, respectively. (c-d) Effect of alcohol dehydrogenase overexpression on BLFL production. Alcohol profiles of strain BO33A (without *adh* overexpression) are compared with those from strain BO33E1 (expressing *adhA* from *L. lactis*), BO33E2 (expressing *yqhD* from *E. coli*), and BO33E3 (expressing *yjgB* from *E. coli*). All cultures were supplemented with 1 g/L 4-methyl-2-oxopentanoic acid. Cells were cultivated and induced as described in Methods.

I first sought to test the three Alcohol Formation Modules by assessing their capacities to convert branched-chain acyl-ACPs to BLFLs. Strains BO33A-C were cultivated at previously determined optimal temperatures for each pathway (See methods) [92, 98, 124] and supplemented with 1 g/L of 4-methyl-2-oxopentanoic acid, the most favorable α-keto acids for BCFA production [113]. Each strain produced some BLFLs, representing the first report of BLFL production in *E. coli*. The CAR pathway (BO33B) and the ACR pathway (BO33C) produced 28 mg/L and 18 mg/L BLFLs, respectively. In addition, the chain lengths of the products range from C14 to C18, consistent with the FFA profile of the TesA-overexpressing strain [39]. Meanwhile, the AAR pathway (BO33A) produced the highest BLFL titer among these three strains: 54 mg/L, comprising 84% of the total fatty alcohols (Figure 3-2a). The branch and chain-length profile of BLFLs produced in BO33A is consistent with the profile of BCFAs produced by strains with similar genetic backgrounds as previously reported (Figure 3-2b) [112], indicating that the AAR pathway has little preference between straight-chain and branched-chain acyl-ACP substrates. Interestingly, the CAR pathway produced 2-fold more straight-chain fatty alcohols but 6-fold less BLFLs than the AAR pathway, indicating that the CAR pathway is primarily straight-chain-specific. While these results serve as a proof-of-principle that BLFL can be produced at high percentages in *E. coli*, the initial low titers indicate that additional engineering efforts are needed to obtain desirable titers and yields of branched-chain products.

All of the above strains relied upon *E. coli* native ADHs to convert fatty aldehydes to alcohols. I next sought to increase BLFL production in strain BO33A by overexpression of ADHs. Three unique ADHs, *adhA* from *Lactoccocus lactis* [122], and *yqhD* and *yjgB* [92, 122, 125] from *E. coli*, were overexpressed in strain BO33A, resulting in strains BO33E1, BO33E2, and BO33E3, respectively. When cultivated under the same conditions and with 1 g/L 4-methyl-2-oxopentanoic

acid, strains BO33E1 and BO33E2 produced 85 and 69 mg/L BLFLs, respectively (Figure 3-2c & 2d). Strain BO33E3 produced 130 mg/L BLFLs, comprising 83% of total alcohols, a 2.4-fold enhancement over BO33A. Specifically, 73 mg/L of 15-methylhexadecanol and 42 mg/L of 13-methyltetradecanol were produced (Figure 3-2c), converting 8% of the supplemented 4-methyl-2-oxopentanoic acid and making odd-chain-iso alcohols the major BC alcohol species. Both BO33E1 and BO33E3 had similar fatty alcohol production profiles to that of strain BO33A, indicating that AdhA and YjgB did not selectively determine chain length or structure. In addition, no aldehyde was detected in BO33E3 culture, indicating the conversion of aldehyde to alcohol is complete.

3.3.2 Engineering 3-methyl-2-oxobutyric acid Generation Module to produce even-chain-iso fatty alcohols from glucose

Modular pathway assembly can facilitate step-wise optimizations. With the downstream Alcohol Formation Module optimized, I next sought to improve the production of BLFL from glucose by engineering and optimizing the α-Keto Acid Generation Module. In this module, I built upon the downstream-optimized strain BO33E3 to add the capacity for even-chain-iso fatty alcohol production from glucose via the precursor 3-methyl-2-oxobutyric acid (Figure 3-3a).

Since the *B. subtilis alsS* and the *E. coli ilvCD* have been used to accumulate intracellular 3-methyl-2-oxobutyric acid, I first cloned them with *yjgB* under the control of a strong P_{tet} promoter in a medium-copy-number BBR1 origin plasmid (Table 3-1). The resulting plasmid, pB2k-*alsS-ilvCD-yjgB*, was co-transformed with pA8c-*aar-lplA* (*aar* and *lplA* under the control of a P_{BAD} promoter in a pA15a origin plasmid) into strain BC33. Cultivation of the resulting strain BO33F in the absence of α-keto acid supplementation produced 34 mg/L of BLFLs, comprising 44% of the total alcohols (Figure 3-3b, Supplementary Figure 3-1). Because the composition of the α-keto acid determines the final chain structure, the final BLFL composition should mirror the cellular

pool of α-keto acids. The titer of even-chain-iso BLFLs produced by strain BO33F is 14 mg/L, lower than the 25 mg/L produced by strain BO33E3 when supplemented with 3-methyl-2-oxobutyric acid. It should be noted that the odd-chain-iso BLFLs are elongated from 4-methyl-2-oxopentanoic acid, which is generated from 3-methyl-2-oxobutyric acid. The comparable total BLFL production of these two strains, including both even-chain-iso and odd-chain-iso BLFLs, indicates that the 3-methyl-2-oxobutyric acid Generation Module was effective, although higher expression level of this module might generate more even-chain-iso products.

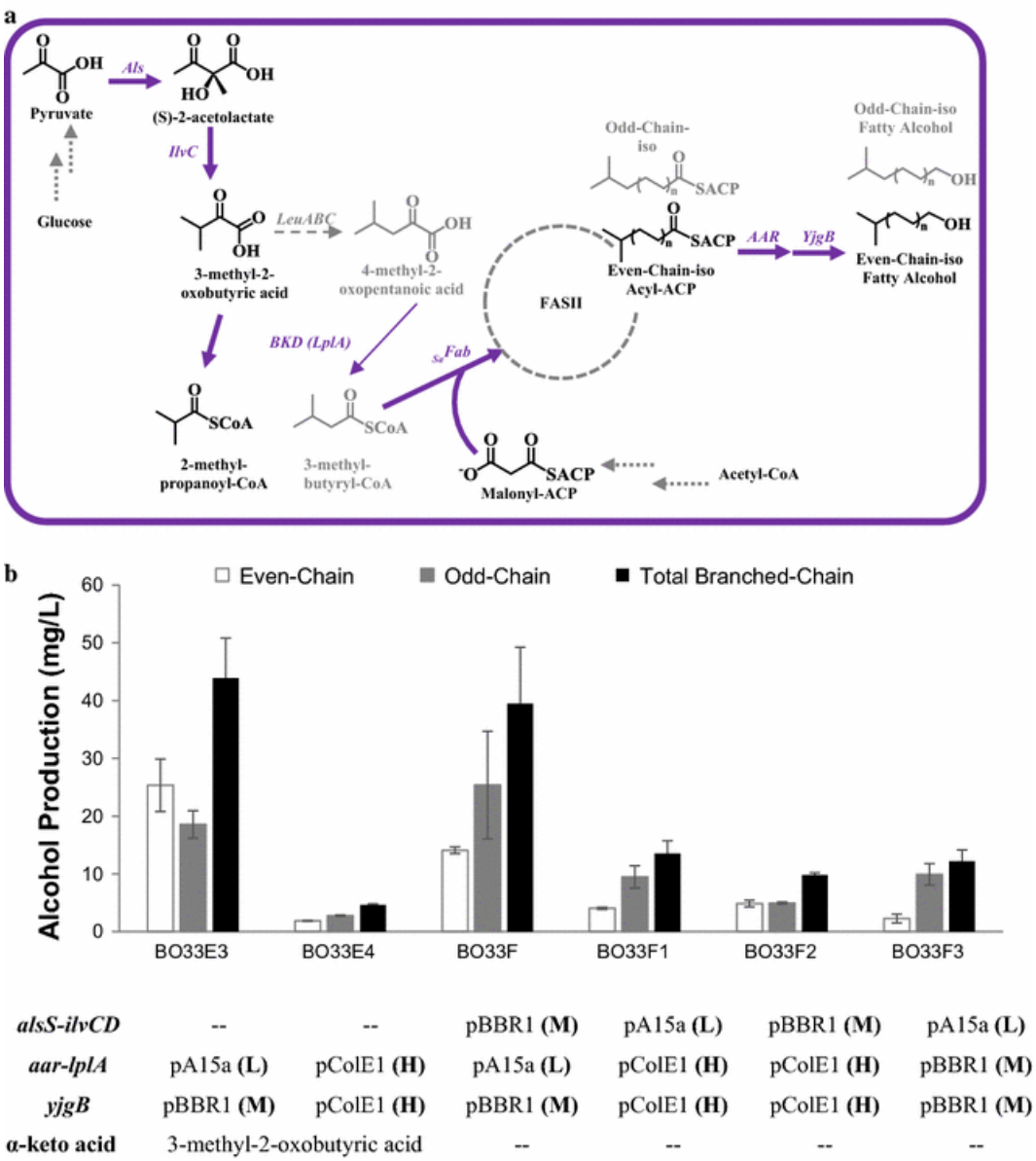

alsS-ilvCD	--	--	pBBR1 **(M)**	pA15a **(L)**	pBBR1 **(M)**	pA15a **(L)**
aar-lplA	pA15a **(L)**	pColE1 **(H)**	pA15a **(L)**	pColE1 **(H)**	pColE1 **(H)**	pBBR1 **(M)**
yjgB	pBBR1 **(M)**	pColE1 **(H)**	pBBR1 **(M)**	pColE1 **(H)**	pColE1 **(H)**	pBBR1 **(M)**
α-keto acid	3-methyl-2-oxobutyric acid		--	--	--	--

Figure 3- 3 Balancing three modules to produce even-chain-iso fatty alcohols
Plasmids with different copy numbers and promoters are used to optimize the expression level of the involved pathways. (a) Biosynthetic pathways for the production of even-chain-iso fatty alcohols. (b) Titers of even-chain, odd-chain, and total BLFL of engineered strains. Plasmids with different copy numbers and promoters were employed to bear the involved genes in different strains. The copy number of the plasmids are defined as low (L), medium (M), and high (H). For strain BO33E3-4, 1 g/L 3-methyl-2-oxobutyric acid was supplemented.

3.3.3 Optimizing 4-methyl-2-oxopentanoic acid Generation Module to produce odd-chain-iso fatty alcohols

In *E. coli*, the *leuABCD* operon converts 3-methyl-2-oxobutyric acid to 4-methyl-2-oxopentanoic acid, which is the precursor for odd-chain-iso BLFL biosynthesis. Previous work demonstrated that the ribosome binding sequence (RBS) of native *leuA* results in weak translation initiation, and *leuA* is heavily negatively auto-regulated by free leucine synthesized from 4-methyl-2-oxopentanoic acid [87] (Figure 3-4a). In this study, I engineered a mutant operon *leuA*^{mut}*BCD* that contained a feedback-resistant *leuA* [87] and a strong synthetic RBS(TTTAAGAAGGAGATATACAT). The *leuA*^{mut}*BCD* was cloned in either a low (pA15a) or a high (pColE1) copy number plasmid to create two engineered strains, BO33G1 and BO33G2, respectively. To test the conversion efficiency of the *leuA*^{mut}*BCD* operon, both strains were supplemented with 3-methyl-2-oxobutyric acid (the substrate for LeuABCD, Figure 3-4a) during cultivation. Fully functional *leuA*^{mut}*BCD* would result in odd-chain-iso BLFL compositions in a similar ratio to the previous best-performing strain (strain BO33A) when supplemented with 4-methyl-2-oxopentanoic acid. Strain BO33G1 produced 50 mg/L total BLFL and 47 mg/L odd-chain-iso fatty alcohol, statistically indistinguishable from the BLFL titer of strain BO33A supplemented with 4-methyl-2-oxopentanoic acid (Figure 3-4b, Supplementary Figure 3-2). Strain BO33G1 generated 94% odd-chain-iso fatty alcohol, indicating complete conversion of 3-methyl-2-oxobutyric acid by the modified LeuA^{mut}BCD. Conversely, when *leuA*^{mut}*BCD* was expressed under the high copy number plasmid (strain BO33G2), the BLFL titers decreased (p = 0.07) and had large standard variations (Figure 3-4b), even when the inducer concentration was reduced. Furthermore, overexpression of *leuA*^{mut}*BCD* from the high-copy number plasmid also decreased cell growth rate and cell density (Data not shown). These results indicate that expression of the

leuA^{mut}*BCD* operon at too high a level affects cell growth and BLFL production, thus needs to be avoided.

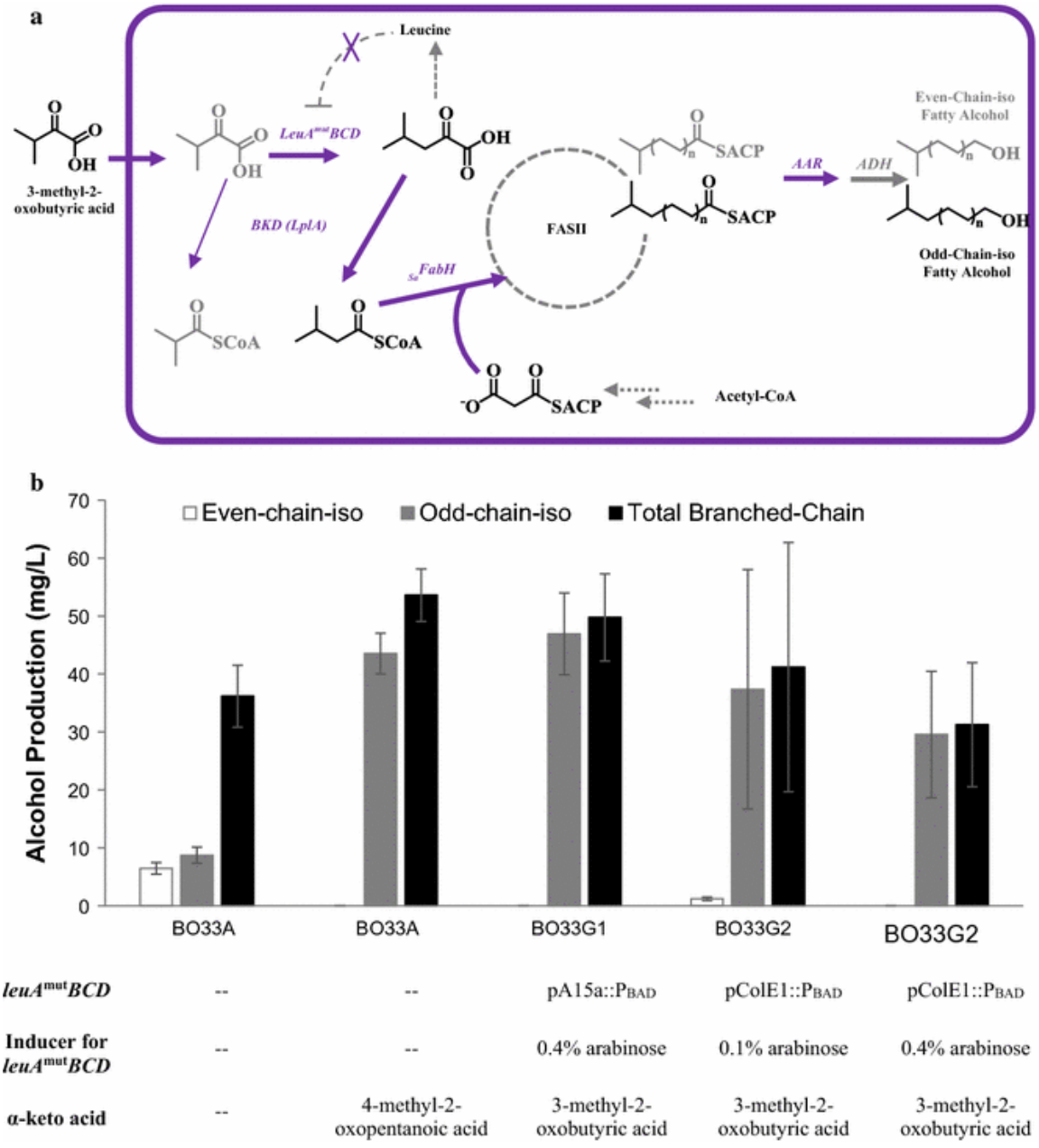

Figure 3- 4 Optimizing the 4-methyl-2-oxopentanoic acid Generation Module to produce odd-chain-iso fatty alcohols

(A) Biosynthetic pathways for the production of odd-chain-iso fatty alcohols. (B) Titers of engineered odd-chain-iso BLFL-producing strains. Strains BO33G1-2 containing *leuA*^{mut}*BCD* in plasmids with different copy numbers were cultivated as described in Methods and supplemented with 1 g/L 3-methyl-2-oxobutyric acid. Strain BO33G2 was induced with either 0.1% or 0.4% arabinose.

3.3.4 Balancing gene expression levels in all three modules for enhanced BLFL production from glucose

With the α-Keto Acid Generation and the Alcohol Formation modules optimized separately, I next sought to balance the gene expression levels within the completed pathway. I selected the best-performing genetic elements of each individual module to complete the full pathway: the α-Keto Acid Generation Module, including *alsS* & *ilvCD*, the Acyl-ACP Synthesis Module, including *aar* & *lplA*, and the Alcohol Formation Module, including *yjgB* (Figure 3-3a). To perform this optimization, I altered gene copy numbers to change the expression level of each module. Compatible plasmids with three different copy numbers were used for this purpose: a high copy number (pColE1, 50 copies per cell), a medium copy number (pBBR1, 17-20 copies per cell), and a low copy number (pA15a, 7-10 copies per cell) [64] (Figure 3-3b, Supplementary Figure 3-1). Three additional strains BO33E4, BO33F1, and BO33F2 were created (Figure 3-3b, Supplementary Figure 3-1). All three strains expressed *aar*, *lplA*, and *yjgB* from the high copy number plasmids under the control of a very tight promoter (P_{tet}), but produced less BLFL than strains BO33E3 and BO33F, which expressed *aar*, *lplA*, and *yjgB* from the low or the medium copy number plasmid. The low titer is potentially caused by the insolubility of highly overexpressed AAR [99]. Meanwhile, compared to strain BO33F3 with the low-copy *alsS-ilvCD* expression, strain BO33F with the medium-copy *alsS-ilvCD* expression improved BLFL production by 3.2-fold. These results suggest that the optimal *aar* expression level was medium to low, and that *alsS-ilvCD* required overexpression in a medium to high-copy number plasmid for optimal BLFL production (Figure 3-3b, Supplementary Figure 3-1).

3.3.5 BLFL production from glucose using the acyl-ACP reductase Maqu2220

During the course of this work, Haushalter *et al.* published the production of straight LCFLs in high titers by overexpression of a marine acyl-ACP reductase, Maqu2220 from *M. aquaeolei* VT8 [121]. Maqu2220 was first characterized as a fatty aldehyde reductase, reducing fatty aldehydes to fatty alcohols [126]. However, it was later confirmed to have acyl-ACP reductase activity and is capable of converting acyl-ACPs or acyl-CoAs directly to fatty alcohols [127], thus significantly simplifying the fatty alcohol pathway. I tested the efficiency of BLFL production via Maqu2220 by replacing the *S. elongatus aar* in strain BO33A with *maqu2220*, resulting in strain BO33D. When supplemented with 1 g/L of 4-methyl-2-oxopentanoic acid, BO33D produced 198 mg/L (89%) BC alcohols, 3.7-fold higher than that of strain BO33A (Figure 3-5). Even compared with the previous best-performing strain BO33E3, the BLFL titer of strain BO33D enhanced by 1.5-fold. Most BLFLs (> 99%) were identified in the cell pellet, consistent with previous study [128]. Moreover, overexpression of the ADHs *yjgB*, *yqhD*, or *adhA* did not enhance BLFL titer (Figure 3-5), further confirming the previous hypothesis that Maqu2220 contains a catalytic domain with ADH activity.

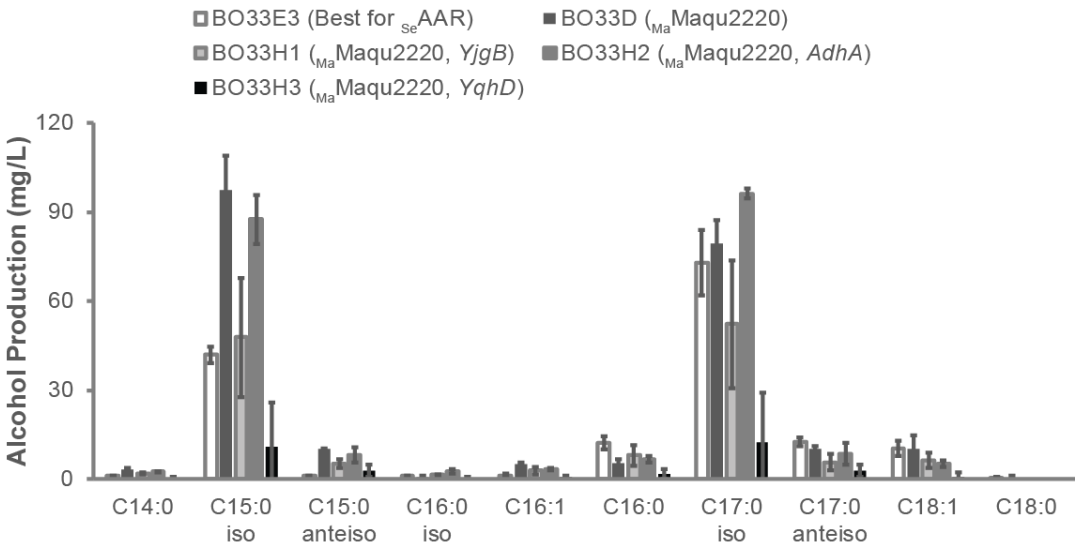

Figure 3- 5 BLFL profiles of engineered *E. coli* strains containing Maqu2220
While strain BO33D does not contain additional *adh*, BO33H1-3 overexpressed *L. lactis adhA*, *E. coli yqhD*, and *E. coli yjgB*, respectively. BLFL profiles are compared with that of strains BO33E3 (the best performing strain in section 3.1). All cultures were supplemented with 1 g/L 4-methyl-2-oxopentanoic acid.

After confirming the capability of Maqu2220 to convert branched-chain acyl-ACPs to BLFLs, I sought to use Maqu2220 to produce BLFLs from glucose by applying the knowledge learned from optimizing the α-Keto Acid Synthesis Module. After constructing and validating strains, I found that the optimal expression level of each module mimicked those characterized using the *aar* pathway. First, the high-copy number-expression (pColE1) of the *alsS-ilvCD* operon increased even-chain-iso fatty alcohol production by 9.2-fold over the low-copy number-expression (pA15a) (as seen by comparing strains BO33I1 with BO33I2 in Figure 3-6a). Second, when supplemented with 3-methyl-2-oxobutyric acid, the low-copy number-expression of the *leuA*^{mut}*BCD* operon produced 2.8-fold more odd-chain-iso fatty alcohols than the medium-copy number-expression (as seen for strains OB33J1 and OB33J2 in Figure 3-6a).

Next, I attempted to combine all three modules to produce BLFLs from glucose, which requires overexpression of 14 genes from 6 synthetic operons: P_{tet}-*alsS-ilvCD*, P_{BAD}-leu*A*^{mut}*BCD*,

P_{lacUV5}-*bs*lpdV-*bs*bkdAA-*bs*bkdAB-*bs*bkdB, P_{lacUV5}-*lplA*, P_{ecfabH}-Sa*fabH*, and P_{lacUV5}-*maqu2220*. To reduce the burden imposed by multiple plasmids while maintaining a sufficient enzyme expression level, I tried to integrate some operons into the genome. Based on the findings above, I first created strain BC43 with a single copy *leuA*^{mut}*BCD* from strain BC33. Using the Type II CRISPR-Cas9 system, I replaced the native promoters of the genomic *leuABCD* operon with the strong IPTG-inducible P_{lacUV5} promoter, and replaced the RBS of *leuA* (including all regulatory sites) with the previously-used strong synthetic RBS. Simultaneously, I replaced the *leuA*-coding gene with the feedback-resistant *leuA*^{mutant}. However, when the resulting strain BC43 was transformed with corresponding plasmids for fermentation, even-chain-iso products predominated over odd-chain-iso products (as seen for strains BO43I in Figure 3-6a). This result indicated that the *leuA*^{mut}*BCD* requires very fine-tuning and that a single copy of *leuA*^{mut}*BCD* was insufficient to convert all the intracellular 3-methyl-2-oxobutyric acid to 4-methyl-2-oxopentanoic acid, further proving that pA15a::P_{BAD}-leu*A*^{mut}*BCD* provides optimal expression level for the α-Keto Acid Synthesis Module. Consistency in expression parameters indicates that the optimal levels derived in this work may be applicable in other systems requiring the use of an α-keto acid pathway.

Then, I chose *lplA* as the gene to be integrated into the host cell's genome; low expression was previously determined to be sufficient to fully functionalize the BKD E2 subunit [112]. Furthermore, it has been demonstrated that even low-level overexpression of the global regulator of fatty acid metabolism *fadR* increases fatty acid production [7, 48]. Thus, *fadR* was cloned to the same operon of *lplA* under the control of the P_{LacUV5} promoter. The synthetic P_{LacUV5}-*fadR*-*lplA* operon was then integrated into the native *ldhA* (involved in lactate production) site of strain BC43, resulting in strain BC63 (Figure 3-6b). Deletion of *ldhA* was expected to reduce lactate formation during fermentation [25].

Strain BC63 was then engineered to produce BLFL with controlled chain structure. To produce even-chain-iso BLFLs from glucose, I created strain BO63V by co-transforming the plasmids pB5k-*maqu2220* and pE2s-*alsS-ilvCD* into strain BC63 (Table 3-2, Figure 3-6b). When fermented in the absence of α-keto acid, BO63V produced 52.4 mg/L of even-chain-iso fatty alcohols (Figure 3-6a, Supplementary Figure 3-4). To produce odd-chain-iso fatty alcohols from glucose, the plasmid pA8c-*leuA*^{mut}*BCD* was further transformed to strain BO63V (Figure 3-6b). The resulting strain BO63L produced 122 mg/L of odd-chain-iso BLFLs, comprising 70% of the total BLFLs (Figure 3-6a, Supplementary Figure 3-4). Although the odd-chain-iso BLFL pathway is less carbon efficient than the even-chain-iso BLFL pathway due to the loss of a CO_2 during 4-methyl-2-oxopentanoic acid biosynthesis, the $_{Sa}$FabH has higher specificity towards 3-methylbutyryl-CoA (the precursor for odd-chain-iso products) than 2-methyl-propanoyl-CoA (the precursor for even-chain-iso products) [113], thus leading to higher odd-chain-iso BLFL titer.

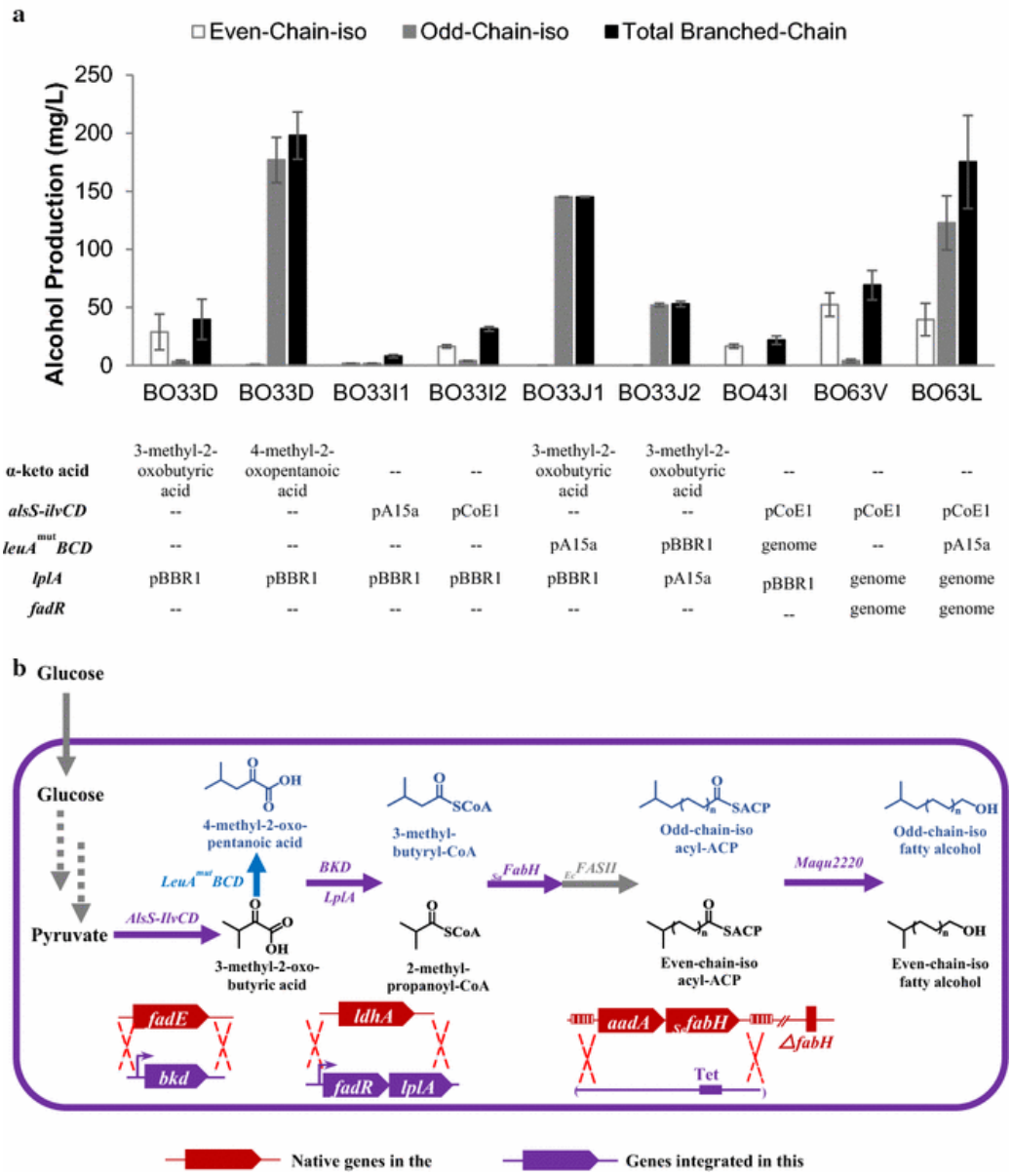

Figure 3- 6 Optimizing α-keto acid biosynthetic pathways in alcohol-producing strains containing $_{Ma}$Maqu2220

(a) Plasmids with different copy numbers and promoters were employed to bear the involved genes in different strains. The titers of even-chain-iso, odd-chain-iso, and total alcohol from all the strains containing α-keto acid biosynthetic pathways are compared with that of strain BO33D with either 1 g/L 3-methyl-2-oxobutyric acid or 1 g/L 4-methyl-2-oxopentanoic acid supplementation. (b) The complete pathways and genome modifications involved in strain BC63V (purple) and BC63L (purple and blue).

a

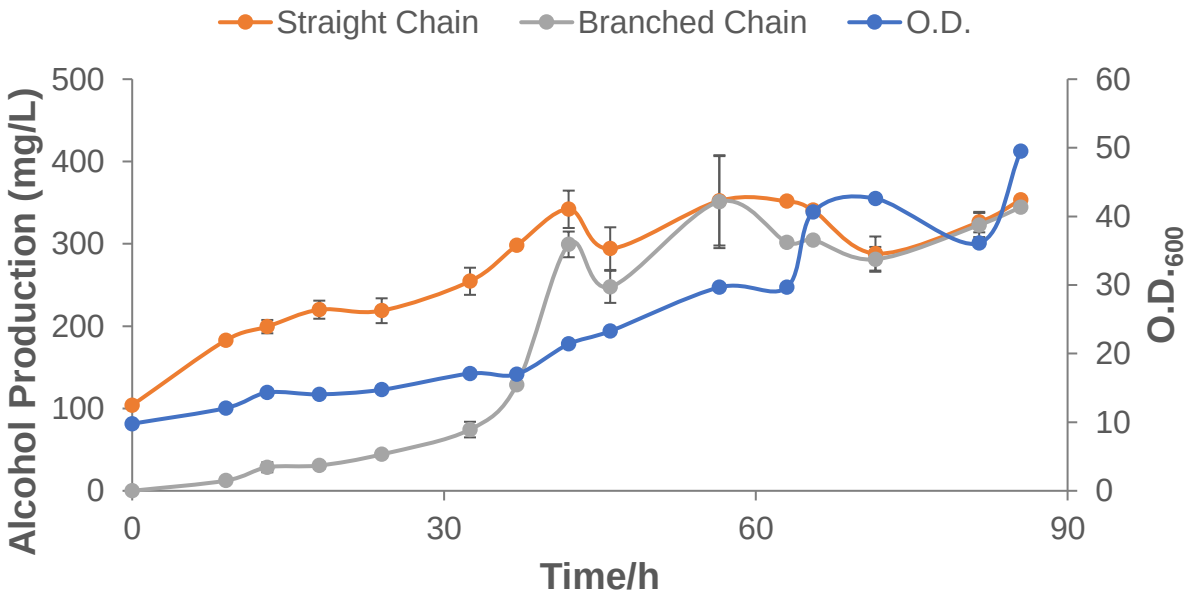

b

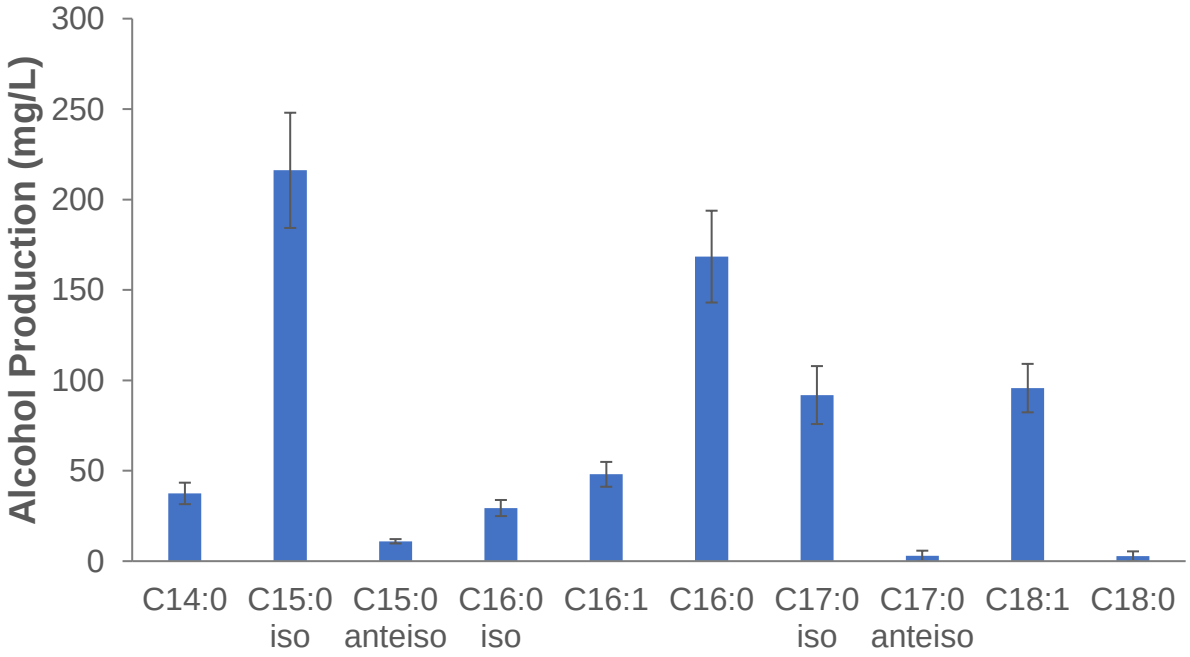

Figure 3- 7 Fed-batch production by strain BO63L
(a) Time-course plots of SCFL and BCFL titer and cell density. (b) BCFL profile at 85 hours during batch-fed fermentation.

Finally, I assessed the performance of strain BO63L in a 1 L glucose fed-batch fermenter (Section 3.2.4). After 85 hours of cultivation, BLFLs accumulated to 350 mg/L (Figure 3-7a). The concentration of 14-methyl-pentadecanol, the most abundant product, reached 217 mg/L (Figure 3-7b). Interestingly, straight LCFLs accumulated rapidly after induction, while BLFL titers did not increase until 32 h (Figure 3-7a). I suspect that the initial straight-chain alcohol accumulation may result from the leaky expression of Maqu2220 prior to induction. Further optimization of fermentation conditions (such as pH, air flowing rate, stirring rate, etc.) might improve the percentage and yield of BLFL. Overall, these results demonstrate the potential of strain BO63L for high-titer production of BLFLs and suggest that further studies might lead to its use on an industrial scale.

3.4 Discussion

Although alcohol-producing pathways have been previously engineered to produce straight LCFLs and short-chain alcohols, little effort has been made to produce BLFLs. In this work, I characterized the capability and substrate specificity of four different alcohol-producing pathways for BLFL production. I demonstrated the highly selective production of two types of BLFLs (odd-chain-iso and even-chain-iso) by engineering the upstream pathways for precursor synthesis. I obtained high BLFL proportions out of total fatty alcohols (strain BO63L, yielded 80%). I also obtained comparable BLFL titers (strain BO63L, 175 mg/L in the absence of any precursor) to BCFA titers, despite the extensive additional engineering required for BLFLs production. The modular engineering strategy allowed us to apply the knowledge learned from the AAR pathway to the new identified Maqu2220 pathway for rapid optimization, quickly yielded strain BO63L that produced 350 mg/L BLFLs in a fed-batch fermenter. Because BLFLs can be directly used in

skin-care or sunscreen products, and are good candidates for diesel fuels, the production of specific BLFL species in high percentages may directly benefit the cosmetics and bioenergy fields.

Meanwhile, I partitioned the complete pathway into three modules: a precursor formation module (the α-Keto Acid Synthesis Module), an acyl-CoA activation and malonyl-ACP consumption module (the Acyl-ACP Generation Module), and a final product synthesis module (the Alcohol Formation Module). Each module can be separately engineered and tuned for novel chemical synthesis. Furthermore, when the tuned modules are combined, the expression level of each module can be tuned to avoid imbalance and to improve product titer. I demonstrated consistent expression parameters that result in optimal productivities, which can be used for the production of other chemicals. Together with previous successes in modular engineering of the isoprenoid pathway [129], the FFA pathways [46] and the ester pathways [130], I confirm that modular pathway engineering is an effective approach to improve product titer and yield.

The top-performing strain BO63L produced 350 mg/L BLFLs in fed-batch fermenter, still low compared to that of the best straight LCFL-producing strain (3.82 g/L in shake flask) [121]. Current pathway is not limited by α-keto acid because increasing the supplemented 4-methyl-2-oxopentanoic acid from 1 g/L to 8 g/L did not increase BLFL titer (Supplementary Figure 3-3). Furthermore, conversion of acyl-ACPs to BLFLs is not likely to be the limiting step due to the high conversion efficiency of Maqu2220 [121]. Thus, I believe the current bottleneck lies in the Acyl-ACP Generation Module, which requires further engineering to improve BLFL titer and yield. Previous engineering strategies developed to optimize free fatty acids production could be potentially used to further improve BLFL yield. These strategies include modulation of the fatty acid and the phospholipid biosynthesis pathway [131], implementing synthetic control systems to

dynamically regulate pathway gene expression [13, 14, 24, 48], and enriching the high-performing subpopulation using PopQC [24].

3.5 Conclusions

I have constructed and tested the capability of four different alcohol-producing pathways for BLFL production in engineered *E. coli*. Moreover, by engineering the α-keto acid biosynthetic pathways and balancing the expression levels of three different modules, I achieved BLFL titers of up to 350 mg/L from glucose, and BLFL percentages up to 79%. Overall, this work generates pathways and knowledge for the production of BLFLs in high percentages that will have broader industrial applications than straight LCFLs.

Supplementary Materials

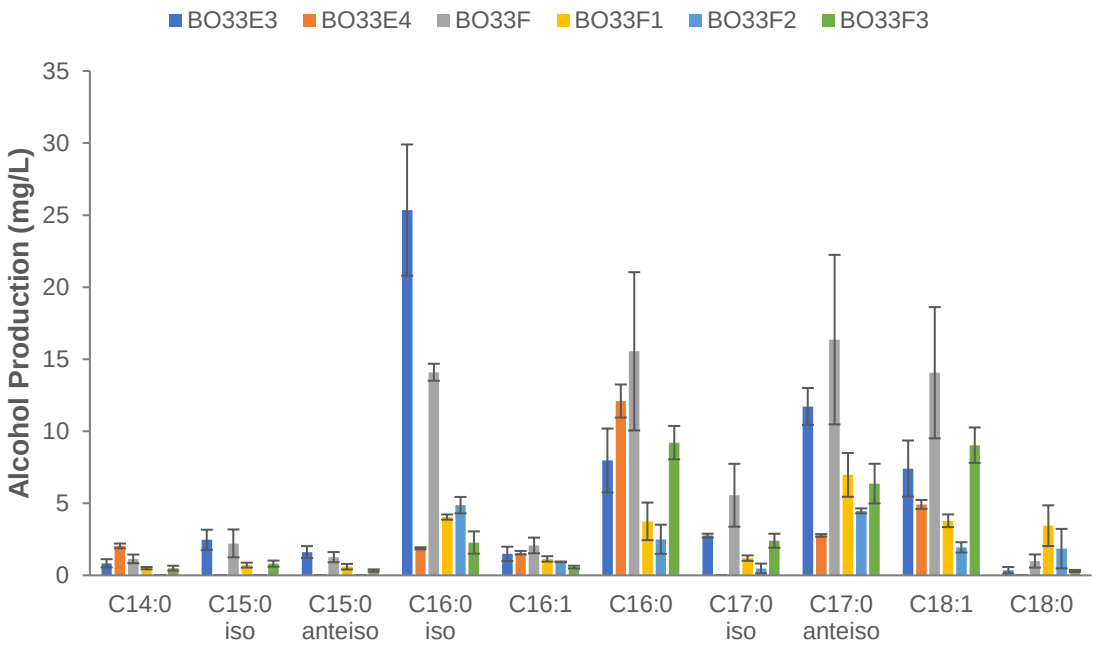

Supplementary Figure 3-1. Fatty alcohol profiles of strains involved in Figure 3-3b.

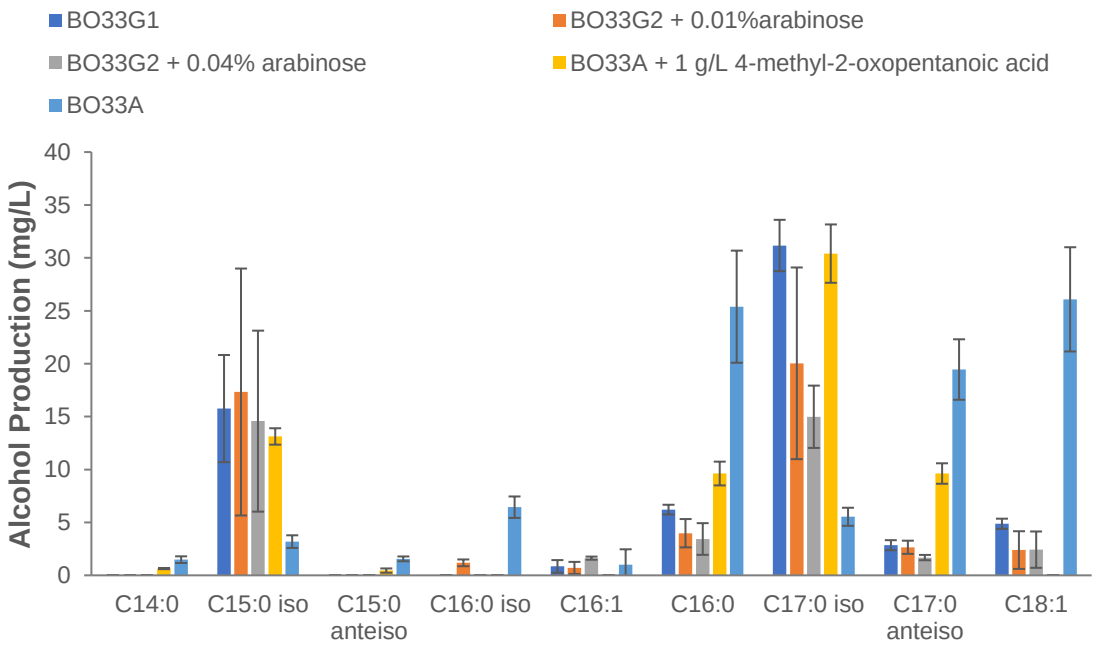

Supplementary Figure 3-2. Fatty alcohol profiles of strains involved in Figure 3-4b.

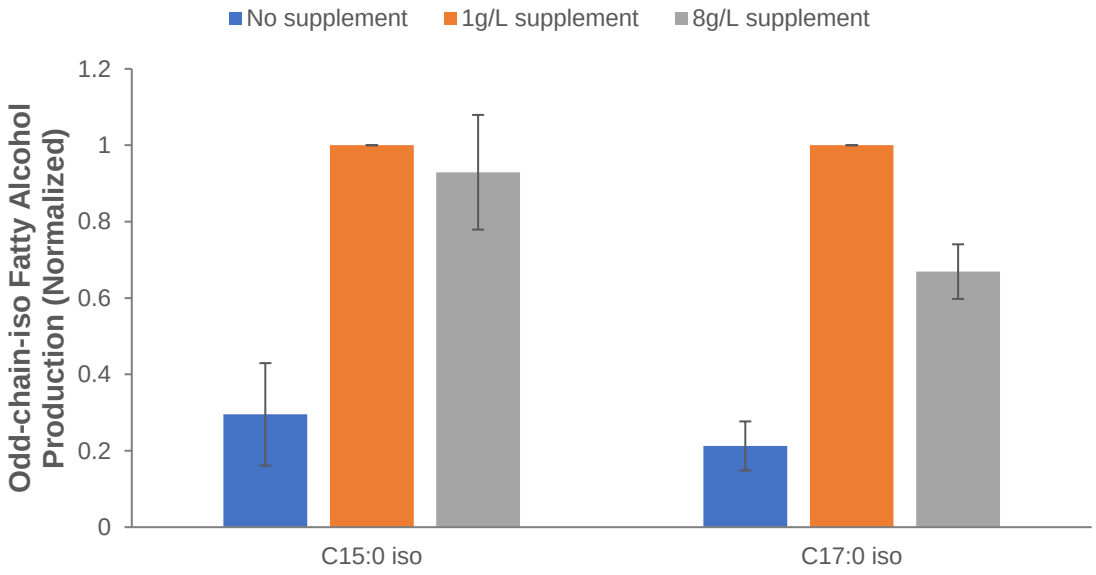

Supplementary Figure 3-3. Odd-chain-iso fatty alcohol production in strain BO33D with different concentrations of 4-methyl-2-oxopentanoic acid supplementation. The data has been normalized to the odd-chain-iso fatty alcohol production in strain BO33D with 1g/L 4-methyl-2-oxopentanoic acid supplementation.

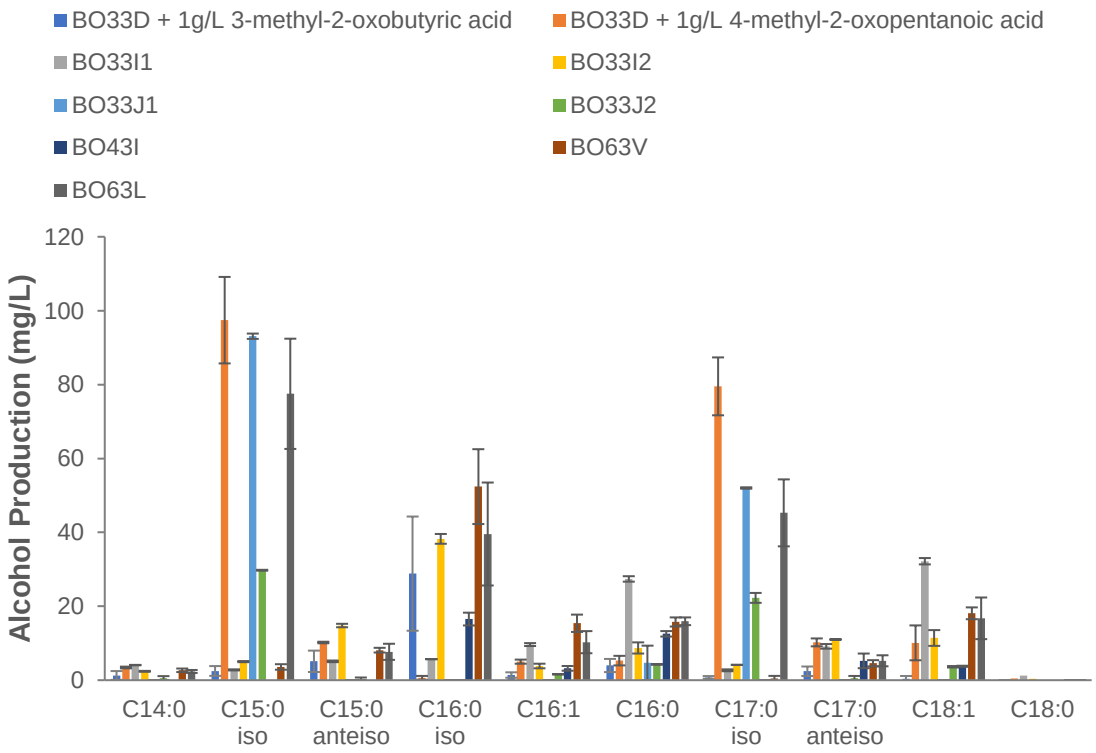

Supplementary Figure 3-4. Fatty alcohol profiles of strains involved in Figure 3-6a.

Chapter 4: Production of other fatty-acid-derived chemicals based on the established non-natural fatty acid biosynthetic pathway

4.1 Introduction

Increasing concerns about national security and the global petroleum supply have driven the development of state-of-art technologies for the sustainable production of chemicals, materials, and fuels that are currently derived from petroleum [132]. Engineering microbes for chemical production is particularly attractive because it allows the conversion of renewable and low-cost feedstocks (such as lignocellulosic biomass and CO_2) into products with precise structures [55, 133] without the use of high temperatures and pressures. Currently, extensive research focuses on engineering the fatty acid biosynthetic pathway [134-137], and especially on the efficient bioconversion of produced fatty acids to other chemicals including alkanes [124], alkenes [50], alcohols [138], aldehydes [124], and esters [48]. These chemicals can be used as biofuels [55, 138], pharmaceuticals [139], polymer precursors [140], and lubricants [141].

The biosynthesis of alkanes and esters are of particularly great interest because they are biofuels with promising physiochemical and combustion properties that are similar to those of petroleum-based fuels. Like fatty alcohol, fatty acid esters and alkanes can be synthesized from the same intermediates of the fatty acid synthetic pathway: fatty acyl-ACP or fatty acyl-CoA. Fatty acid esters have been produced by esterifying acyl-CoA with methanol or ethanol using a wax ester synthase (AtfA), while alkanes have been generated from fatty aldehyde by aldehyde-deformylating oxygenases (ADO) from various origins (Figure 4-1).

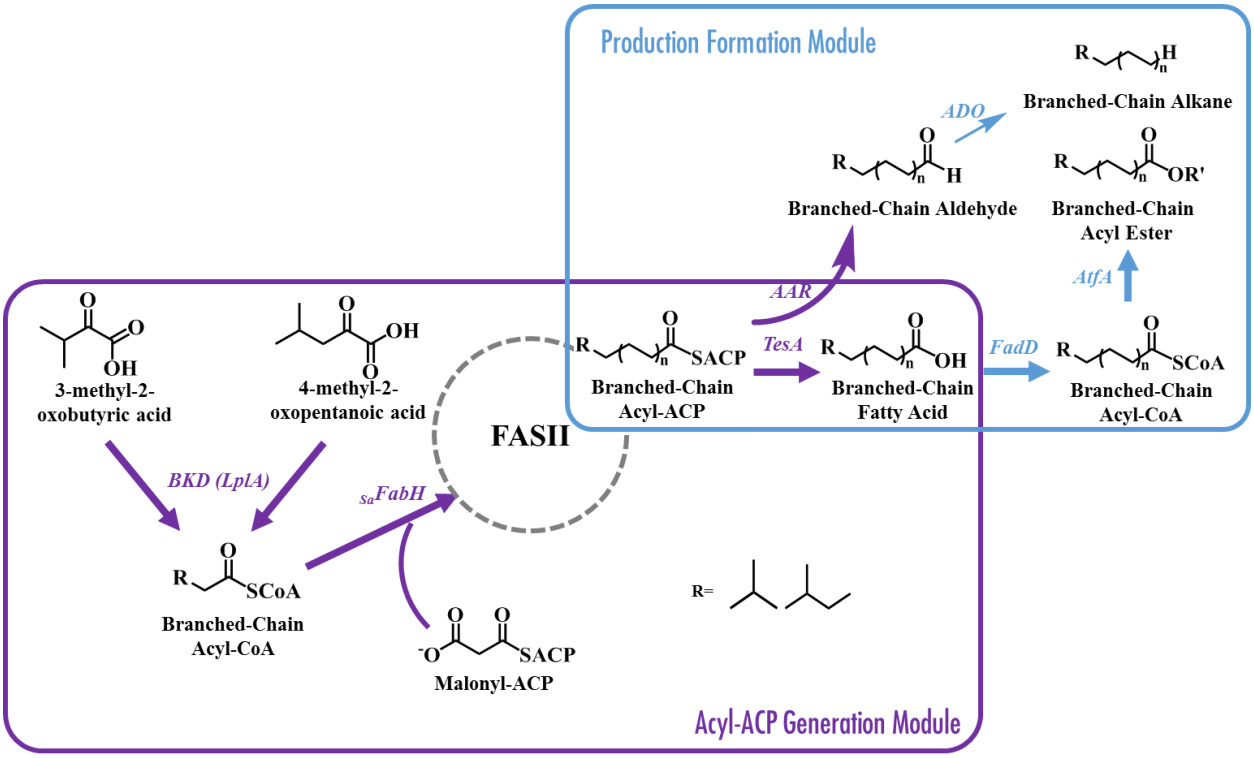

Figure 4- 1 Biosynthetic pathways for alkane and ester production
The Acyl-ACP Generation Module (Module B) incorporates α-keto acid into the fatty acid biosynthetic pathway. The Product Formation Module (Module C) converts branched-chain acyl-ACPs to alkanes and esters.

Most previously biosynthesized alkanes and fatty acid esters have straight aliphatic chains, which have relatively higher freezing points than their petroleum-derived, branched-chain counterparts, limiting their low-temperature operability. Thus, there is much impetus to biosynthesize fuels derived from branched-chain fatty acids (BCFAs) to such improved properties as a lower freezing point and better cold flow. In this chapter, I applied the modular engineering strategy in Chapter 3 to produce branched-chain alkanes and branched-chain fatty acid ethyl esters (BCFAEEs).

4.2 Materials and Methods

4.2.1 Materials and Media

Phusion DNA polymerase was purchased from New England Biolabs (Beverly, MA, USA). Restriction enzymes, T4 ligase, gel purification kits, and plasmid miniprep kits were purchased from Thermo Fisher Scientific (Waltham, Massachusetts, USA). All primers were synthesized by Integrated DNA Technologies (Coralville, IA, USA). BCFA standards (Bacterial Acid Methyl Ester Mix), SCFA standards (GLC-20 and GLC-30), and all the other reagents were purchased from Sigma Aldrich (St. Louis, MO, USA).

Minimal medium (M9 medium supplemented with 75 mM MOPS at pH 7.4, 2 mM $MgSO_4$, 1 mg/L thiamine, 50 μg/mL lipoic acid, 10 μM $FeSO_4$, 0.1 mM $CaCl_2$, and micronutrients, including 3 μM $(NH_4)_6Mo_7O_{24}$, 0.4 mM boric acid, 30 μM $CoCl_2$, 15 μM $CuSO_4$, 80 μM $MnCl_2$, and 10 μM $ZnSO_4$) containing 2% glucose and 0.5% yeast extract as carbon sources was used for cell growth and fatty alcohol production.

4.2.2 Plasmids and strains

Plasmids and oligonucleotides used in this study were listed in Table 4-1. Genes encoding *Prochlorococcus merinus* ADO (ADO), *Alicyclobacillus acidocaldarius* FabH ($_{Aa}$FabH), and *Megasphaera elsdenii* Pct (Pct) were codon-optimized for *E. coli* expression and synthesized by Integrated DNA Technologies (Coralville, IA, USA), whereas other genes were amplified by PCR and assembled into the backbones of BioBrick plasmids [64] using either restriction sites or Golden-Gate DNA assembly method [65].

Table 4- 1 Plasmids used in Chapter 4

Plasmids	Replication ori	Overexpressed operon	Resistance	Refs
pB5k-tesA	pBBR1	P_{lacUV5}-*tesA*(*E. coli*)	Kan^R	This study
pE8c-pct	ColE1	P_{BAD}-*pct*(*M. elsdenii*)	Cm^R	This study
pSa-P_{ecfabH}-$_{Aa}$fabH	SC101	P_{ecfabH}-*fabH* (*A. acidocaldarius*)	Amp^R	This study
pE5c-fadD-atfA	pBBR1	P_{lacUV5}-*fadD*(*E.coli*)-*atfA*	Cm^R	This study
pE8c-ado	ColE1	P_{BAD}-*ado*(*P. merinu*)	Cm^R	This study
pE8k-lplA	ColE1	P_{BAD}-*lplA*(*E. coli*)	Kan^R	This study
pB5k-tesA-lplA	pA15a	P_{lacUV5}-*tesA*-*lplA* (*E. coli*)	Kan^R	This study

Table 4- 2 Strains used in Chapter 4

Strains	**Relevant genotype**	**Reference**
CL111	UB1005, attHK022::(*plsX'fabH*; *aadA*) *fabH*::kan	[67]
CL111(*⊿Kan*)	CL111 ⊿kan	Chapter 2
BC73	BC63 *⊿yjgB*	This study
BC14	CL111(*⊿Kan*) pSa-P_{ecfabH}-$_{Aa}$*fabH*	This study
BA33A	BC63 pB5k-*aar*-*lplA*, pE8c-*ado*	This study
BA73A	BC73 pA8c-*aar*-*lplA*, pB5k-*ado*	This study
BE33A	BC33 pB5k-*tesA*-*lplA*, pE5c-*fadD*-*atfA*	This study
BC14A	BC14 pB5k-*tesA*, pE8c-*pct*	This study
BO14D	BC14 pB5k-*maqu2220*, pE8c-*pct*	This study

E. coli DH10B was used for cloning purposes. *E. coli* strains CL111 [67] was used for production purposes. To created strain BC14, plasmid pSa-P_{ecfabH}-$_{Aa}$fabH was transformed into CL111(*⊿Kan*) strain, and the $_{Se}$*fabH* was knocked out by P1 transduction [67]. The genomic *yjgB* was deleted in BC63 strain using a previously described CRISPR-Cas9 gene replacement method (Jiang Y. et al. 2015), creating strain BC73. Other strains were created by transforming the corresponding plasmids (Table 4-2) into corresponding parental strains, respectively.

4.2.3 Cell culturing and α-keto acids supplementation

Overnight cultures were inoculated 2% v/v into M9 minimal medium (in section 4.2.1) with corresponding antibiotics for adaptation. Overnight cultures in minimal medium were then used to inoculate 5 mL of the same fresh minimal medium with an initial OD_{600} of 0.08. Cells were induced

with proper inducers (1mM IPTG, 0.4% arabinose, and/or 200 nM aTc) when OD_{600} reached 0.8 or as otherwise specified. For α-keto acids supplementation experiments, one of the α-keto acids (3-methyl-2-oxobutyric acid, 4-methyl-2-oxopentanoic acid, or glycolic acid) was added at OD_{600} = 0.8 to a final concentration of 1 g/L. For alkane production experiments, 0.5 mL decane was added to each sample as an organic layer to extract alkanes. For ester production experiments, ethanol or isopropanol was added at a final concentration of 5% v/v, respectively. Cells were harvested three days after induction.

4.2.4 Quantification of the products

For the quantification of diols and fatty acid esters, 1 mL of cell culture was acidified with 100 μL of concentrated HCl (12N). Diols and esters were extracted twice with 0.5 mL of ethyl acetate. For derivatization of diols, 200 μL of supernatant from each sample was transferred to 2 mL clear glass GC vials (Agilent Technologies, Santa Clara, CA), mixed with 200 μL of N,OBis(trimethylsilyl)trifluoroacetamide with 1% v/v chlorotrimethylsilane, and incubated at 60 °C for 2 h. Both diol derivatives and fatty acid esters were quantified using a GC-MS (Hewlett-Packard model 7890A, Agilent Technologies) equipped with a 30 m DB5-MS column (J&W Scientific) and a mass spectrometer (5975C, Agilent Technologies) or a FID (Agilent Technologies) detector. For each ester sample, the column was equilibrated at 80 °C, followed by a ramp to 280 °C at 30°C/min, and was then held at 280 °C for 3 min. For each diol sample, the column was equilibrated at 80 °C, followed by a ramp to 300 °C at 20°C/min, and was then held at 300 °C for 3 min. Individual peaks were identified by comparing their retention time to those of diol standards (mixture of 12-hydroxy-1-dodecanol, 14-hydroxy-1-tetradecanol and 16-hydroxy-1-hexadecanol, prepared and derivatized identically to samples) or FAEE mixtures (Sigma Aldrich).

Concentrations of each component were determined by comparing the area of each peak to a standard curve generated by corresponding standards eluted using the same method.

To quantify alkanes, the decane organic layer was extracted and diluted 10 times. Then the samples were quantified using a GC-FID (Agilent 6890A) equipped with a 30 m Rtx-1 column (Restek, Bellefonte, PA). For each sample, the column was equilibrated at 45 °C for 4 min, followed by a ramp to 300 °C at 15°C/min, and was then held at 300 °C for 5 min. Individual alkane peaks were identified by comparing their retention time to those of standard alkane solutions (Sigma Aldrich). Concentrations of each alkane were determined by comparing the area of each alkane peak to a standard curve generated by standard alkane mixtures eluted using the same method.

Product titer for each strain was measured in biological triplicate (starting from three different colonies), and average values are reported.

4.3 Results

4.3.1 Testing alkane-producing pathways in BCFA-producing strains

Based on the optimal expression level for all three Modules in Chapter 3, I expanded the application of Module (C) for various chemical productions (Figure 3-1). First, I focused on alkane, another important product derived from the fatty acid synthetic pathway. The alkane-producing pathway is well-known in cyanobacteria and plants [124, 142]. The key enzyme, aldehyde-deformylating oxygenase (ADO), has been isolated and characterized to catalyze the reducing reaction from aldehyde to alkanes. In this chapter, I selected AAR to construct the alkane-producing pathways, because I suspected that Maqu2220 already contained a subunit functioning as ADH, which would direct the metabolic flux towards alcohol production. In order to produce

branched-chain alkane, the *ado* gene from *Prochlorococcus merinus* [143-146] that encodes ADO was overexpressed in strain BO33A, to generate strain BA33A (Figure 4-1). When cultivated in 37°C without supplementation, strain BA33A produced 8 mg/L total alkane, and 1.7 mg/L branched-chain alkane. When 4-methyl-2-oxopentanoic acid was supplemented, the BC alkane titer increased to 10 mg/L, comprising 74% of total alkane production (Figure 4-2) and representing the highest BC alkane titer and percentage published to date.

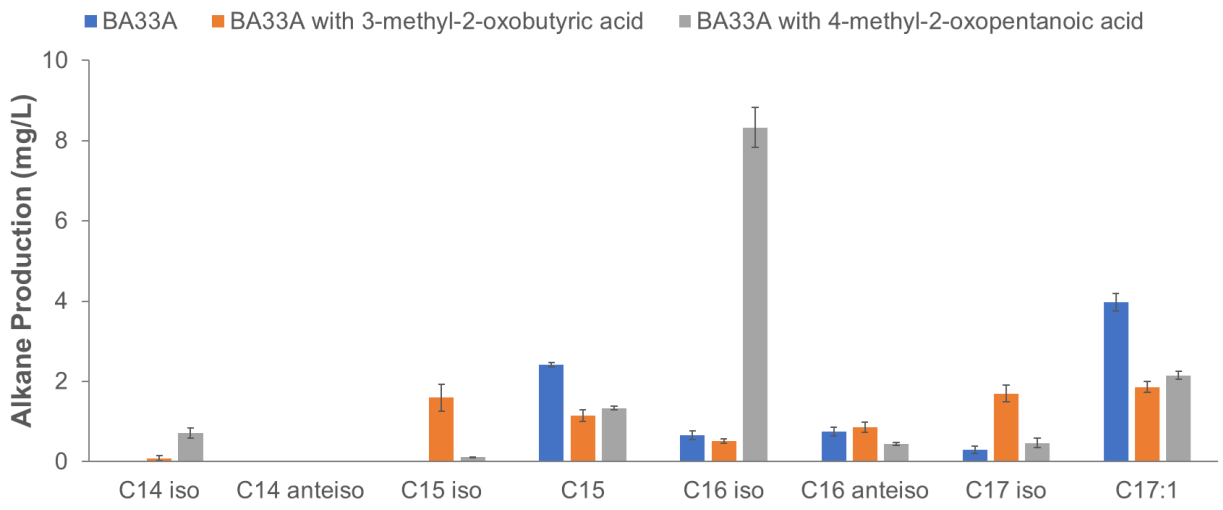

Figure 4- 2 Branched-chain alkane production from strain BA33A

Many studies have shown that the deletion of *E. coli* endogenous alcohol dehydrogenase increases the aldehyde accumulation and thus improves the alkane production [147, 148]. As shown in Figure 3-2c, endogenous ADH YjgB has a high specificity toward long-branched-chain aldehyde, so I deleted the *yjgB* gene in strain BC63 genome by CRISPR-Cas9, followed by transforming corresponding plasmids into the resulting strain BC73, hoping the branched-chain alkane production would improve in the resulting strain, BA73A. However, BA73A produced similar amounts of alkane regardless of whether α-keto acid was supplemented or not (data not shown). One possible reason might be that the alkane generation rate of ADO was so slow that the

deletion of endogenous *adh*s could not help to redirect the flux towards alkane. Or there are too many endogenous *adh*s that could reduce the long-branched-chain aldehyde to alcohols, thus the deletion of a single *adh* gene (*yjgB*) would not decrease the alcohol generation rate. Other strategies, such as overexpression of fatty alcohol oxidase (FAO) and/or manipulation all the factors related to fatty aldehyde dynamic pools [149], might further improve the branched-chain alkane production.

4.3.2 Assembling the ester-producing pathway in BCFA-producing strains

The production of fatty acid ethyl esters (FAEE), the major component of biodiesel, has been demonstrated in *E. coli*. However, the microbially-produced FAEE primarily consist of ethyl-palmitate, which has a melting point of 23ºC, and so is not suitable in cold weather. Alternatively, ethyl-anteiso-methyl-palmitate does not freeze until the temperature reaches 3.8ºC, a much more amenable temperature for direct usage in a variety of climates, demonstrating the value of BCFAEEs [150, 151].

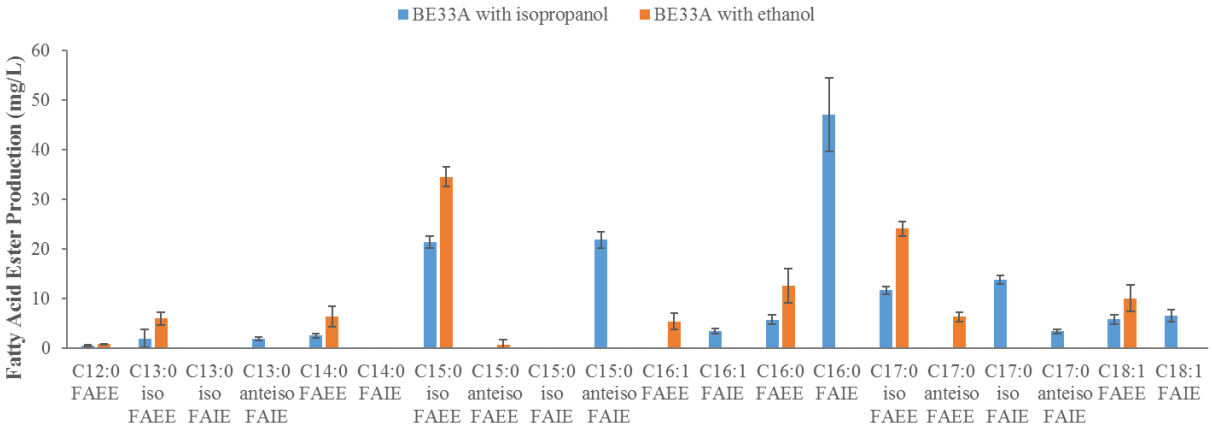

Figure 4- 3 Fatty acid ester production from strain BE33A
Data generated by Dr. Gayle Bentley.

Just as for the BCFL production, I first focused on the Module C to produce BCFAEEs from BCFAs. Strain BE33A was constructed by transforming the plasmid pB5k-fadD-atfA into BCFA-producing strain BC33A (Table 4-2). Free BCFAs were converted into branched-chain acyl-CoAs by an acyl-CoA synthase (encoded by *fadD*) and then transesterified to BCFAEEs by a wax ester synthase (encoded by *atfA*). When cultivated with supplementation of 1 mg/L of 4-methyl-2-oxopentanoic acid and 5% ethanol, strain BE33A produced 71 mg/L FAEE, with BCFAEE comprising 66.9% of the total FAEE (Figure 4-3).

Finally, I attempted to generate branched-chain esters with branches at both termini (branched-chain fatty acid isopropyl esters), through the *in vivo* transesterification of isopropanol rather than ethanol. Strain BE33A was supplemented with 5% isopropanol at the point of induction. Fatty acid esters from BE33A, observed by GC-MS, contained branches at both the fatty acyl terminus and the ester terminus, reaching 68 mg/L and 61.4% of the total fatty acid isopropyl esters produced (Figure 4-3**)**. There is no data describing the freezing point of these branched-chain fatty acid isopropyl esters (BCFAIEs), but theoretically, the freezing point of the double-branched fatty acyl esters will be lower than that of the esters with a single branched terminus, increasing the value of the resultant fuel.

4.3.3 α, ω-diol production by switching the *fabH* and engineering the precursor formation module

After exploring the different possibilities for product generation module (Module C) to produce branched-chain alcohols, alkanes and esters, I sought to engineer the acyl-CoA activation (Module A) and malonyl-ACP consumption module (Module B) to incorporate other ω-functional groups into fatty acid chain (Figure 3-1). I first chose ω-hydroxy group, because ω-hydroxy fatty acids and α,ω-diols are valuable precursors to polyesters [152], and the enzyme Pct from *M.*

elsdenii has been identified to produce 2-hydroxyacetyl-CoA from 2-hydroxyacetic acid (glycolic acid).

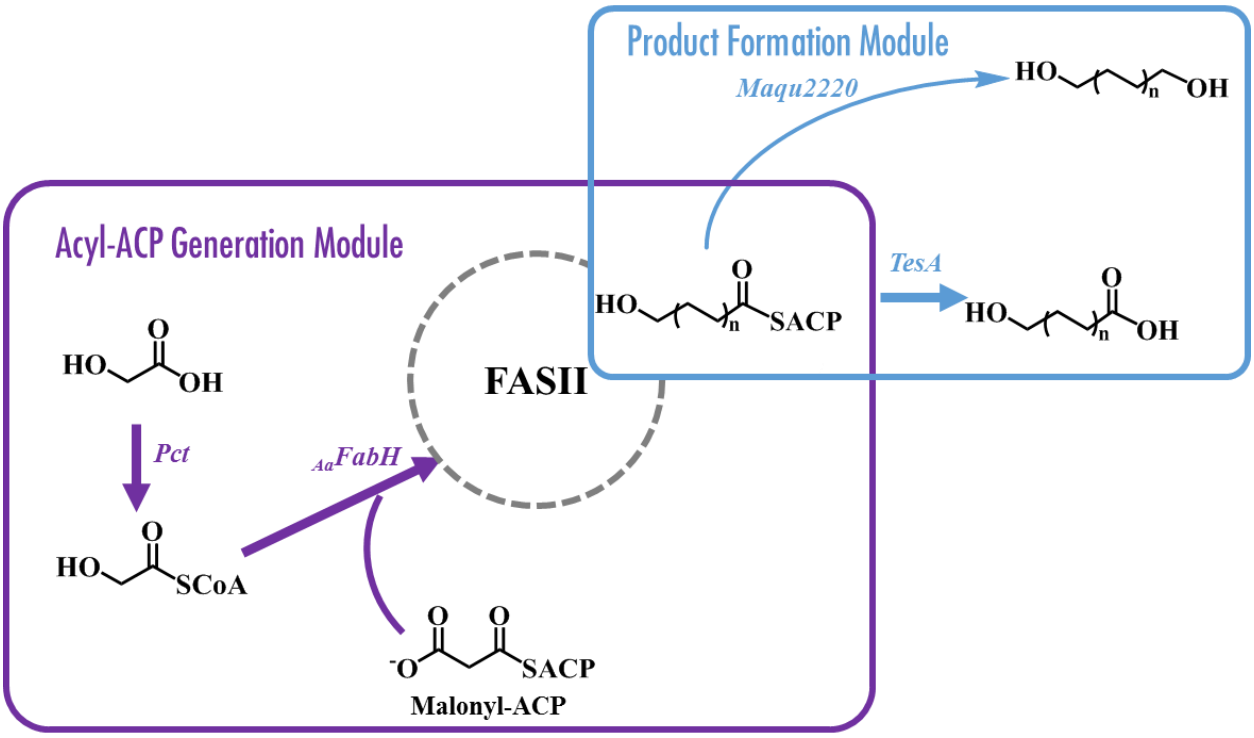

Figure 4- 4 Biosynthetic pathways to generate ω-hydroxy products
The Acyl-ACP Generation Module (Module B) incorporates ω-hydroxy-acyl-CoA into the fatty acid biosynthetic pathway. The Product Formation Module (Module C) converts ω-hydroxy-acyl-ACP to ω-hydroxy acid and diols.

I first sought to engineer the Module B by replacing *E. coli* native *fabH* with a ω-hydroxy acyl-CoA-specific *fabH* using similar strategy described in Chapter 2. Because no FabH has ever been reported to uptake ω-hydroxy acyl-CoA, I selected the FabH from *Alicyclobacillus acidocaldarius*, which was reported to uptake 3-hydroxybutyryl-CoA as a substrate. Strain BC14 carrying $_{Aa}$*fabH* was constructed from parental strain CL111(*ΔKan*) through P1 transduction in the same way as strain BC13. Then plasmids pE8c-pct and pB5k-maqu2220/pB5k-tesA were transformed into strain BC14 to create the producing strains BC14A and BO14D, respectively.

However, when glycolic acid was supplemented in the cell culture, no ω-hydroxy products were detected in either strains. This result indicated that either $_{Aa}$FabH or FASII elongation enzymes could not uptake ω-hydroxy substrates.

4.4 Discussion

In this chapter, I applied the modular BCFA synthetic pathway to generate biofuels with desirable cold-flow properties for specific fuels. Strain BA33A can produce branched-chain alkane with a percentage of 74%, which can be readily used as jet fuel. Similarly, strain BE33A, which can produce BCFAEE and BCFAIE in high percentages, will also benefit the biodiesel industry.

The next step was to expand the profile of the products from this NNFA biosynthetic pathway to include bifunctional chemicals. Here I started by incorporating the ω-hydroxy group, but was unsuccessful, probably due to the unsuitable FabH. On the other hand, to generate ω-hydroxy fatty acid, the ω-hydroxy group can also be introduced by P450 enzymes after FASII elongation steps [152]. I tried this pathway to produce α, ω-diols, but it suffered from low titers and the significant co-production of fatty alcohols (data not shown). This fact also demonstrated the superiority of this NNFA synthetic pathway to produce ω-functionalized fatty acid derivatives in a high percentage and called for an effective method to screen and select for suitable FabHs.

4.5 Conclusion

In this chapter, I engineered the BCFA-producing strains to generate branched-chain alkanes and esters in high percentages, which can be readily used as biofuels with desirable cold-flow properties. I also explored the possibility of producing ω-hydroxy fatty acids and α,ω-diols by engineering Module A and Module B in the NNFA synthetic pathway.

Chapter 5: Establish a cell-free platform for producing fatty acid and derivatives

5.1 Introduction

The success of BCFA production in engineered *E. coli* demonstrated the versatility of *E. coli* FASII elongation enzymes in accepting substrates with branched terminal groups, paving the way for the bioproduction of bifunctional fatty-acid-based chemicals, such as ω-hydroxy acids, ω-ethenyl acids, ω-ethynyl acids, and ω-azido acids. These chemicals have appealing applications: ω-hydroxy acids are monomer building blocks for polymers, and acids with ethenyl, ethynyl, or azido groups have the potential for protein tagging and labelling in protein chemistry. In addition, the engineered BCFA synthetic pathway can provide a suitable platform to test the capacity of the FASII enzymes to uptake the ω-functionalized substrates, while the modular pathway engineering strategy can simplify the test by decoupling it from the generation of acyl-CoA precursors.

However, even with the supplementation of those specific α-keto acids or acyl-CoA precursors, there would still be several obstacles to running the test *in vivo*, including the intracellular transport barriers of the precursors and the toxicity of those bi-functional molecules to the cells. Meanwhile, the *in vitro* system offers a complementary approach, which can also overcome other shortages for *in vivo* biomanufacturing practices, most notably, these are the cell's inherent limitations (mainly the cost of carbon and energy for cell growth, maintenance, and byproduct formation [64]) and the unwieldy complexity of cells [64-66].

Although the *in vitro* reconstitution of the fatty acid synthase in *E. coli* has been achieved using purified enzyme systems [88], I chose crude lysates to build this biosynthetic pathway for several reasons: 1) The fatty acid productivity could be easily affected by the molar ratio of the FASII enzymes, and the fatty acid overproducing cell lines have molar protein ratios that are close to optimal; 2) The native metabolic enzymes and cofactor regeneration in the crude lysates will result in a higher titer than that of the purified systems, which will make identification of products much easier; 3) The crude lysates inherently provide the context of native-like metabolic networks [153-156].

Quick and efficient biosynthesis of several chemicals has been achieved with high productivities by cell-free metabolic engineering (CFME) using crude lysates, such as mevalonate [155], n-butanol [153], and 2,3-butanediol [157]. In all these cases, the enzymes involved in the metabolic pathways have been overexpressed. However, considering the robustness and integrity of FASII enzymes, I used cell endogenous FASII enzymes without any engineering or overexpression in this work (except heterologous overexpressed FabH). I used several strategies to construct and optimize the CFME reaction and achieved both straight-chain and branched-chain fatty alcohol production *in vitro*.

5.2 Materials and Methods

5.2.1 Strains, plasmids and media

Strains used in this study were listed in Table 5-1. Genes encoding *E. coli accABCD* was amplified from the genome and assembled into the pE8c backbone using Golden-Gate DNA assembly method [65].

2×YTPG media (16 g/L tryptone, 10 g/L yeast extract, 5 g/L NaCl, 7 g/L KH_2PO_4, 3 g/L K_2HPO_4, 18 g/L glucose) without any antibiotics was used to cultivate cells for lysate preparation.

Table 5- 1 Strains used in Chapter 5

Strains	Relevant genotype	Reference
JBEI-9018	MG1655 *ΔfadE*, *araD: acpS* (*C. glutamicum*), pB5k-maqu2220	[121]
DH1acc	DH1(*ΔfadE*) pE8c-accABCD	This study
BC13A	CL111 (*plsX'fabH*; *aadA*)::Tet^A pSa-$P_{ecfabH\text{-}Sa}$fabH, pB5c-tesA-bkd	Chapter 2
BO33D	CL111 (*plsX'fabH*; *aadA*)::Tet^A, *△Kan, fadE::bkd,* pSa-$P_{ecfabH\text{-}Sa}$fabH, pB5k-maqu2220-lplA	Chapter 3

5.2.2 Cell extract preparation

Cell lysates were prepared using a previously published protocol [158]. In detail, *E. coli* cells were pre-cultivated in LB medium with proper antibiotics. Overnight cultures were inoculated 2% v/v into 2×YTPG minimal medium (described in section 5.2.1) at 37 °C with vigorous shaking at 250 rpm. When OD_{600} reached 0.8, cells were induced with proper inducers (1mM IPTG, 0.4% arabinose and/or 200 nM aTc, or as otherwise specified) and grown for 4h at 30 °C. The cells were harvested by centrifuging at 8000 g at 4 °C for 15 min and were washed twice with ice-cold S30 buffer (10 mM Tris-acetate (pH8.2), 14mM $Mg(Ac)_2$, and 60 mM potassium glutamate). Then the pelleted wet cells were weighed and suspended in 0.8 mL of S30 buffer per1g wet cell mass. Suspended cells were lysed using a Qsonica Sonicator Q700 (Qsonica, Newtown, CT) with a 1.6 mm diameter probe at frequency of 20 kHz and 50% of amplitude. The various input energies (Joules) were used, and the optimal input energies for different strains were identified by following cell-free protein synthesis (CFPS) reactions. The lysates were then centrifuged twice at 21,100 g at 4 °C for 15 min. All the prepared cell extracts were flash frozen in liquid nitrogen and stored at -80 °C until use.

5.2.3 Protein quantification in cell lysates and CFPS reactions

The total protein concentration of the extracts was measured by Bradford protein assay with a bovine serum albumin standard. The extracts were subsequently run on a 12% SDS-PAGE gel with Coomassie-blue staining analysis.

The CFPS reactions were carried out following a published protocol [158]. In detail, a 25 μl CFPS reaction was prepared by mixing the following components in a 1.5 mL microtube: 1.2 mM ATP; 0.85 mM each of GTP, UTP, and CTP; 34.0 mg/mL L-5-formyl-5, 6, 7, 8-tetrahydrofolic acid (folinic acid); 170.0 mg/mL of *E. coli* tRNA mixture; 130 mM potassium glutamate; 10 mM ammonium glutamate; 12 mM magnesium glutamate; 2 mM each of 20 amino acids; 0.33 mM nicotinamide adenine dinucleotide (NAD); 0.27 mM coenzyme-A (CoA); 1.5 mM spermidine; 1 mM putrescine; 33 mM phosphoenolpyruvate (PEP); 13.3 mg/mL plasmid pJL1-sfGFP; 100 mg/mL T7 RNA polymerase, and 10 mg/mL of cell extract. The CFPS reactions were carried out at 37 °C for 24 h. For each sample, 2 μL of reaction mix was diluted with 48 μL of purified water, and the fluorescence of active sfGFP was measured by an Infinite F200PRO (TECAN) plate reader at excitation and emission wavelengths of 485 and 528 nm, respectively.

5.2.4 CFME reactions and products quantification

Reactions were carried out at 37 °C in 25 μl volumes for 4 h (or as otherwise specified). Each reaction consisted of mixing the cell-extracts along with 8 mM magnesium glutamate, 10 mM ammonium glutamate, 134 mM potassium glutamate, 10 mM K_2HPO_4 (pH = 7.2), 100mM BisTris, and various substrates and cofactors. Reactions were terminated by adding ethyl acetate in a 1:1 ratio. Then products were extracted and analyzed following the methods in section 2.2.4 and 3.2.5.

5.3 Results

5.3.1 Cell-free metabolic engineering for fatty acid production

To achieve cell-free biosynthesis of fatty acids, I first used strain BC13A for lysis and extract preparation. Various conditions were set up to produce straight-chain or branched-chain fatty acid as shown in Table 5-2 (A-D). The reaction mixtures were incubated at 37 °C for 4 h, then the amount of fatty acids in each sample was measured using previous analytical methods. As this was the first trial to test whether *in vitro* production of fatty acid from CFME reaction was even feasible, so I just used a well-established reaction protocol from Jewett Lab in Northwestern University. Further investigation and/or optimization of the reaction buffer setting/running time might be performed after the verification of the feasibility.

However, more than 30 mg/L C18:0 fatty acid (stearic acid) was observed in all the conditions (Figure 5-1), which the exceeded the theoretical yield (9 mg/L in the form of C18:0 fatty acid) calculated from the supplied NADPH. I sought to trace the source of the excess FFA by setting up different control reactions (Table 5-2 E-H). A high amount of FFA was detected in all the sources (Figure 5-1), including water, all the reagents, and the cell extract, which indicated that the detected FFA came from universal contamination rather than the reactions.

Table 5- 2 Reactions for fatty acid production from CFME

	A	B	C	D	E	F	G	H
15× SS	1×	1×	1×	1×	1×	1×	--	--
glucose (mM)	200	--	--	--	200	--	--	--
acetyl-CoA	--	25	--	25	--	25	--	--
α-keto acid (g/L)	--	--	1	1	1	1	--	--
K_2HPO_4 (mM)	10	--	10	--	10	--	--	--
Bis Tris Buffer (mM)	100	--	100	--	100	--	--	--
NAD^+ (mM)	0.5	--	0.5	--	0.5	--	--	--
$NADP^+$ (mM)	0.5	--	0.5	--	0.5	--	--	--
NADPH (mM)	--	1	--	1	--	1	--	--
ATP (mM)	1	1	1	1	1	1	--	--
CoA (mM)	0.5	--	0.5	--	0.5	--	--	--
BC13A lysate (mg/mL)	10	10	10	10	--	--	--	10

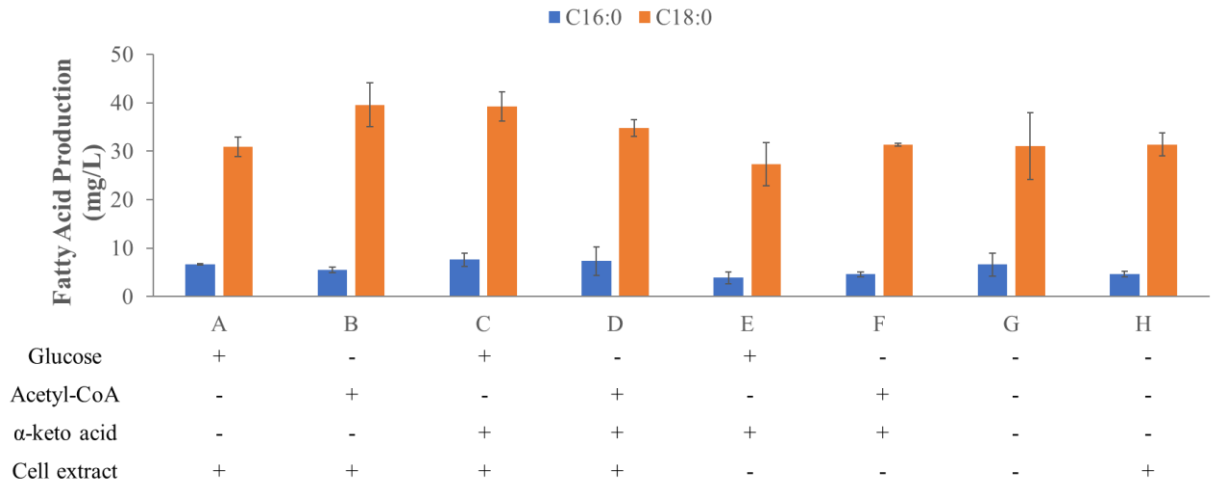

Figure 5- 1 Fatty acid production from CFME reactions

Because the amounts of detected FFA were comparable, indicating they were introduced from common steps, I assumed that the FFA contamination resulted from three external major sources: the surface of the tubes, the water used, and the incubation process. The effect of each factor was quantified by setting up various reactions (Supplementary Table 5-1). The results showed that the contamination induced during incubation was negligible (data not shown), but a large amount of

C16:0 and C18:0 fatty acids was introduced from the tube and water (Supplementary section). For a 25 μL reaction in a 1.5 mL tube, the C18:0 fatty acid contamination from the environment was roughly 20 mg/L.

5.3.2 Cell-free metabolic engineering for fatty alcohol production

Considering the difficulty of eliminating FFA contamination from the environment, I switched to the fatty alcohol pathway for this research. After confirming that no fatty alcohol would be introduced from the environment, I lysed two strains to generate cell extracts for straight-chain and branched-chain alcohol productions. Strain JBEI-9018 was reported to produce the highest amount of straight-chain alcohols to date [121], while BO33D strain is currently the best performing strain for branched-chain alcohol production.

I first tested the feasibility of the cell extracts to produce fatty alcohols *in vitro* by setting up a series of reactions (Table 5-3). Similarly, I used the same well-established protocol to run the reactions. Reaction O was set to detect the trace amount of alcohol in all the reagents and cofactors, while reactions A- and B- were used to evaluate the alcohol amounts in the cell extracts. All the reactions started with acetyl-CoA and malonyl-CoA as the substrate to uncouple the FASII synthesis from other endogenous reactions (such as glycolysis), and 4-methyl-2-oxopentanoic acid was supplemented as the precursor for branched-chain fatty alcohol production.

Table 5- 3 Reactions to produce fatty alcohols from CFME

	O	A-	A+	B-	B+
JBEI-9018 lysate	--	10 mg/mL	10 mg/mL	--	--
BO33D lysate	--	--	--	10 mg/mL	10 mg/mL
Acetyl-CoA	25 mM	--	25 mM	--	--
Malonyl-CoA	0.5 mM	--	0.5 mM	--	0.5 mM
Keto acid	1 g/L	--	--	--	1 g/L
NADPH	1 mM	--	1 mM	--	1 mM
ATP	1 mM	--	1 mM	--	1 mM
15× SS	1×		1×		1×

The comparison between A- and A+ indicated that 2 mg/L of C18:0 alcohol (stearyl alcohol) was produced *in vitro*. Similarly, with supplemented α-keto acid, 1 mg/L of C17:0 iso alcohol (15-methyl-1-hexadecanol) was generated from reaction B+ (Figure 5-2). Both results demonstrated that all the enzymes involved in alcohol producing pathway, including FASII elongation enzymes, BKD, and Maqu2220 were active in the cell lysates. However, more than 20 mg/L of C16:0 alcohol was detected in both cell lysates, even without any substrates or cofactors, which made the identification of the *in vitro* produced portion impossible.

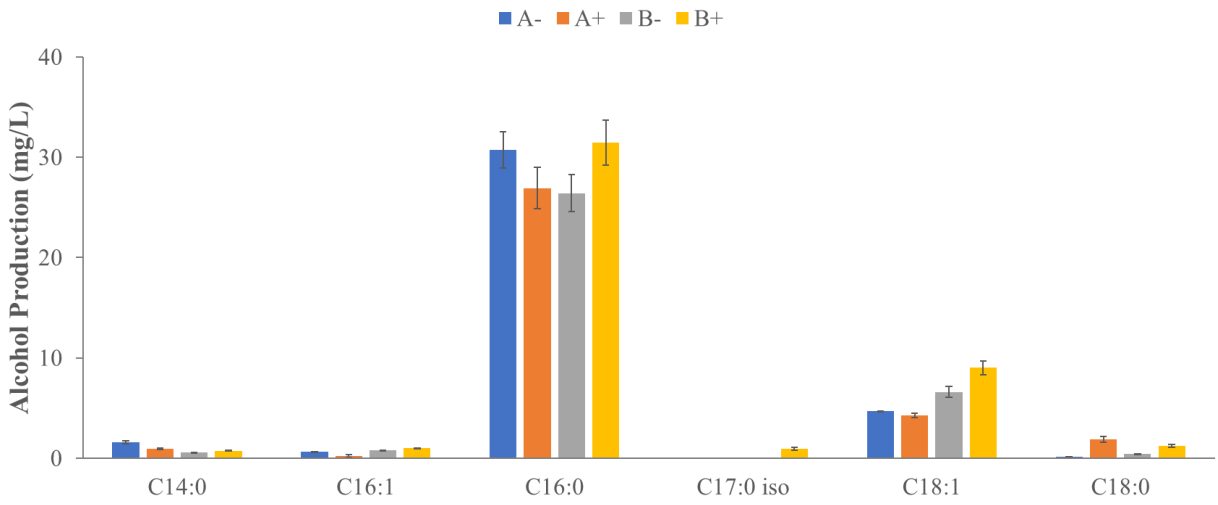

Figure 5- 2 Fatty alcohol production from CFME reactions

5.3.3 Improve the cell-free platform for fatty alcohol production

I reasoned that a large amount of C16:0 alcohol might be generated during the post-induction incubation, that is, once the Maqu2220 was overexpressed, it would immediately convert acyl-ACPs to alcohols during the incubation before lysis. Therefore, I designed two ways to differentiate this portion with *in vitro* produced portion: one way is to attenuate the *in vivo* produced portion, and the other is to increase the *in vitro* produced portion.

I first decreased the cell extract concentration in hope to directly decrease the *in vivo* produced portion. However, when the cell extract concentration was decreased to 1 mg/mL, although no C16:0 alcohol was detected in all the reactions, the concentrations of C18:0 and C17:0 iso products, which were identified as synthesized *in vitro*, were also below the detection limit. This result indicated that the FASII enzymes and/or the Maqu2220 enzyme need to be accumulated to a threshold to run the cell-free reactions and to produce detectable amount of the alcohols. While under this threshold, it is almost impossible to omit the *in vivo* produced portion using the cell extract from a single strain.

As direct decreasing the *in vivo* produced portion was unsuccessful, I sought to increase the *in vitro* produced portion by studying the necessity of the substrates and cofactors, i.e. acetyl-CoA, malonyl-CoA, and NADPH. Some of the cofactors might either already exist or be regenerated in the cell lysate, but the low titer in section 5.3.2 demonstrated that at least one of the substrates or cofactors would be the limiting step. Reactions A1-A5 were carried out using the cell extract from JBEI-9018 (Table 5-4), and the results clearly showed that external malonyl-CoA is required for *in vitro* fatty alcohol production (Figure 5-3A). I also evaluated the impact of the malonyl-CoA amount on *in vitro* branched-chain fatty alcohol production by setting up reactions B1 to B3 with various malonyl-CoA concentrations (Table 5-4). When the malonyl-CoA concentration was

increased by 6-fold, the C17:0 iso titer increased by 8-fold (Figure 5-3B). Again, no branched-chain product was observed in reaction B3 lacking malonyl-CoA.

Table 5- 4 Cofactor necessity test for fatty alcohol production from CFME

	A1	A2	A3	A4	A5	B1	B2	B3
Cell lysate (10 mg/mL)	JBEI-9018	JBEI-9018	JBEI-9018	JBEI-9018	JBEI-9018	BO33D	BO33D	BO33D
Acetyl-CoA (mM)	25	--	25	--	25	--	--	--
Malonyl-CoA (mM)	0.5	--	--	0.5	0.5	3	0.5	--
Keto acid (g/L)	--	--	--	--	--	1	1	1
NADPH (mM)	--	1	1	1	1	1	1	1
ATP (mM)	1	1	1	1	1	1	1	1
15× SS	1×	1×	1×	1×	1×	1×	1×	1×

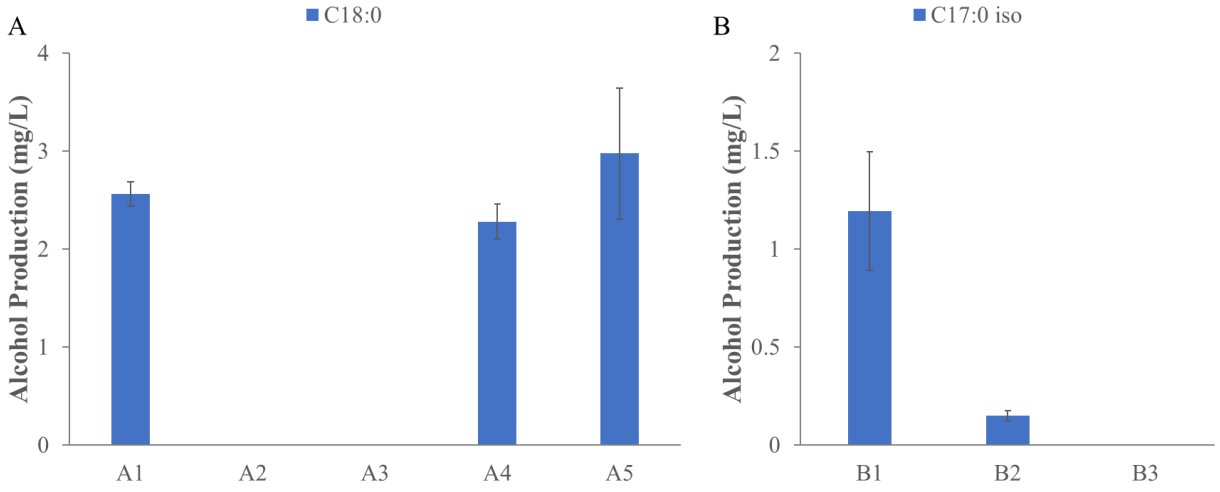

Figure 5- 3 The role of different cofactors in fatty alcohol production from CFME reactions

5.3.4 Straight-chain fatty alcohol production from lysate mix

Although I found that the malonyl-CoA is the limiting resource for *in vitro* production, I could not supplement it to a very high concentration, due to its solubility and high price. Thus, I next sought to overexpress the *accABCD* operon to endogenously produce malonyl-CoA from acetyl-CoA. However, the overexpression of *accABCD* was reported to increases the rate of fatty acid

biosynthesis. Considering that a large proportion of C16:0 alcohol was already generated *in vivo* before the cell lysis process in a *maqu2220* overexpressed strain, I decided to separate the overexpression of *accABCD* from the *maqu2220* overexpressed strain. Here I overexpressed these two operons in two strains and mix their cell lysates to reduce the *in vivo* production.

The *accABCD* operon was overexpressed in strain DH1(*ΔfadE*) to create strain DH1acc. The lysate of DH1acc was mixed with that of JBEI-9018 at two different ratios for a rough optimization (Table 5-5 A0 to A2 *vs*. B0 to B2). The total amount of the cell lysates was kept at 10 mg/mL to guarantee the performance of FASII enzymes *in vitro*. I used glucose rather than acetyl-CoA as the substrate, because glycolysis has been reported to be active in cell-extract. Considering about the conversion of glucose to acetyl-CoA, and their solubilities and prices, the use of glucose would undoubtedly increase the acetyl-CoA pool in the reaction, which might increase the product titer. Additionally, malonyl-CoA was supplemented in reaction A2 and B2 to evaluate the *accABCD* efficiency.

Table 5- 5 Mix and match approach for straight-chain alcohol production from CFME

	A0	A1	A2	B0	B1	B2
JBEI-9018 (mg/mL)	9	9	9	5	5	5
DH1acc (mg/mL)	1	1	1	5	5	5
Glucose (mM)	--	200	200	--	200	200
Malonyl-CoA (mM)	--	--	0.5	--	--	0.5
K_2HPO_4 (mM)	10	10	10	10	10	10
Bis Tris Buffer (mM)	100	100	100	100	100	100
NAD^+ (mM)	0.5	0.5	0.5	0.5	0.5	0.5
$NADP^+$ (mM)	0.5	0.5	0.5	0.5	0.5	0.5
CoA (mM)	0.5	0.5	0.5	0.5	0.5	0.5
15× SS	1×	1×	1×	1×	1×	1×

Surprisingly, no fatty alcohol was detected in the cell mix (reaction A0 and B0), which demonstrated the effectiveness of the mixture in reducing the final concentration of *in vivo*

produced alcohols. Also, no fatty alcohol was generated *in vitro* in reactions A1 and A2, indicating that the Maqu2220 amount was not sufficient when the JBEI-9018 cell extract concentration was only 1 mg/mL. Reaction B1 produced 5 mg/L total fatty alcohol, a 2.5-fold enhancement compared to the titer of reaction A+ in section 5.3.2 (Figure 5-5), as expected that glucose will yield a higher titer than acetyl-CoA when used as the sole substrate. Moreover, reaction B2 produced 7 mg/L total fatty alcohol, indicating that AccABCD amount in this reaction needed further optimization.

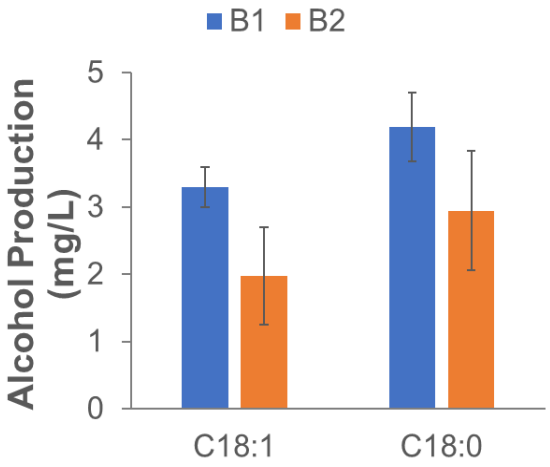

Figure 5- 4 Fatty alcohol production from lysate mix

5.4 Discussion

In this chapter, I tried to develop a new cell-free framework for *in vitro* fatty acid production. Unlike previous published CFME, this framework relied heavily on *E. coli* native fatty acid biosynthetic pathway. Once the enzyme catalyzing the final step, Maqu2220, was overexpressed in the strain, fatty alcohols were accumulated even before the cells were lysed. Therefore, how to differentiate the *in vitro* synthesized products from *in vivo* products generated after induction remained a big challenge. Here I decreased the *in vivo* proportion of the fatty alcohol in the reaction by diluting the JBEI-9018 cell extract with the cell extract from a non-alcohol-producing strain.

The result is a proof-of-concept for both straight-chain and branched-chain fatty alcohol production via CFME.

Although I have achieved the *in vitro* alcohol production, a lot of parameters and conditions could be further investigated and optimized. First, there are two different reaction buffers used in Jewett Lab, gluconate-based buffer and acetate-based buffer. Here I chose gluconate-based buffer due to its excellent performance in 1-butanol production, but I did not have a solid evidence that the same buffer will improve long-chain alcohol production. Second, although I have identified that malonyl-CoA is the rate-limiting factor, the limits for the maximum amounts of all the substrates and cofactors are still unknown. Then, by careful examination, it is highly possible that the titer would increase by several folds using the maximum limits of all the reagents.

More importantly, after characterizing the maximum limit of all the reagents (which indicate the reaction capacity), the amounts of enzymes could also be tuned to improve the reaction capacity. For example, the overexpression of FASII enzymes individually in the cells for lysate preparations, followed by mixing and matching lysates in cell-free cocktails might provide another strategy to increase the reaction capacity and dilute the *in vivo* portion of the fatty alcohol while enhancing the *in vitro* production. However, because FabH plays an essential role in incorporating ω-functionalized acyl-CoA, *E. coli* native FabH needs to be cleared in all the cell extracts. The *ΔfabH* strain in the K.O. collection is a promising parental strain, but the effects of its endogenous regulations on protein synthesis remain unclear. For instance, when pA5a-maqu2220 plasmid was transformed into the *ΔfabH* strain, the cells grew very slowly (data not shown), and no Maqu2220 was detected by SDS-PAGE (Supplementary Figure 5-1).

Therefore, to further improve the titer for either scale-up production or product identification, a large number of reactions are required to be carried out to optimize the reaction buffer, the reaction condition, the optimal amount of all the reagents and the ratio of the cell extracts.

Meanwhile, cell-free protein synthesis (CFPS) offers a complementary solution to fast enrich the enzymes separately before adding into the reactions. The CFPS-ME framework will also enable rapid prototyping of ω-functionalized fatty alcohol production from the combination of FASII with specific FabH. With the progress of bioinformatics, this platform can be further applied for fast screening of optimal enzyme combinations for the production of bifunctional fatty acid derivatives.

5.5 Conclusion

In this chapter, I established a new cell-free framework for *in vitro* fatty alcohol production and characterized the necessity of several cofactors. The production of both straight-chain and branched-chain fatty alcohol from this cell-free framework has been achieved. In addition, I overcame a major obstacle arising from the fact that fatty acid synthesis is an endogenous pathway. A large proportion of fatty alcohol was produced *in vivo* during the post-induction incubation time but was diluted in the final reaction solution through the mix-and-match approach. This result is a proof-of-concept for fatty alcohol production via CFME and provides guidance for future CFPS-ME frameworks to produce bifunctional fatty acid derivatives, while intensive optimizations are still needed before the goal could be achieved.

Supplementary Materials

Quantification of FFA contamination from three major sources.

Steps:

1. Prepare the reactions as listed below

Supplementary Table 5-1 Recipes for quantification of FFA contamination

	1	2	3	4	5	6	7	8	9
Water (μL)	25	50	300	50	100	150	300	500	1000
Tube (mL)	0.5	0.5	0.5	1.5	1.5	1.5	1.5	1.5	1.5
Incubation	Yes	No	No	Yes	No	Yes	No	Yes	No
Ethyl Acetate (μL)	25	25	150	50	50	150	150	500	500

1) For samples that need incubation (1, 4, 6, 8), add the indicated amount of water into 1.5 mL tubes and incubate at 37 °C for 4 h;

2) Add the same amount of water into those tubes. For sample 1, transfer into 0.5 mL tubes for extraction;

3) Prepare the samples 2, 3, 5, 7, 9;

2. Extract each sample with the indicated amount of ethyl acetate twice and derivatize and inject as usual;

3. Normalize the final concentration as the concentration in water;

4. Calculate the FA concentrations in all the samples

1) Models for C16:0 fatty acid

In 0.5 mL tube

$$c_w + \frac{m_t}{50} = 5.1$$

$$c_w + \frac{m_t}{300} = 1.67$$

$$c_w = 1ng/\mu L$$

$$m_t = 0.2\mu g$$

c_w = ~2 mg/L

In 1.5 mL tube

$$c_w + \frac{m_t}{100} = 16.6$$

$$c_w + \frac{m_t}{300} = 7.66$$

$$c_w + \frac{m_t}{1000} = 5.01$$

$$c_w = 3ng/\mu L$$

$$m_t = 1.4\mu g$$

2) Models for C18:0 fatty acid

In 0.5 mL tube

$$c_w + \frac{m_t}{50} = 11.77$$

$$c_w + \frac{m_t}{300} = 3.83$$

$$c_w = 2ng/\mu L$$

$$m_t = 0.5\mu g$$

c_w = ~3 mg/L

In 1.5 mL tube

$$c_w + \frac{m_t}{100} = 16.6$$

$$c_w + \frac{m_t}{300} = 7.91$$

$$c_w + \frac{m_t}{1000} = 4.68$$

$$c_w = 3.5ng/\mu L$$

$$m_t = 1.3\mu g$$

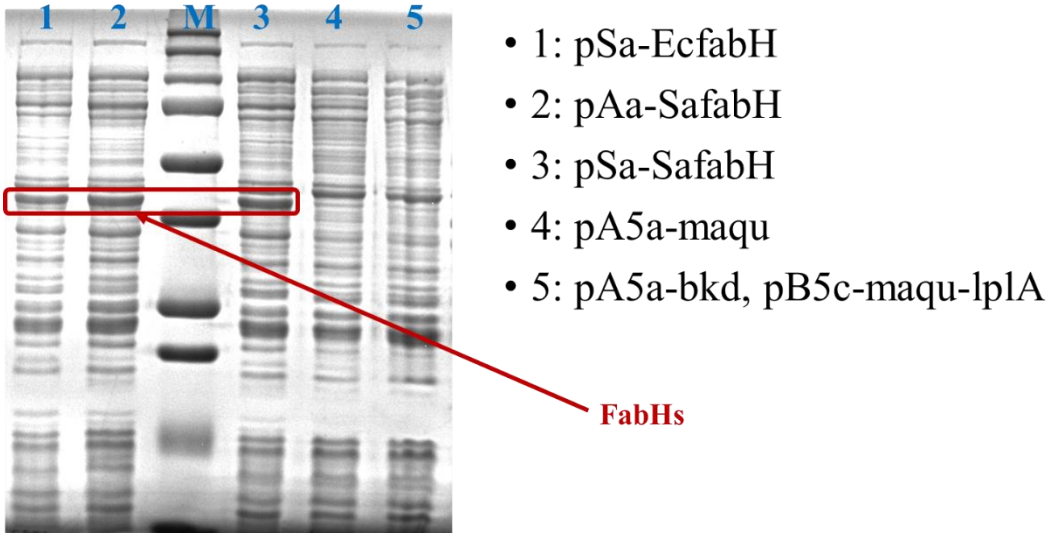

Supplementary Figure 5-1 SDS-PAGE results for protein expression in *ΔfabH* strain

Chapter 6: Conclusion and future directions

6.1 Conclusions

In this work, I have established a modular pathway for producing NNFA and derivatives production. To start, I achieved branched-chain fatty acid production. In Chapter 2, I directed the carbon flux to the synthesis of BCFAs by replacing the acetyl-CoA-specific *E. coli* FabH, the only β-ketoacyl-(acyl-carrier-protein) synthase that catalyzes the initial fatty acid condensation reaction, with a branched-chain-acyl-CoA-specific FabH, enhancing BCFA titer by 81-fold over a strain containing both acetyl-CoA- and branched-chain-acyl-CoA-specific FabHs. I further discovered that the overexpression of BKD, a member of the 2-oxoacid dehydrogenase family needed to synthesize branched-chain-acyl-CoA precursors, is toxic to *E. coli* due to depletion of the protein lipoylation capacity. Engineering a complementary protein lipoylation pathway alleviated the toxicity and improved BCFA production to 276 mg/L and 85% of total free fatty acids, the highest BCFA titer and percentage to-date. Furthermore, I achieved fine-tuning of BCFA branch positions by engineering the upstream pathway to control the supply of branched-chain acyl-CoAs, eventually producing 181 mg/L BCFA at 72% of total FFA from glucose.

In Chapter 3, I partitioned the complete pathway into three modules: a precursor formation module (the α-Keto Acid Synthesis Module), an acyl-CoA activation and malonyl-ACP consumption module (the Acyl-ACP Generation Module), and a final product synthesis module (the Alcohol Formation Module). I engineered and tuned each module separately and combined the optimal modules to produce a high percentage of branched fatty alcohols from glucose. In Chapter 4, I further utilized this modular pathway engineering strategy to produce branched-chain alkanes and esters. I also tested the feasibility of ω-hydroxy fatty acid production by engineering

the precursor formation module. In Chapter 5, I moved the modular NNFA synthetic pathway into a new cell-free framework to give a proof-of-concept for *in vitro* production of fatty acid derivatives and provided guidance for future CFPS-ME framework to produce bifunctional fatty acid derivatives.

Overall, this work establishes a platform for the microbial synthesis of branched biofuels and chemical in high percentages, paving the way for bioproduction of structurally-defined molecules with desired properties.

6.2 Future directions

In this work, although I have established a modular pathway platform to produce non-natural fatty acids, I have achieved the production of only branched-chain fatty acid and derivatives. Diversifying the ω-terminal structure requires comprehensive studies on the precursor formation module and the acyl-CoA activation and malonyl-ACP consumption module. The enzyme selection, screening, and pathway prototyping can be facilitated by bioinformatics and the CFPS-ME framework. Thus, one future direction would be the optimization of all the factors in current CFME framework, and the establishment of an improved CFPS-ME platform to perform the prototyping work.

Meanwhile, although the titer of straight-chain fatty acid and alcohol production can reach more than 3 g/L, the results from this dissertation showed that their branched-chain counterparts can be produced only at the level of 200 mg/L. Since the low titer might result from the metabolic burden caused by protein synthesis and/or product accumulation, studying the metabolic limits of the engineered strains will be another future direction. In detail, the burden caused by protein synthesis, $NADP^+$/NADPH recycling, and BCFA intracellular distribution, are potential research

targets to study about in the fatty acid synthetic pathway. In addition, the heterogeneity of producing cells has been demonstrated to affect ensemble production [22, 23], so studies on cell-to-cell variations based on this platform are other potential directions, including the strategy to enrich the high-producing variants and ultimately enhance product titers. These studies will provide a general strategy to improve cell performance in metabolic engineering.

References/Bibliography/Works Cited

1. Frederix M, Mingardon F, Hu M, Sun N, Pray T, Singh S, Simmons BA, Keasling JD, Mukhopadhyay A: **Development of an E. coli strain for one-pot biofuel production from ionic liquid pretreated cellulose and switchgrass.** *Green Chemistry* 2016, **18:**4189-4197.
2. Gaeta-Bernardi A, Parente V: **Organic municipal solid waste (MSW) as feedstock for biodiesel production: A financial feasibility analysis.** *Renewable Energy* 2016, **86:**1422-1432.
3. Price JV, Chen L, Whitaker WB, Papoutsakis E, Chen W: **Scaffoldless engineered enzyme assembly for enhanced methanol utilization.** *Proceedings of the National Academy of Sciences* 2016, **113:**12691-12696.
4. Oliver NJ, Rabinovitch-Deere CA, Carroll AL, Nozzi NE, Case AE, Atsumi S: **Cyanobacterial metabolic engineering for biofuel and chemical production.** *Current Opinion in Chemical Biology* 2016, **35:**43-50.
5. Jung J, Lim JH, Kim SY, Im D-K, Seok JY, Lee S-JV, Oh M-K, Jung GY: **Precise precursor rebalancing for isoprenoids production by fine control of gapA expression in Escherichia coli.** *Metabolic Engineering* 2016, **38:**401-408.
6. Rodriguez GM, Atsumi S: **Toward aldehyde and alkane production by removing aldehyde reductase activity in Escherichia coli.** *Metabolic Engineering* 2014, **25:**227-237.
7. Zhang F, Ouellet M, Batth TS, Adams PD, Petzold CJ, Mukhopadhyay A, Keasling JD: **Enhancing fatty acid production by the expression of the regulatory transcription factor FadR.** *Metabolic Engineering* 2012, **14:**653-660.
8. Lim JH, Jung GY: **A simple method to control glycolytic flux for the design of an optimal cell factory.** *Biotechnology for Biofuels* 2017, **10**.
9. Ohtake T, Pontrelli S, Laviña WA, Liao JC, Putri SP, Fukusaki E: **Metabolomics-driven approach to solving a CoA imbalance for improved 1-butanol production in Escherichia coli.** *Metabolic Engineering* 2017, **41:**135-143.
10. Ceroni F, Algar R, Stan G-B, Ellis T: **Quantifying cellular capacity identifies gene expression designs with reduced burden.** *Nat Meth* 2015, **12:**415-418.
11. Guo W, Sheng J, Zhao H, Feng X: **Metabolic engineering of Saccharomyces cerevisiae to produce 1-hexadecanol from xylose.** *Microbial Cell Factories* 2016, **15:**24.
12. George KW, Thompson MG, Kang A, Baidoo E, Wang G, Chan LJG, Adams PD, Petzold CJ, Keasling JD, Lee TS: **Metabolic engineering for the high-yield production of isoprenoid-based C5 alcohols in E. coli.** *Scientific Reports* 2015, **5**.
13. Liu D, Xiao Y, Evans BS, Zhang F: **Negative Feedback Regulation of Fatty Acid Production Based on a Malonyl-CoA Sensor-Actuator.** *ACS Synth Biol* 2015, **4:**132-140.
14. Xu P, Li LY, Zhang FM, Stephanopoulos G, Koffas M: **Improving fatty acids production by engineering dynamic pathway regulation and metabolic control.** *Proceedings of the National Academy of Sciences of the United States of America* 2014, **111:**11299-11304.
15. Yu X, Xu J, Liu X, Chu X, Wang P, Tian J, Wu N, Fan Y: **Identification of a highly efficient stationary phase promoter in Bacillus subtilis.** 2015, **5:**18405.

16. Gupta A, Reizman IMB, Reisch CR, Prather KLJ: **Dynamic regulation of metabolic flux in engineered bacteria using a pathway-independent quorum-sensing circuit.** *Nat Biotech* 2017, **35:**273-279.
17. Blazeck J, Hill A, Liu L, Knight R, Miller J, Pan A, Otoupal P, Alper HS: **Harnessing Yarrowia lipolytica lipogenesis to create a platform for lipid and biofuel production.** 2014, **5:**3131.
18. Kang M-K, Zhou YJ, Buijs NA, Nielsen J: **Functional screening of aldehyde decarbonylases for long-chain alkane production by Saccharomyces cerevisiae.** *Microbial Cell Factories* 2017, **16:**74.
19. Jiang G-Z, Yao M-D, Wang Y, Zhou L, Song T-Q, Liu H, Xiao W-H, Yuan Y-J: **Manipulation of GES and ERG20 for geraniol overproduction in Saccharomyces cerevisiae.** *Metabolic Engineering* 2017, **41:**57-66.
20. Tan Z, Yoon JM, Nielsen DR, Shanks JV, Jarboe LR: **Membrane engineering via trans unsaturated fatty acids production improves Escherichia coli robustness and production of biorenewables.** *Metabolic Engineering* 2016, **35:**105-113.
21. Tan Z, Khakbaz P, Chen Y, Lombardo J, Yoon JM, Shanks JV, Klauda JB, Jarboe LR: **Engineering Escherichia coli membrane phospholipid head distribution improves tolerance and production of biorenewables.** *Metabolic Engineering* 2017, **44:**1-12.
22. Schmitz AC, Hartline CJ, Zhang F: **Engineering Microbial Metabolite Dynamics and Heterogeneity.** *Biotechnology Journal***:**1700422-n/a.
23. Delvigne F, Zune Q, Lara AR, Al-Soud W, Sørensen SJ: **Metabolic variability in bioprocessing: implications of microbial phenotypic heterogeneity.** *Trends in Biotechnology* 2014, **32:**608-616.
24. Xiao Y, Bowen CH, Liu D, Zhang F: **Exploiting nongenetic cell-to-cell variation for enhanced biosynthesis.** *Nature Chemical Biology* 2016, **12:**339-+.
25. Atsumi S, Hanai T, Liao JC: **Non-fermentative pathways for synthesis of branched-chain higher alcohols as biofuels.** *Nature* 2008, **451:**86-U13.
26. Marcheschi RJ, Li H, Zhang KC, Noey EL, Kim S, Chaubey A, Houk KN, Liao JC: **A Synthetic Recursive "+1" Pathway for Carbon Chain Elongation.** *Acs Chemical Biology* 2012, **7:**689-697.
27. Yu AQ, Juwono NKP, Foo JL, Leong SSJ, Chang MW: **Metabolic engineering of Saccharomyces cerevisiae for the overproduction of short branched-chain fatty acids.** *Metabolic Engineering* 2016, **34:**36-43.
28. Zhang L, Liang Y, Wu W, Tan X, Lu X: **Microbial synthesis of propane by engineering valine pathway and aldehyde-deformylating oxygenase.** *Biotechnology for Biofuels* 2016, **9:**80.
29. Rodriguez GM, Tashiro Y, Atsumi S: **Expanding ester biosynthesis in Escherichia coli.** *Nature Chemical Biology* 2014, **10:**259-265.
30. Shen CR, Liao JC: **Metabolic engineering of Escherichia coli for 1-butanol and 1-propanol production via the keto-acid pathways.** *Metabolic Engineering* 2008, **10:**312-320.
31. Connor MR, Cann AF, Liao JC: **3-Methyl-1-butanol production in Escherichia coli: random mutagenesis and two-phase fermentation.** *Applied Microbiology and Biotechnology* 2010, **86:**1155-1164.
32. Cann AF, Liao JC: **Production of 2-methyl-1-butanol in engineered Escherichia coli.** *Applied Microbiology and Biotechnology* 2008, **81:**89-98.

33. Chen GS, Siao SW, Shen CR: **Saturated mutagenesis of ketoisovalerate decarboxylase V461 enabled specific synthesis of 1-pentanol via the ketoacid elongation cycle.** *Scientific Reports* 2017, **7:**11284.
34. Barker HA, Taha SM: **Clostridium kluyverii, an Organism Concerned in the Formation of Caproic Acid from Ethyl Alcohol.** *Journal of Bacteriology* 1942, **43:**347-363.
35. Dellomonaco C, Clomburg JM, Miller EN, Gonzalez R: **Engineered reversal of the beta-oxidation cycle for the synthesis of fuels and chemicals.** *Nature* 2011, **476:**355-U131.
36. Cheong S, Clomburg JM, Gonzalez R: **Energy- and carbon-efficient synthesis of functionalized small molecules in bacteria using non-decarboxylative Claisen condensation reactions.** *Nat Biotech* 2016, **34:**556-561.
37. Dickschat JS: **Bacterial terpene cyclases.** *Natural Product Reports* 2016, **33:**87-110.
38. Yamada Y, Kuzuyama T, Komatsu M, Shin-ya K, Omura S, Cane DE, Ikeda H: **Terpene synthases are widely distributed in bacteria.** *Proceedings of the National Academy of Sciences* 2015, **112:**857-862.
39. Steen EJ, Kang YS, Bokinsky G, Hu ZH, Schirmer A, McClure A, del Cardayre SB, Keasling JD: **Microbial production of fatty-acid-derived fuels and chemicals from plant biomass.** *Nature* 2010, **463:**559-U182.
40. Torella JP, Ford TJ, Kim SN, Chen AM, Way JC, Silver PA: **Tailored fatty acid synthesis via dynamic control of fatty acid elongation.** *Proceedings of the National Academy of Sciences* 2013, **110:**11290-11295.
41. Gajewski J, Pavlovic R, Fischer M, Boles E, Grininger M: **Engineering fungal de novo fatty acid synthesis for short chain fatty acid production.** *Nature Communications* 2017, **8:**14650.
42. Choi YJ, Lee SY: **Microbial production of short-chain alkanes.** *Nature* 2013, **502:**571-+.
43. Youngquist JT, Schumacher MH, Rose JP, Raines TC, Politz MC, Copeland MF, Pfleger BF: **Production of medium chain length fatty alcohols from glucose in Escherichia coli.** *Metabolic Engineering* 2013, **20:**177-186.
44. Fan L, Liu J, Nie K, Liu L, Wang F, Tan T, Deng L: **Synthesis of medium chain length fatty acid ethyl esters in engineered Escherichia coli using endogenously produced medium chain fatty acids.** *Enzyme and Microbial Technology* 2013, **53:**128-133.
45. Lennen RM, Braden DJ, West RM, Dumesic JA, Pfleger BF: **A Process for Microbial Hydrocarbon Synthesis: Overproduction of Fatty Acids in Escherichia coli and Catalytic Conversion to Alkanes.** *Biotechnology and Bioengineering* 2010, **106:**193-202.
46. Xu P, Gu Q, Wang WY, Wong L, Bower AGW, Collins CH, Koffas MAG: **Modular optimization of multi-gene pathways for fatty acids production in E. coli.** *Nature Communications* 2013, **4**.
47. Liu TG, Khosla C: **Genetic Engineering of Escherichia coli for Biofuel Production.** *Annual Review of Genetics, Vol 44* 2010, **44:**53-69.
48. Zhang F, Carothers JM, Keasling JD: **Design of a dynamic sensor-regulator system for production of chemicals and fuels derived from fatty acids.** *Nature Biotechnology* 2012, **30:**354-U166.
49. Schirmer A, Rude MA, Li X, Popova E, del Cardayre SB: **Microbial Biosynthesis of Alkanes.** *Science* 2010, **329:**559-562.

50. Rude MA, Baron TS, Brubaker S, Alibhai M, Del Cardayre SB, Schirmer A: **Terminal olefin (1-alkene) biosynthesis by a novel p450 Fatty Acid decarboxylase from jeotgalicoccus species.** *Appl Environ Microbiol* 2011, **77:**1718-1727.
51. Liu R, Zhu F, Lu L, Fu A, Lu J, Deng Z, Liu T: **Metabolic engineering of fatty acyl-ACP reductase-dependent pathway to improve fatty alcohol production in Escherichia coli.** *Metabolic Engineering* 2014, **22:**10-21.
52. Guo D, Zhu J, Deng Z, Liu T: **Metabolic engineering of Escherichia coli for production of fatty acid short-chain esters through combination of the fatty acid and 2-keto acid pathways.** *Metabolic Engineering* 2014, **22:**69-75.
53. Thompson RA, Trinh CT: **Enhancing fatty acid ethyl ester production in Saccharomyces cerevisiae through metabolic engineering and medium optimization.** *Biotechnology and Bioengineering* 2014, **111:**2200-2208.
54. Rodriguez GM, Tashiro Y, Atsumi S: **Expanding ester biosynthesis in Escherichia coli.** *Nature Chemical Biology* 2014, **10:**259-265.
55. Peralta-Yahya PP, Zhang F, del Cardayre SB, Keasling JD: **Microbial engineering for the production of advanced biofuels.** *Nature* 2012, **488:**320-328.
56. Tang HY, Salley SO, Ng KYS: **Fuel properties and precipitate formation at low temperature in soy-, cottonseed-, and poultry fat-based biodiesel blends.** *Fuel* 2008, **87:**3006-3017.
57. Ghanei R: **Improving cold-flow properties of biodiesel through blending with nonedible castor oil methyl ester.** *Environmental Progress & Sustainable Energy* 2014**:**n/a-n/a.
58. Knothe G, Dunn RO: **A Comprehensive Evaluation of the Melting Points of Fatty Acids and Esters Determined by Differential Scanning Calorimetry.** *Journal of the American Oil Chemists Society* 2009, **86:**843-856.
59. Choi KH, Heath RJ, Rock CO: **beta-ketoacyl-acyl carrier protein synthase III (FabH) is a determining factor in branched-chain fatty acid biosynthesis.** *Journal of Bacteriology* 2000, **182:**365-370.
60. Lowe PN, Hodgson JA, Perham RN: **Dual role of a single multienzyme complex in the oxidative decarboxylation of pyruvate and branched-chain 2-oxo acids in Bacillus subtilis.** *Biochem J* 1983, **215:**133-140.
61. McCully V, Burns G, Sokatch JR: **Resolution of branched-chain oxo acid dehydrogenase complex of Pseudomonas aeruginosa PAO.** *Biochem J* 1986, **233:**737-742.
62. Sokatch JR, McCully V, Gebrosky J, Sokatch DJ: **Isolation of a specific lipoamide dehydrogenase for a branched-chain keto acid dehydrogenase from Pseudomonas putida.** *Journal of Bacteriology* 1981, **148:**639-646.
63. Howard TP, Middelhaufe S, Moore K, Edner C, Kolak DM, Taylor GN, Parker DA, Lee R, Smirnoff N, Aves SJ, Love J: **Synthesis of customized petroleum-replica fuel molecules by targeted modification of free fatty acid pools in Escherichia coli.** *Proceedings of the National Academy of Sciences of the United States of America* 2013, **110:**7636-7641.
64. Lee TS, Krupa RA, Zhang F, Hajimorad M, Holtz WJ, Prasad N, Lee SK, Keasling JD: **BglBrick vectors and datasheets: A synthetic biology platform for gene expression.** *J Biol Eng* 2011, **5:**12.

65. Engler C, Kandzia R, Marillonnet S: **A one pot, one step, precision cloning method with high throughput capability.** *PLoS One* 2008, **3:**e3647.
66. Gibson DG, Young L, Chuang RY, Venter JC, Hutchison CA, Smith HO: **Enzymatic assembly of DNA molecules up to several hundred kilobases.** *Nature Methods* 2009, **6:**343-U341.
67. Lai CY, Cronan JE: **beta-ketoacyl-acyl carrier protein synthase III (FabH) is essential for bacterial fatty acid synthesis.** *Journal of Biological Chemistry* 2003, **278:**51494-51503.
68. Doublet B, Douard G, Targant H, Meunier D, Madec JY, Cloeckaert A: **Antibiotic marker modifications of lambda Red and FLP helper plasmids, pKD46 and pCP20, for inactivation of chromosomal genes using PCR products in multidrug-resistant strains.** *Journal of Microbiological Methods* 2008, **75:**359-361.
69. Datsenko KA, Wanner BL: **One-step inactivation of chromosomal genes in Escherichia coli K-12 using PCR products.** *Proceedings of the National Academy of Sciences of the United States of America* 2000, **97:**6640-6645.
70. He L, Xiao Y, Gebreselassie N, Zhang F, Antoniewicz MR, Tang YJ, Peng L: **Central Metabolic Responses to the Overproduction of Fatty Acids in Escherichia coli Based on C-13-Metabolic Flux Analysis.** *Biotechnology and Bioengineering* 2014, **111:**575-585.
71. Haushalter RW, Kim W, Chavkin TA, The L, Garber ME, Nhan M, Petzold CJ, Katz L, Keasling JD: **Production of anteiso-branched fatty acids in Escherichia coli; next generation biofuels with improved cold-flow properties.** *Metabolic Engineering* 2014.
72. Bennett BD, Kimball EH, Gao M, Osterhout R, Van Dien SJ, Rabinowitz JD: **Absolute metabolite concentrations and implied enzyme active site occupancy in Escherichia coli.** *Nature Chemical Biology* 2009, **5:**593-599.
73. Zhang Y, Cronan JE: **Transcriptional analysis of essential genes of the Escherichia coli fatty acid biosynthesis gene cluster by functional replacement with the analogous Salmonella typhimurium gene cluster.** *Journal of Bacteriology* 1998, **180:**3295-3303.
74. Qiu XY, Choudhry AE, Janson CA, Grooms M, Daines RA, Lonsdale JT, Khandekar SS: **Crystal structure and substrate specificity of the beta-ketoacyl-acyl carrier protein synthase III (FabH) from Staphylococcus aureus.** *Protein Science* 2005, **14:**2087-2094.
75. Vonderha.Ra, Umbarger HE: **Isoleucine and Valine Metabolism in Escherichia-Coli .19. Inhibition of Isoleucine Biosynthesis by Glycyl-Leucine.** *Journal of Bacteriology* 1972, **112:**142-&.
76. Gollop N, Damri B, Barak Z, Chipman DM: **Kinetics and Mechanism of Acetohydroxy Acid Synthase Isozyme-Iii from Escherichia-Coli.** *Biochemistry* 1989, **28:**6310-6317.
77. Stieglitz BI, Calvo JM: **Distribution of the isopropylmalate pathway to leucine among diverse bacteria.** *Journal of Bacteriology* 1974, **118:**935-941.
78. Machado RS, Clark DP, Guest JR: **Construction and properties of pyruvate dehydrogenase complexes with up to nine lipoyl domains per lipoate acetyltransferase chain.** *FEMS Microbiology Letters* 1992, **100:**243-248.
79. Jordan SW, Cronan JE: **The Escherichia coli lipB Gene Encodes Lipoyl (Octanoyl)-Acyl Carrier Protein:Protein Transferase.** *Journal of Bacteriology* 2003, **185:**1582-1589.
80. Zhao X, Miller JR, Jiang Y, Marletta MA, Cronan JE: **Assembly of the Covalent Linkage between Lipoic Acid and Its Cognate Enzymes.** *Chemistry & Biology* 2003, **10:**1293-1302.

81. Cicchillo RM, Lee K-H, Baleanu-Gogonea C, Nesbitt NM, Krebs C, Booker SJ: **Escherichia coli Lipoyl Synthase Binds Two Distinct [4Fe−4S] Clusters per Polypeptide [†].** *Biochemistry* 2004, **43:**11770-11781.
82. Cicchillo RM, Iwig DF, Jones AD, Nesbitt NM, Baleanu-Gogonea C, Souder MG, Tu L, Booker SJ: **Lipoyl Synthase Requires Two Equivalents of S -Adenosyl- l -methionine To Synthesize One Equivalent of Lipoic Acid [†].** *Biochemistry* 2004, **43:**6378-6386.
83. Hermes FAM, Cronan JE: **Scavenging of Cytosolic Octanoic Acid by Mutant LplA Lipoate Ligases Allows Growth of Escherichia coli Strains Lacking the LipB Octanoyltransferase of Lipoic Acid Synthesis.** *Journal of Bacteriology* 2009, **191:**6796-6803.
84. Morris TW, Reed KE, Cronan JE: **Lipoic acid metabolism in Escherichia coli: the lplA and lipB genes define redundant pathways for ligation of lipoyl groups to apoprotein.** *Journal of Bacteriology* 1995, **177:**1-10.
85. Cronan JE: **Biotin and Lipoic Acid: Synthesis, Attachment, and Regulation.** *EcoSal Plus* 2013, **1**.
86. Zhang F, Ouellet M, Batth TS, Adams PD, Petzold CJ, Mukhopadhyay A, Keasling JD: **Enhancing fatty acid production by the expression of the regulatory transcription factor FadR.** *Metabolic Engineering* 2012, **14:**653-660.
87. Connor MR, Liao JC: **Engineering of an Escherichia coli Strain for the Production of 3-Methyl-1-Butanol.** *Appl Environ Microbiol* 2008, **74:**5769-5775.
88. Yu XY, Liu TG, Zhu FY, Khosla C: **In vitro reconstitution and steady-state analysis of the fatty acid synthase from Escherichia coli.** *Proceedings of the National Academy of Sciences of the United States of America* 2011, **108:**18643-18648.
89. Yadav VG, De Mey M, Giaw Lim C, Kumaran Ajikumar P, Stephanopoulos G: **The future of metabolic engineering and synthetic biology: Towards a systematic practice.** *Metabolic Engineering* 2012, **14:**233-241.
90. Garg S, Rizhsky L, Jin HN, Yu XC, Jing FY, Yandeau-Nelson MD, Nikolau BJ: **Microbial production of bi-functional molecules by diversification of the fatty acid pathway.** *Metabolic Engineering* 2016, **35:**9-20.
91. Zargar A, Bailey CB, Haushalter RW, Eiben CB, Katz L, Keasling JD: **Leveraging microbial biosynthetic pathways for the generation of 'drop-in' biofuels.** *Curr Opin Biotechnol* 2017, **45:**156-163.
92. Akhtar MK, Turner NJ, Jones PR: **Carboxylic acid reductase is a versatile enzyme for the conversion of fatty acids into fuels and chemical commodities.** *Proceedings of the National Academy of Sciences of the United States of America* 2013, **110:**87-92.
93. Knaut J, Richtler HJ: **Trends in Industrial Uses of Palm and Lauric Oils.** *Journal of the American Oil Chemists Society* 1985, **62:**317-327.
94. Carroll AL, Desai SH, Atsumi S: **Microbial production of scent and flavor compounds.** *Curr Opin Biotechnol* 2016, **37:**8-15.
95. Washecheck PH: **Manufacture of Higher Straight-Chain Alcohols by the Ethylene Chain Growth Process.** In *Monohydric Alcohols. Volume* 159: AMERICAN CHEMICAL SOCIETY; 1981: 87-100: *ACS Symposium Series*].
96. Voeste T, Buchold H: **Production of Fatty Alcohols from Fatty-Acids.** *Journal of the American Oil Chemists Society* 1984, **61:**350-352.

97. Zheng YN, Li LL, Liu Q, Yang JM, Wang XW, Liu W, Xu X, Liu H, Zhao G, Xian M: **Optimization of fatty alcohol biosynthesis pathway for selectively enhanced production of C12/14 and C16/18 fatty alcohols in engineered Escherichia coli.** *Microb Cell Fact* 2012, **11:**65.
98. Liu A, Tan X, Yao L, Lu X: **Fatty alcohol production in engineered E. coli expressing Marinobacter fatty acyl-CoA reductases.** *Appl Microbiol Biotechnol* 2013, **97:**7061-7071.
99. Liu R, Zhu FY, Lu L, Fu AS, Lu JK, Deng ZX, Liu TG: **Metabolic engineering of fatty acyl-ACP reductase-dependent pathway to improve fatty alcohol production in Escherichia coli.** *Metabolic Engineering* 2014, **22:**10-21.
100. Sheng JY, Stevens J, Feng XY: **Pathway Compartmentalization in Peroxisome of Saccharomyces cerevisiae to Produce Versatile Medium Chain Fatty Alcohols.** *Scientific Reports* 2016, **6**.
101. Sheng JY, Feng XY: **Metabolic engineering of yeast to produce fatty acid-derived biofuels: bottlenecks and solutions.** *Frontiers in Microbiology* 2015, **6**.
102. Gabriels D, Hernandez WY, Sels B, Van Der Voort P, Verberckmoes A: **Review of catalytic systems and thermodynamics for the Guerbet condensation reaction and challenges for biomass valorization.** *Catalysis Science & Technology* 2015, **5:**3876-3902.
103. O'Lenick AJ: **Guerbet chemistry.** *Journal of Surfactants and Detergents* 2001, **4:**311-315.
104. Mueller G, Bongardt F, Fies M, Daute P: **Hydraulic oils containing biodegradable guerbet alcohols.** Google Patents; 1996.
105. Vinson PK, Foley PR, Cripe TA, Connor DS, Willman KW: **Detergent compositions containing selected mid-chain branched surfactants.** Google Patents; 2001.
106. Dyer DJ, Walba DM: **Improvement of Thermotropic Liquid Crystallinity by Incorporation of Unsaturated Fatty Alcohol Tail Units.** *Chemistry of Materials* 1994, **6:**1096-1098.
107. Kozlowski JT, Davis RJ: **Heterogeneous Catalysts for the Guerbet Coupling of Alcohols.** *Acs Catalysis* 2013, **3:**1588-1600.
108. Anbarasan P, Baer ZC, Sreekumar S, Gross E, Binder JB, Blanch HW, Clark DS, Toste FD: **Integration of chemical catalysis with extractive fermentation to produce fuels.** *Nature* 2012, **491:**235-239.
109. Carlini C, Macinai A, Galletti AMR, Sbrana G: **Selective synthesis of 2-ethyl-1-hexanol from n-butanol through the Guerbet reaction by using bifunctional catalysts based on copper or palladium precursors and sodium butoxide.** *Journal of Molecular Catalysis a-Chemical* 2004, **212:**65-70.
110. Sheppard MJ, Kunjapur AM, Wenck SJ, Prather KLJ: **Retro-biosynthetic screening of a modular pathway design achieves selective route for microbial synthesis of 4-methyl-pentanol.** *Nature Communications* 2014, **5**.
111. Lennen RM, Pfleger BF: **Microbial production of fatty acid-derived fuels and chemicals.** *Current Opinion in Biotechnology* 2013, **24:**1044-1053.
112. Bentley GJ, Jiang W, Guaman LP, Xiao Y, Zhang F: **Engineering Escherichia coli to produce branched-chain fatty acids in high percentages.** *Metabolic Engineering* 2016, **38:**148-158.
113. Jiang W, Jiang Y, Bentley GJ, Liu D, Xiao Y, Zhang F: **Enhanced production of branched-chain fatty acids by replacing -ketoacyl-(acyl-carrier-protein) synthase III (FabH).** *Biotechnology and Bioengineering* 2015, **112:**1613-1622.

114. McMahon MD, Prather KLJ: **Functional Screening and In Vitro Analysis Reveal Thioesterases with Enhanced Substrate Specificity Profiles That Improve Short-Chain Fatty Acid Production in Escherichia coli.** *Applied and Environmental Microbiology* 2014, **80:**1042-1050.
115. Martin CH, Dhamankar H, Tseng HC, Sheppard MJ, Reisch CR, Prather KLJ: **A platform pathway for production of 3-hydroxyacids provides a biosynthetic route to 3-hydroxy-gamma-butyrolactone.** *Nature Communications* 2013, **4**.
116. Jones JA, Toparlak OD, Koffas MAG: **Metabolic pathway balancing and its role in the production of biofuels and chemicals.** *Current Opinion in Biotechnology* 2015, **33:**52-59.
117. Zhao SJ, Jones JA, Lachance DM, Bhan N, Khalidi O, Venkataraman S, Wang ZT, Koffas MAG: **Improvement of catechin production in Escherichia coli through combinatorial metabolic engineering.** *Metabolic Engineering* 2015, **28:**43-53.
118. Jones JA, Vernacchio VR, Lachance DM, Lebovich M, Fu L, Shirke AN, Schultz VL, Cress B, Linhardt RJ, Koffas MAG: **ePathOptimize: A Combinatorial Approach for Transcriptional Balancing of Metabolic Pathways.** *Scientific Reports* 2015, **5**.
119. Fang MY, Wang TM, Zhang C, Bai JL, Zheng X, Zhao XJ, Lou CB, Xing XH: **Intermediate-sensor assisted push-pull strategy and its application in heterologous deoxyviolacein production in Escherichia coli.** *Metabolic Engineering* 2016, **33:**41-51.
120. Jiang Y, Chen B, Duan CL, Sun BB, Yang JJ, Yang S: **Multigene Editing in the Escherichia coli Genome via the CRISPR-Cas9 System.** *Appl Environ Microbiol* 2015, **81:**2506-2514.
121. Haushalter RW, Groff D, Deutsch S, The L, Chavkin TA, Brunner SF, Katz L, Keasling JD: **Development of an orthogonal fatty acid biosynthesis system in E. coli for oleochemical production.** *Metabolic Engineering* 2015, **30:**1-6.
122. Atsumi S, Wu TY, Eckl EM, Hawkins SD, Buelter T, Liao JC: **Engineering the isobutanol biosynthetic pathway in Escherichia coli by comparison of three aldehyde reductase/alcohol dehydrogenase genes.** *Applied Microbiology and Biotechnology* 2010, **85:**651-657.
123. Willis RM, Wahlen BD, Seefeldt LC, Barney BM: **Characterization of a Fatty Acyl-CoA Reductase from Marinobacter aquaeolei VT8: A Bacterial Enzyme Catalyzing the Reduction of Fatty Acyl-CoA to Fatty Alcohol.** *Biochemistry* 2011, **50:**10550-10558.
124. Schirmer A, Rude MA, Li XZ, Popova E, del Cardayre SB: **Microbial Biosynthesis of Alkanes.** *Science* 2010, **329:**559-562.
125. Jarboe LR: **YqhD: a broad-substrate range aldehyde reductase with various applications in production of biorenewable fuels and chemicals.** *Appl Microbiol Biotechnol* 2011, **89:**249-257.
126. Wahlen BD, Oswald WS, Seefeldt LC, Barney BM: **Purification, Characterization, and Potential Bacterial Wax Production Role of an NADPH-Dependent Fatty Aldehyde Reductase from Marinobacter aquaeolei VT8.** *Appl Environ Microbiol* 2009, **75:**2758-2764.
127. Hofvander P, Doan TTP, Hamberg M: **A prokaryotic acyl-CoA reductase performing reduction of fatty acyl-CoA to fatty alcohol.** *Febs Letters* 2011, **585:**3538-3543.
128. Liu YL, Chen S, Chen JJ, Zhou JM, Wang YY, Yang MH, Qi XN, Xing JM, Wang QH, Ma YH: **High production of fatty alcohols in Escherichia coli with fatty acid starvation.** *Microbial Cell Factories* 2016, **15**.

129. Ajikumar PK, Xiao W-H, Tyo KEJ, Wang Y, Simeon F, Leonard E, Mucha O, Phon TH, Pfeifer B, Stephanopoulos G: **Isoprenoid Pathway Optimization for Taxol Precursor Overproduction in Escherichia coli.** *Science* 2010, **330:**70-74.
130. Layton DS, Trinh CT: **Expanding the modular ester fermentative pathways for combinatorial biosynthesis of esters from volatile organic acids.** *Biotechnology and Bioengineering* 2016, **113:**1764-1776.
131. Fatma Z, Jawed K, Mattam AJ, Yazdani SS: **Identification of long chain specific aldehyde reductase and its use in enhanced fatty alcohol production in E. coli.** *Metabolic Engineering* 2016, **37:**35-45.
132. Chu S, Majumdar A: **Opportunities and challenges for a sustainable energy future.** *Nature* 2012, **488:**294-303.
133. Zhang F, Rodriguez S, Keasling JD: **Metabolic engineering of microbial pathways for advanced biofuels production.** *Curr Opin Biotechnol* 2011, **22:**775-783.
134. Yu X, Liu T, Zhu F, Khosla C: **In vitro reconstitution and steady-state analysis of the fatty acid synthase from Escherichia coli.** *Proc Natl Acad Sci U S A* 2011, **108:**18643-18648.
135. Dellomonaco C, Clomburg JM, Miller EN, Gonzalez R: **Engineered reversal of the beta-oxidation cycle for the synthesis of fuels and chemicals.** *Nature* 2011, **476:**355-359.
136. Handke P, Lynch SA, Gill RT: **Application and engineering of fatty acid biosynthesis in Escherichia coli for advanced fuels and chemicals.** *Metab Eng* 2011, **13:**28-37.
137. Zhang F, Ouellet M, Batth TS, Adams PD, Petzold CJ, Mukhopadhyay A, Keasling JD: **Enhancing fatty acid production by the expression of the regulatory transcription factor FadR.** *Metab Eng* 2012, **14:**653-660.
138. Steen EJ, Kang Y, Bokinsky G, Hu Z, Schirmer A, McClure A, Del Cardayre SB, Keasling JD: **Microbial production of fatty-acid-derived fuels and chemicals from plant biomass.** *Nature* 2010, **463:**559-562.
139. Hopkins H, Small LD: **An investigation of some pharmaceutical applications of certain fatty acid esters of sucrose.** *J Am Pharm Assoc Am Pharm Assoc* 1960, **49:**220-224.
140. Liu C, Liu F, Cai J, Xie W, Long TE, Turner SR, Lyons A, Gross RA: **Polymers from fatty acids: poly(omega-hydroxyl tetradecanoic acid) synthesis and physico-mechanical studies.** *Biomacromolecules* 2011, **12:**3291-3298.
141. Aoshima H, Miyagisnima A, Nozawa Y, Sadzuka Y, Sonobe T: **Glycerin fatty acid esters as a new lubricant of tablets.** *Int J Pharm* 2005, **293:**25-34.
142. Choi YJ, Lee SY: **Microbial production of short-chain alkanes.** *Nature* 2013, **502:**571-574.
143. Li N, Norgaard H, Warui DM, Booker SJ, Krebs C, Bollinger JM: **Conversion of Fatty Aldehydes to Alka(e)nes and Formate by a Cyanobacterial Aldehyde Decarbonylase: Cryptic Redox by an Unusual Dimetal Oxygenase.** *Journal of the American Chemical Society* 2011, **133:**6158-6161.
144. Andre C, Kim SW, Yu XH, Shanklin J: **Fusing catalase to an alkane-producing enzyme maintains enzymatic activity by converting the inhibitory byproduct H2O2 to the cosubstrate O-2.** *Proceedings of the National Academy of Sciences of the United States of America* 2013, **110:**3191-3196.
145. Khara B, Menon N, Levy C, Mansell D, Das D, Marsh ENG, Leys D, Scrutton NS: **Production of Propane and Other Short-Chain Alkanes by Structure-Based**

Engineering of Ligand Specificity in Aldehyde-Deformylating Oxygenase. *Chembiochem* 2013, **14:**1204-1208.
146. Kallio P, Pasztor A, Thiel K, Akhtar MK, Jones PR: **An engineered pathway for the biosynthesis of renewable propane.** *Nature Communications* 2014, **5**.
147. Rodriguez GM, Atsumi S: **Toward aldehyde and alkane production by removing aldehyde reductase activity in Escherichia coli.** *Metabolic Engineering* 2014, **25:**227-237.
148. Cao YX, Xiao WH, Zhang JL, Xie ZX, Ding MZ, Yuan YJ: **Heterologous biosynthesis and manipulation of alkanes in Escherichia coli.** *Metabolic Engineering* 2016, **38:**19-28.
149. Andre C, Kim SW, Yu XH, Shanklin J: **Fusing catalase to an alkane-producing enzyme maintains enzymatic activity by converting the inhibitory byproduct H2O2 to the cosubstrate O2.** *Proc Natl Acad Sci U S A* 2013, **110:**3191-3196.
150. Knothe G, Dunn RO: **A Comprehensive Evaluation of the Melting Points of Fatty Acids and Esters Determined by Differential Scanning Calorimetry.** *Journal of the American Oil Chemists' Society* 2009, **86:**843-856.
151. Knothe G: **Dependence of biodiesel fuel properties on the structure of fatty acid alkyl esters.** *Fuel Processing Technology* 2005, **86:**1059-1070.
152. Bowen CH, Bonin J, Kogler A, Barba-Ostria C, Zhang F: **Engineering Escherichia coli for Conversion of Glucose to Medium-Chain omega-Hydroxy Fatty Acids and alpha,omega-Dicarboxylic Acids.** *Acs Synthetic Biology* 2016, **5:**200-206.
153. Karim AS, Jewett MC: **A cell-free framework for rapid biosynthetic pathway prototyping and enzyme discovery.** *Metabolic Engineering* 2016, **36:**116-126.
154. Hold C, Billerbeck S, Panke S: **Forward design of a complex enzyme cascade reaction.** *Nature Communications* 2016, **7:**12971.
155. Dudley QM, Anderson KC, Jewett MC: **Cell-Free Mixing of Escherichia coli Crude Extracts to Prototype and Rationally Engineer High-Titer Mevalonate Synthesis.** *ACS Synth Biol* 2016, **5:**1578-1588.
156. Bujara M, Schumperli M, Pellaux R, Heinemann M, Panke S: **Optimization of a blueprint for in vitro glycolysis by metabolic real-time analysis.** *Nature Chemical Biology* 2011, **7:**271-277.
157. Kay JE, Jewett MC: **Lysate of engineered Escherichia coli supports high-level conversion of glucose to 2,3-butanediol.** *Metabolic Engineering* 2015, **32:**133-142.
158. Kwon YC, Jewett MC: **High-throughput preparation methods of crude extract for robust cell-free protein synthesis.** *Scientific Reports* 2015, **5**.

Curriculum Vitae

Wen Jiang

Department of Energy, Environmental and Chemical Engineering

Washington University in St. Louis, St. Louis, MO 63130

Email: w.jiang@wustl.edu

EDUCATION

Aug. 2013 to Aug. 2018

Ph.D., Energy, Environmental and Chemical Engineering, Washington University in St. Louis, St. Louis, USA

Sep. 2011 to Aug. 2013

M.S., Chemical Engineering, Pohang University of Science and Technology, Pohang, South Korea

Sep. 2008 to Jul. 2011

B.S. (Double Major), Biochemistry and Molecular Biology, Peking University, Beijing, China

Sep. 2007 to Jul. 2011

B.S., Chemistry, Peking University, Beijing, China

JOURNAL PAPER

Jiang W., Gu P., Zhang F., Steps towards "drop-in" biofuels: focusing on metabolic pathways. Current Opinion in Biotechnology. 53, 26-32, (2018)

Jiang W., Qiao J.B., Bentley G.J., Liu D., Zhang F., Modular pathway engineering for the Production of Branched-Chain Fatty Alcohols. Biotechnology for Biofuels. 10, 244, (2017)

Xiao Y., Jiang W., Zhang F., Developing a genetically-encoded, cross-species ammonium biosensor for detecting nitrogen and regulating biosynthesis of cyanophycin. ACS Synthetic Biology. 6, 1807-1815, (2017)

Bentley G.J., Jiang W., Guaman L.P., Xiao Y., Zhang F., Engineering Escherichia coli to produce branched-chain fatty acids in high percentages. Metabolic Engineering. 38, 148-158, (2016).

Jiang W, Jiang Y, Bentley GJ, Liu D, Xiao Y, Zhang F. Enhanced production of branched-chain fatty acids by replacing β-ketoacyl-(acyl-carrier-protein) synthase III (FabH). *Biotechnology and Bioengineering*, 112, 1613, (2015)

CONFERENCE

Jiang W., Qiao J.B., Bentley G.J., Liu D., Zhang F., Modular pathway engineering for the Production of Branched-Chain Fatty Alcohols. Poster, 2018 EBRC Spring Retreat, Mar. 23-24, Seattle, WA (2018)

Jiang W., Bentley G.J., Qiao J.B., Zhang F., Production of branched-chain fatty acid and derivatives in high percentage. 2017 ACS Spring National Meeting, Apr. 2, San Francisco, CA (2017)

Xiao Y., Jiang W., Zhang F., Developing a genetically-encoded, cross-species ammonium biosensor for detecting nitrogen and regulating biosynthesis of cyanophycin. Poster, 2017 EBRC Spring Retreat, Mar. 24-25, Evanston, IL (2017)

Jiang W., Bentley G.J., Xiao Y., Zhang F., Explore the capacity of engineered E. coli to produce branched-chain fatty acids (BCFAs), Poster, 2016 EBRC Fall Retreat, Nov. 2-3 Pasadena, CA (2016)

Jiang W, Jiang Y, Bentley GJ, Liu D, Xiao Y, Zhang F. 2015. Enhanced production of branched-chain fatty acids by replacing β-ketoacyl-(acyl-carrier-protein) synthase III (FabH). Poster, 2015 Synberc Spring Retreat, April 1-3, Berkeley, CA

Appendix Chapter: Developing a genetically-encoded, cross-species ammonium biosensor for detecting nitrogen and regulating biosynthesis of cyanophycin